

NASA CR-122414

NUS-772

**EMITTED RADIATION CHARACTERISTICS OF PLUTONIUM DIOXIDE
RADIOISOTOPE THERMOELECTRIC GENERATORS**

For

**NATIONAL AERONAUTICS AND SPACE ADMINISTRATION
GODDARD SPACE FLIGHT CENTER
Glenn Dale Road
Greenbelt, Maryland**

NASA Contract Number: NAS5-11359

By

P. J. GINGO

and

J. J. STEYN

March 1971

**NUS CORPORATION
4 Research Place
Rockville, Maryland 20850**

NUS-772

ABSTRACT

The nuclear and emitted radiation characteristics of the radioisotope elements and impurities in commercial grade plutonium dioxide are presented in detail. The development of the methods of analysis are presented.

Radioisotope thermoelectric generators (RTG) of 1575, 3468 and 5679 thermal watts are characterized with respect to neutron and gamma photon source strength as well as spatial and number flux distribution. The results are presented as a function of detector position and light element contamination concentration for fuel age ranging from 'fresh' to 18 years. The data may be used to obtain results for given ^{18}O and ^{236}Pu concentrations.

The neutron and gamma photon flux and dose calculations compare favorably with reported experimental values for SNAP-27

TABLE OF CONTENTS

	<u>Page</u>
Abstract	i
List of Figures	iv
List of Tables	vi
Foreward and Acknowledgements	x
1. Introduction	1
2. Gamma Photon Radiation Characteristics	8
2.1 Introduction	8
2.2 Gamma Photon Source Spectra	9
2.3 Gamma Photon Fluxes	12
3. Neutron Radiation Characteristics	53
3.1 Introduction	53
3.2 Neutron Source Spectra	55
3.2.1 Fission Neutrons	55
3.2.2 Oxygen (α , n) Neutrons	56
3.2.3 Impurity (α , n) Neutron Yield	59
3.3 Neutron Fluxes	60
4. Discussion of Results	76
Appendix A Gamma Activity Due to Direct Decay of ^{241}Pu and Daughter Nuclides	81
Appendix B Tabulation of Prompt Fission and Equilibrium Fission Product Gamma Photons	85
Appendix C ^{236}Pu Gamma Photon Activity	88
Appendix D ^{236}Pu Daughter Nuclide Gamma Photon Activity	90
Appendix E $^{18}\text{O}(\alpha, n)^{21}\text{Ne}$ Gamma Photon Activity	93
Appendix F Example Flux Calculations	95
Appendix G The Dynamics of the $^{18}\text{O}(\alpha, n)^{21}\text{Ne}$ Reaction	97
Appendix H Alpha Particle Energy Loss per Unit Path Length	101

		<u>Page</u>
Appendix I	$^{18}\text{O}(\alpha, n) ^{21}\text{Ne}$ Neutron Yield	102
Appendix J	Integration of $^{18}\text{O}(\alpha, n) ^{21}\text{Ne}$ Spectral Yield	107
Appendix K	Contaminant Light Element (α, n) Neutron Yield	112
References		116

LIST OF FIGURES

		<u>Page</u>
Figure 2-I	Typical Plutonium Fuelled RTG Capsule	15
Figure 2-II	Geometry of Model Fuel Capsule	16
Figure 2-III	RTG Coordinate System	17
Figure 2-IV	Gamma Photon Flux as a Function of Detector Radial Distance from 1575 w(th) Capsule Axis with Fuel Age as the Parameter	18
Figure 2-V	Gamma Photon Flux as a Function of Detector Radial Distance from 3468 w(th) Capsule Axis with Power as the Parameter	19
Figure 2-VI	Gamma Photon Flux as a Function of Detector Radial Distance from 5679 w(th) Capsule Axis with Fuel Age as the Parameter	20
Figure 2-VII	Gamma Photon Flux as a Function of Detector Axial Distance from 1575 w(th) Capsule Mid-plane with Fuel Age as the Parameter	21
Figure 2-VIII	Gamma Photon Flux as a Function of Detector Axial Distance from 3468 w(th) Capsule Mid-plane with Fuel Age as the Parameter	22
Figure 2-IX	Gamma Photon Flux as a Function of Detector Axial Distance from 5679 w(th) Capsule Mid-plane with Fuel Age as the Parameter	23
Figure 2-X	Gamma Photon Radial and Axial One-Meter Photon Flux as a Function of Capsule Power with Fuel Age as the Parameter	24
Figure 2-XI	One-Meter Gamma Photon Radial Photon Flux as a Function of Fuel Age with Capsule Power as the Parameter	25

		<u>Page</u>
Figure 3-I	Neutron Flux as a Function of Detector Radial Distance from Capsule Axis with Power as the Parameter (Neutron Source: $^{18}\text{O}(\alpha, n)^{21}\text{Ne}$ and Fission)	63
Figure 3-II	Neutron Flux as a Function of Detector Radial Distance from Capsule Axis with Power as the Parameter (Neutron Source: Fission)	64
Figure 3-III	Neutron Flux as a Function of Detector Axial Distance from Capsule Axis with Power as the Parameter (Neutron Source: $^{18}\text{O}(\alpha, n)^{21}\text{Ne}$ and Fission)	65
Figure 3-IV	Neutron Flux as a Function of Detector Axial Distance from Capsule Axis with Power as the Parameter (Neutron Source: Fission)	66
Figure 4-I	1575 w(th) Capsule Gamma Photon Dose Rate at 1.0 Meter as a Function of Fuel Age	79
Figure I-I	Neutron Fractional Yield as a Function of Energy	105
Figure I-II	Neutron Energy as a Function of Angle of Scatter in the C-M System with Alpha Particle Energy as the Parameter	106

LIST OF TABLES

		<u>Page</u>
Table 1-I	Radiation Properties of PuO ₂	5
Table 1-II	Specific Neutron Yields from Light Element Impurities	6
Table 1-III	PuO ₂ Source Neutron Activity	7
Table 2-I	Natural Nuclear Properties of Plutonium Isotopes	26
Table 2-II	Gamma Photons from Decay of Plutonium Isotopes and their Decay Products	27
Table 2-III	Gamma Photons Emitted from Equilibrium Fission	28
Table 2-IV	Gamma Photons from ²³⁶ Pu and Daughter Nuclides	29
Table 2-V	Gamma Photons due to ¹⁸ O(α,n) ²¹ Ne Reaction	30
Table 2-VI(a)	Gamma Photon Activity at Time Zero	31
Table 2-VI(b)	Gamma Photon Activity at Time Zero	32
Table 2-VII(a)	Gamma Photon Activity at Time One Year	33
Table 2-VII(b)	Gamma Photon Activity at Time One Year	34
Table 2-VIII(a)	Gamma Photon Activity at Time Five Years	35
Table 2-VIII(b)	Gamma Photon Activity at Time Five Years	36
Table 2-IX(a)	Gamma Photon Activity at Time Ten Years	37
Table 2-IX(b)	Gamma Photon Activity at Time Ten Years	38
Table 2-X(a)	Gamma Photon Activity at Time Eighteen Years	39
Table 2-X(b)	Gamma Photon Activity at Time Eighteen Years	40
Table 2-XI	Total Photon Activity at Noted Times	41
Table 2-XII	Material Properties of Model Fuel Capsule	42

	<u>Page</u>
Table 2-XIII	43
Gamma Photon Surface Flux (Photons/cm ² -sec) at Capsule Midplane for Fresh Fuels; Source-- Decay of Isotopes and Daughters	
Table 2-XIV	44
Gamma Photon Surface Flux (Photons/cm ² -sec) at Capsule Midplane for Fresh Fuel; Source-- ¹⁸ O(α,n) ²¹ Ne Reaction	
Table 2-XV	45
Gamma Photon Surface Flux (Photons/cm ² -sec) at 1575 w(th) Capsule Midplane at Noted Fuel Age; Source-- ²³⁶ Pu and Daughters	
Table 2-XVI	46
Gamma Photon Surface Flux (Photons/cm ² -sec) at 3468 w(th) Capsule Midplane at Noted Fuel Age; Source-- ²³⁶ Pu and Daughters	
Table 2-XVII	47
Gamma Photon Surface Flux (Photons/cm ² -sec) at 5679 w(th) Capsule Midplane at Noted Fuel Age; Source-- ²³⁶ Pu and Daughters	
Table 2-XVIII	48
Gamma Photon Flux (Photons/cm ² -sec) as a Function of Detector Position for Fresh Fuel; Source--Decay of Isotopes and Daughters	
Table 2-XIX	49
Gamma Photon Flux (Photons/cm ² -sec) as a Function of Detector Position for Fresh Fuel; Source-- ¹⁸ O(α,n) ²¹ Ne Reaction	
Table 2-XX	50
Gamma Photon Flux (Photon/cm ² -sec) for 1575 w(th) Capsule as a Function of Detector Position at Noted Fuel Age; Source-- ²³⁶ Pu and Daughters	
Table 2-XXI	51
Gamma Photon Flux (Photon/cm ² -sec) for 3468 w(th) Capsule as a Function of Detector Position at Noted Fuel Age; Source-- ²³⁶ Pu and Daughters	

	<u>Page</u>	
Table 2-XXII	Gamma Photon Flux (Photons/cm ² -sec) for 5679 w(th) Capsule as a Function of Detector Position at Noted Fuel Age: Source-- ²³⁶ Pu and Daughters	52
Table 3-I	Plutonium Isotope Spontaneous Fission Neutron Spectrum	67
Table 3-II	Total Neutron Emission from the ¹⁸ O(α,n) ²¹ Ne Reaction in PuO ₂ Fuel	68
Table 3-III	¹⁸ O(α,n) ²¹ Ne Neutron Spectrum	69
Table 3-IV	Analysis of Typical Pu(NO ₃) ₄ Feed Stock and Plasma Spheroidized Microspheres	70
Table 3-V	Radial Neutron Flux at Capsule Surface Source: ¹⁸ O(α,n) ²¹ Ne and Fission Neutrons	71
Table 3-VI	Radial Neutron Flux at Capsule Surface Source: Fission Neutrons	72
Table 3-VII	Neutron Flux as a Function of Detector Position Capsule Power 1575 w(th) Neutron Flux (neutron/cm ² -sec)	73
Table 3-VIII	Neutron Flux as a Function of Detector Position Capsule Power 3468 w(th)	74
Table 3-IX	Neutron Flux as a Function of Detector Position Capsule Power 5679 w(th)	75
Table 4-I	Radial Gamma Photon Total Dose Rate at 1.0 Meter as a Function of PuO ₂ Age	80
Table B-I	Prompt Fission and Equilibrium Fission Product Gamma Photons	86
Table B-II	Prompt Fission and Equilibrium Fission Product Gamma Photons	87

		<u>Page</u>
Table J-I	Nuclear Cross Sections for Formation of $^{18}\text{O}(\alpha, n)^{21}\text{Ne}$ Compound Nucleus	111
Table K-I	Data for Light Element (α, n) Yield	114
Table K-II	Light Element (α, n) Yield	115

FOREWORD AND ACKNOWLEDGEMENTS

This report, prepared by NUS Corporation for the National Aeronautics and Space Administration at Goddard Space Flight Center under contract NAS5-11359, consists of a compilation of work performed largely by the first author, Dr. Peter Gingo. The section on 'Gamma Photon Radiation Characteristics' is based on work done at the Jet Propulsion Laboratory, California Institute of Technology, as reported by P. J. Gingo and M. A. Dore, in JPL Engineering Memo 342-84. The section on 'Neutron Radiation Characteristics' was developed by Dr. Gingo at the University of Akron, Akron, Ohio.

The authors gratefully acknowledge on behalf of NASA/GSFC the preliminary manuscript reviews of P. Brown (General Electric Co.), Dr. Albenesius and Dr. Peterson (Savannah River Laboratory), Edward Anderson (Mound Laboratory) and H. Bermanis (United Engineers and Constructors).

The authors also wish to express their gratitude to Mrs. Janet Falibota, Mrs. Stephanie Jones, Mr. Michael T. Kalman and Mr. Charles Whittaker for assistance during compilation.

1. INTRODUCTION

The ever increasing requirement for long-lived and compact power sources has led to the recent evolution of a number of very successful generators. Specifically, the development of the radioisotope thermoelectric generator (RTG) for both terrestrial and space flight applications has progressed very significantly. A number of plutonium dioxide fuelled RTG's are already in actual use. The NIMBUS weather satellite is powered by a Space Nuclear Auxiliary Power system, i.e., SNAP 19. Instrumentation left on the Moon by the Apollo 12 and 14 missions are powered by SNAP 27 units. Future space missions include RTG assemblies. Unlike solar cell generators their power output is not dependent upon solar flux and thus they are suited for deep outer planet space missions of 10 to 20 year duration.

The radioactive properties of RTG's require that special attention be given to their engineering design from both the standpoint of mission safety and mission operational requirements. This report is concerned with these factors as they relate to the gamma photon and neutron radiation emitted by plutonium-oxide fuelled generators. The radiation data presented will be of interest to spacecraft, RTG and science experiment designers. It permits radiation field maps to be developed to aid in location and protection of sensitive electronic packages and science experiments. The data may also be used for determination of personnel exposure and protection.

The RTG gamma photon and neutron radiation result from the natural radioactivity of the plutonium dioxide heat source. The gamma photons are due mainly to the plutonium isotopes and their daughter products with small contributions resulting from induced fission and neutron interactions with materials in the source assembly. The neutrons result mainly from

plutonium decay alpha emission and thus (α , n) reactions with low atomic number impurity elements including the ^{18}O component of the oxide; a small contribution is due to plutonium spontaneous fission. The neutron flux may be decreased by reduction of the impurities and depletion of ^{18}O .

The natural radioactivity of the isotope ^{238}Pu consists of alpha particles accompanied by a spectrum of gamma photons and spontaneous fission neutrons. Commercial grade plutonium consists of ^{238}Pu and other Pu isotopes as indicated in Table 1-I⁽¹⁻³⁾. Even though the ^{238}Pu is only $\sim 80\%$ abundant, it contributes $\sim 99.9\%$ of the total alpha activity. Since the average energy of emitted alphas is ~ 5.5 MeV, (α , n) reactions occur with low atomic number elements such as oxygen which is abundantly present in PuO_2 as indicated in Table 1-I. The use of oxygen in which the ^{18}O isotope is depleted by a factor of 100 reduces this effect correspondingly by ~ 100 . Again, the presence of impurity beryllium or fluorine even in low abundance may give rise to a significant (α , n) neutron yield; some light impurity element yields are given in Table 1-II⁽³⁾. The spontaneous fission (SF) neutron emission of plutonium is primarily that of ^{238}Pu since the other contributing isotope ^{240}Pu , has an SF rate ~ 0.015 that of ^{238}Pu . The SF neutrons have a Maxwellian distribution peaked at ~ 0.7 MeV, an average energy of ~ 2.0 MeV, and a maximum energy of ~ 10 MeV. Fast photo-neutrons are also produced in PuO_2 due to energetic gamma photons from ^{238}Pu spontaneous fission and the ^{236}Pu daughter, ^{208}Tl , interacting with impurity elements.

PuO_2 sources emit X-rays and gamma photons as a result of spontaneous and induced fission, non-fission neutron interactions, decay of fission products and their daughter products, and alpha interactions with light

elements such as ^{18}O . The gamma photons emitted by PuO_2 are presented in detail in Section 2 of this report. The gamma photon activity from Pb, Bi and Tl daughters increases with time after ^{238}Pu purification to a maximum at ~ 18 years; this is readily seen in the decay in

Figure 1-I. Freshly separated plutonium fuel has a 'soft' gamma spectrum. With increasing time the decay daughter products of the small ^{236}Pu impurity increase the intensity of the 0.2 - 0.3 and 2.0 - 3.0 MeV photon groups. Spectral hardening is complete at approximately 18 years.

Long-lived ^{241}Am , a daughter of 13 year ^{241}Pu , yields increasingly intense gamma photon emission rates with age. However, since the photon energy is 0.06 MeV, it is easily shielded and so is not intensely present in the emission spectra of encapsulated sources.

As indicated above fast neutrons are emitted by PuO_2 primarily as the result of the three interaction phenomena: spontaneous fission, alpha-neutron emission rates for these effects; ⁽³⁾ detailed neutron data is presented in Section 3 of this report. The (α, n) neutron emission rate depends on the impurities present in the source, since the reaction requires the presence of low Z elements, as seen from Table 1-II. Table 1-III lists neutron activity due to (α, n) for normal and ^{18}O depleted PuO_2 ; it also gives the photo-neutron production rate.

The alpha and beta radiation emitted by PuO_2 sources does not present any problems if the source encapsulation has a wall thickness greater than $\sim 1000 \text{ mg/cm}^2$. (e.g., ~ 0.06 " Ta).

Section 2 of this report presents gamma photon source and calculated emission flux data for a hypothesized SNAP RTG. The data was determined for 1575, 3468 and 5679 watts of thermal power. The flux data

was calculated as a function of PuO_2 age at the RTG exterior surface and points on both the axial and radial mid-planes. Section 3 of this report presents neutron source and emission flux data similar to the photon data of Section 2. Section 4 consists of a brief review of the data in Sections 2 and 3. A comparison of the calculated data with published data is presented. Pertinent information and methods of calculation are given in Appendices A through J

TABLE I-I
RADIATION PROPERTIES OF PuO₂⁽¹⁻³⁾

A. Chemical Composition PuO₂

Plutonium (total)	88.2%
Oxygen	11.8%

B. Isotopic Composition⁽¹⁾

<u>Isotope</u>	<u>Abundance %= (a)</u>	<u>Activation of Pure Isotope, d/sec-g = (b)</u>	<u>Contribution to the Activity of 1 gram of Product = (a) x (b)/100</u>
236 Pu	1.2×10^{-4}	1.97×10^{13}	2.37×10^7 (α)
238 Pu	81 %	6.35×10^{11}	5.14×10^{11} (α)
239 Pu	15 %	2.27×10^9	3.41×10^8 (α)
240 Pu	2.9 %	8.38×10^9	2.43×10^8 (α)
241 Pu	0.8 %	4.12×10^{12}	3.30×10^{10} (β)
242 Pu	0.1 %	1.44×10^8	1.44×10^5 (α)

C. Specific Activity ^{238}Pu 16.8 Curies/gm

D. Density of PuO₂ 10.0 gm/cm³
 Plutonium Fraction 8.82 gm/cm³ (^{238}Pu 7.15 gm/cm³ PuO₂)
 Oxygen 1.18 gm/cm³

E. Activity of Fuel

$$\begin{aligned}
 7.15 \text{ gm/cm}^3 \times 16.8 \text{ Ci/gm} &= 1.2 \times 10^2 \text{ Curies/cm}^3 \text{-PuO}_2 \\
 &= 4.5 \times 10^{12} \alpha/\text{cm}^3 \text{-sec} \\
 &= 3.92 \text{ watts/cm}^3
 \end{aligned}$$

TABLE I-II
 SPECIFIC NEUTRON YIELDS FROM
 LIGHT ELEMENT IMPURITIES⁽³⁾

<u>Element</u>	<u>Neutrons Per Second*</u> <u>for one Part per Million</u>
Li	4.6
Be	133
B	41
C	0.2
N	0.0 (α, n threshold too high)
O	0.1
F	18
Na	2.2
Mg	2.1
Al	1.0
Si	0.2
P	< 0.03
S	< 0.03

* In 1 gm Pu metal containing 81% ²³⁸Pu

TABLE I-III

PuO_2 SOURCE NEUTRON ACTIVITY⁽³⁾

(i) Spontaneous Fission Rate

^{238}Pu : 2.6×10^3 n/sec-gm ^{238}Pu
 fuel : 1.8×10^3 n/sec-gm PuO_2

(ii) (α , n) Neutron Emission Rate

PuO_2 (normal O): 1.13×10^4 n/sec-gm ^{238}Pu
 PuO_2 (^{18}O reduced to 1/100): $\sim 1.13 \times 10^2$ n/sec-gm ^{238}Pu

(excludes (α , n) due to other impurities)

(iii) Photo-Neutron Production Rate: $\sim 5.0 \times 10^2$ n/sec-gm ^{238}Pu

(varies with concentration of ^{208}Tl daughter of Pu^{236})

2. GAMMA PHOTON RADIATION CHARACTERISTICS

2.1 Introduction

This report section presents the calculation of the gamma photon flux emitted by plutonium dioxide fuelled RTG capsules. Gamma photon fluxes were determined as a function of energy and fuel age for RTG model capsules with thermal power capacities of 1575, 3468 and 5679 w(th). The calculations included the determination of source data to account for plutonium decay, nuclear fission and the (α , n) reaction.

Production grade plutonium dioxide fuel consists of a mixture of plutonium isotopes having the approximate composition shown in Table 1-1⁽¹⁾; other possible compositions may be found in the references (2, 3). Each of the isotopes listed in Table 1-I have the properties of natural radioactivity and neutron fission as given in Table 2-1^(1,4-11). The determination of the total gamma photon source intensity and spectral distribution is described in Section 2.2.

The data presented in this report were determined for a standard RTG, namely: a hypothesized SNAP 27. The radioisotope fuel used in the SNAP 27 fuel capsule is plutonium in the form of plutonium dioxide microspheres. The fuel is contained in a cylindrical annulus as shown in Figure 2-I. The basic model capsule was assumed to produce 1575 watts of thermal power. The 1575 w(th) capsule power was extended volumetrically to 3468 w(th) and 5679 w(th) in order to study the effect of fuel self shielding on radiated photon fluxes. Gamma photon transport in the RTG was determined by the method of discrete ordinates⁽¹²⁾. RTG surface fluxes were extended to

radial and axial midplane spatial detector locations by means of the point kernel technique⁽¹³⁾. The calculation of the photon flux distributions is described in Section 2.3.

2.2 Gamma Photon Source Spectra

The gamma photons emitted by plutonium dioxide were separated into four components, categorized according to their origin, namely:

- I. Plutonium isotopes and their decay products, excluding ^{236}Pu .
- II. Fission and decay of fission products.
- III. Radioactive decay of ^{236}Pu and daughter nuclides.
- IV. The alpha particle reaction, $^{18}\text{O}(\alpha, n)^{21}\text{Ne}$, which yields a gamma spectrum due to the decay of the ^{22}Ne compound nucleus to ^{21}Ne .

Other categories whose contribution to the RTG external radiation field were reasonably neglected are, namely:

- V. Bremsstrahlung and inelastic gamma photons which are a function of spacecraft geometry and materials.
- VI. Gamma photons resulting from the $^{17}\text{O}(\alpha, n)^{20}\text{Ne}$ reaction.

The gamma photon calculations were carried out for twenty (20) energy groups. The upper and lower limits of the highest and lowest energy intervals were taken as 7.0 MeV and 2.0 keV, respectively. In each of the corresponding gamma energy intervals, the sources of prominent gammas emitted by the plutonium dioxide fuel were determined for time periods beginning with the "fresh" (time of chemical extraction) fuel and extending up to 18 years of fuel aging.

The gamma photon spectrum emitted by ^{238}Pu , ^{239}Pu , and ^{241}Pu was calculated as the abundance multiplied by the activity of the isotope at the equilibrium time considered. The activity of daughter nuclides ^{241}Am , ^{237}U and ^{237}Np is calculated in Appendix A. The gamma activity of the plutonium isotopes, exclusive of ^{236}Pu , and their decay products varies only slightly up to 18 years and thus was assumed to remain constant with time. The gamma photons emitted by the plutonium isotopes and their decay products are given in Table 2-II^(1,3,9,14). The reference (9) data was used where available, otherwise references (1) and (14) were used.

The gamma rays emitted by prompt fission were assumed to have the spectral shape provided by the spontaneous fission of ^{235}U ⁽¹⁵⁾. In the gamma photon energy range, 1.30 to 1.0 MeV, the photon spectral distribution was obtained from the relationship

$$N(E) = 26.8e^{-2.30E}, \text{ photons/fission.}$$

In the range, 1.0 to 7.0 MeV, the distribution was obtained from the relationship⁽¹⁵⁾

$$N(E) = 8.03^{-1.10E}, \text{ photons/fission.}$$

Equilibrium fission product gamma photon emission was determined using analytic functions fitted to the data of reference (14). The functions and the reference data are given in Table 2-III. The gamma photons emitted by prompt fission and equilibrium fission products were integrated numerically in each energy interval to yield the total number of photons produced per fission. Details of these calculations are given in Appendix B.

In the present work the ^{236}Pu isotope was considered as a PuO_2 fuel impurity which ranged from 1.2 ppm (1.2×10^{-6} gm ^{236}Pu per gm PuO_2), as typical of the current commercial product grade, down to 0.1 ppm as desirable in the bio-medical grade. The gamma photon activity as a function of time was calculated as detailed in Appendix C. The activity of the ^{236}Pu daughter nuclides was calculated from the growth of 1.91 year ^{228}Th . The calculation is detailed in Appendix D as a function of ^{236}Pu impurity, i.e., 0.1 to 1.2 ppm. The gamma photons emitted by ^{236}Pu and the daughter nuclides are given in Table 2-IV^(1,9). The reference (9) data was used in this work.

Alpha particles interacting with ^{18}O may give rise to the formation of very short-lived compound nuclei which promptly decay accompanied by the emission of a neutron and gamma photons. The photon emission due to $^{18}\text{O}(\alpha, n)^{21}\text{Ne}$ interactions is detailed in Appendix E and tabulated in Table 2-V. The radiated gamma photon fluxes produced by the $^{18}\text{O}(\alpha, n)^{21}\text{Ne}$ reaction at time periods other than "fresh" were obtained by multiplying the fresh $^{18}\text{O}(\alpha, n)^{21}\text{Ne}$ gamma yield values by the time decay factors given in Appendix E.

It is indicated in reference (16) that the ^{17}O abundance and (α, n) cross section are approximately 10% of the corresponding values for ^{18}O . Though the ^{17}O interaction has not been fully investigated and documented, and thus cannot be adequately treated at this time, it can be reasonably neglected.

The gamma photon source spectra derived for each of the source categories I through IV above, are listed in Tables 2-II through 2-V. These sources are detailed for 0 (fresh), 1, 5, 10 and 18 years as a function of energy in

Tables 2-VI(a) and 2-VI(b) through 2-X(a) and 2-X(b). The (b) tables give the sum of the isotopic photons and fission photons, and the ^{236}Pu -chain photons detailed in the (a) tables as well as the ^{18}O reaction photons and their totals. Table 2-XI summarizes these totals for each fuel age as a function of energy.

The calculations assumed the ^{238}Pu half life as 87.4 years⁽⁷⁾ and the fission yield as 2.75 ± 0.01 neutrons/fission⁽⁶⁾. The half-life of ^{241}Pu was taken as 14.0 years⁽⁷⁾.

2.3 Gamma Photon Fluxes

The gamma photon source spectra discussed in Section 2.2 were used to determine flux distributions at the RTG surface and exterior spatial positions. The flux calculations were carried out for 1575, 3468 and 5679 w(th) model capsules. Figure 2-II gives the dimensions of the three model capsules and their material zones as a function of thermal power. The material composition of the capsule zones are detailed in Table 2-XII

Gamma photon flux transport to the RTG surface and exterior spatial positions on the radial and axial midplanes were calculated using the ANISN⁽¹⁷⁾ and QAD⁽¹⁸⁾ computer codes. ANISN, a discrete ordinate⁽¹²⁾ code was used to determine surface fluxes. QAD, an integrating point kernel⁽¹³⁾ code was used to calculate the fluxes at detector points outside the RTG. The gamma spectrum was assumed as unchanging from the capsule surface to detector positions distant from the capsule surface. The calculations were carried out for "fresh," 1, 5, 10, and 18 year old fuel.

The twenty group gamma photon cross sections were determined using a modified version of the GAMLEG⁽¹⁹⁾ computer code. The cross sections in each of the energy intervals were averaged for PuO₂ product fuel with the gamma photon flux spectrum given in reference (1).

Table 2-XIII gives the calculated gamma photon surface flux as a function of energy and power, at the capsule radial midplane for fresh fuel. The fluxes are calculated for the decay of the plutonium isotopes and daughters, and fission but exclude ²³⁶Pu. The calculated values of $k_{\text{effective}}$ are noted as 0.17, 0.30 and 0.40 for the 1575, 3468 and 5679 w(th) capsules. Table 2-XIV presents similar photon flux data for the ¹⁸O(α , n)²¹Ne reaction as the photon source. Tables 2-XV through 2-XVII give similar photon flux data as a function of fuel age for ²³⁶Pu and daughters as the photon source, for the 1575, 3468 and 5679 w(th) capsules, respectively.

Tables 2-XVIII through 2-XXII give the calculated total photon fluxes at axial and radial detector positions at and beyond the capsule surface, i.e., at cylindrical coordinates (r, θ , z) as defined in Figure 2-III. The data in these tables corresponds to the total fluxes given in Tables 2-XIII through 2-XVII at (r, θ , z) = (capsule radial surface, 0, 0). The total fluxes given in Tables 2-XVIII through 2-XXII, integrated over all sources, are shown graphically in Figures 2-IV through 2-IX as a function of detector distance r, with fuel age as the parameter. Figures 2-IV through 2-VI are for the radial midplane while Figures 2-VII through 2-IX are for the axial midplane.

Figure 2-X gives the source-integrated total photon flux as a function of capsule power for r = 100 cm and 1, 5 and 18 year old fuel. The curves demonstrate the ease with which data may be interpolated for other than the tabulated dependent variables. A further example is given in Figure 2-XI

where the total photon flux is plotted as a function of fuel age for the three model capsules.

The calculations presented above allow the prediction of the gamma photon flux as a function of the following variables:

- I fuel impurities such as ^{236}Pu and ^{18}O ,
- II fuel capsule power, and
- III fuel age.

If the ^{18}O impurity is reduced from 100% to 10% as in the case of ^{18}O depleted oxygen then the $^{18}\text{O}(\alpha, n)^{21}\text{Ne}$ photon flux data may be multiplied by the corresponding appropriate value in the range 1.0 to 0.1. Again since the ^{236}Pu and daughter photon flux data corresponds to a concentration of 1.2 ppm it may be readily corrected for other concentrations. For example, if ^{236}Pu is given as 0.1 ppm then it is only necessary to multiply the " ^{236}Pu fluxes" given in Table XV by the ratio 0.1/1.2 to get the correct photon flux.

An example of the use of the calculated data presented in this report section is given in Appendix F. The example computes the photon flux at $r = 100$ cm for a capsule power of 1575 w(th), a ^{236}Pu impurity of 1.6 ppm, "normal" oxygen, and 5 year old PuO_2 fuel.

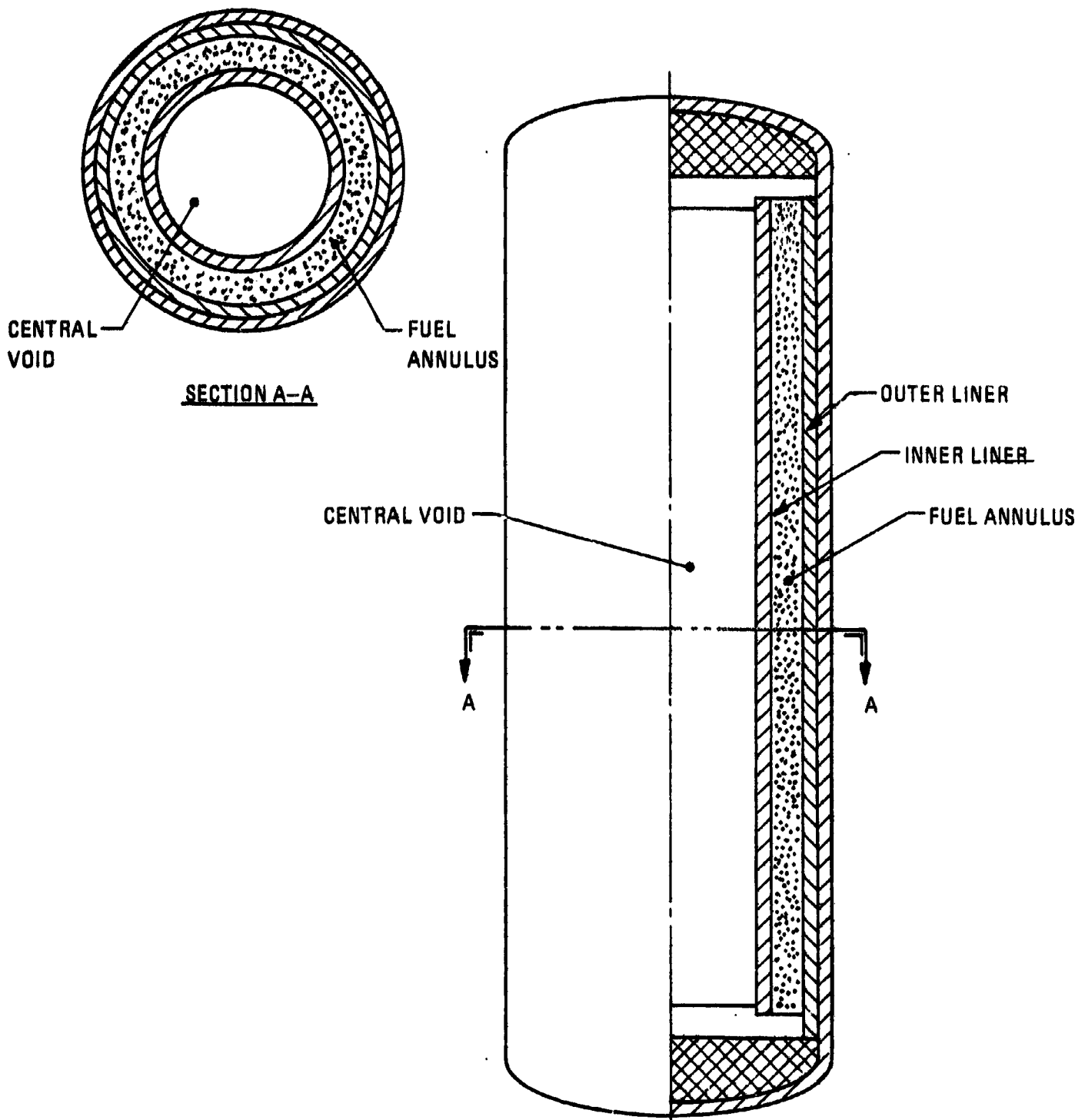
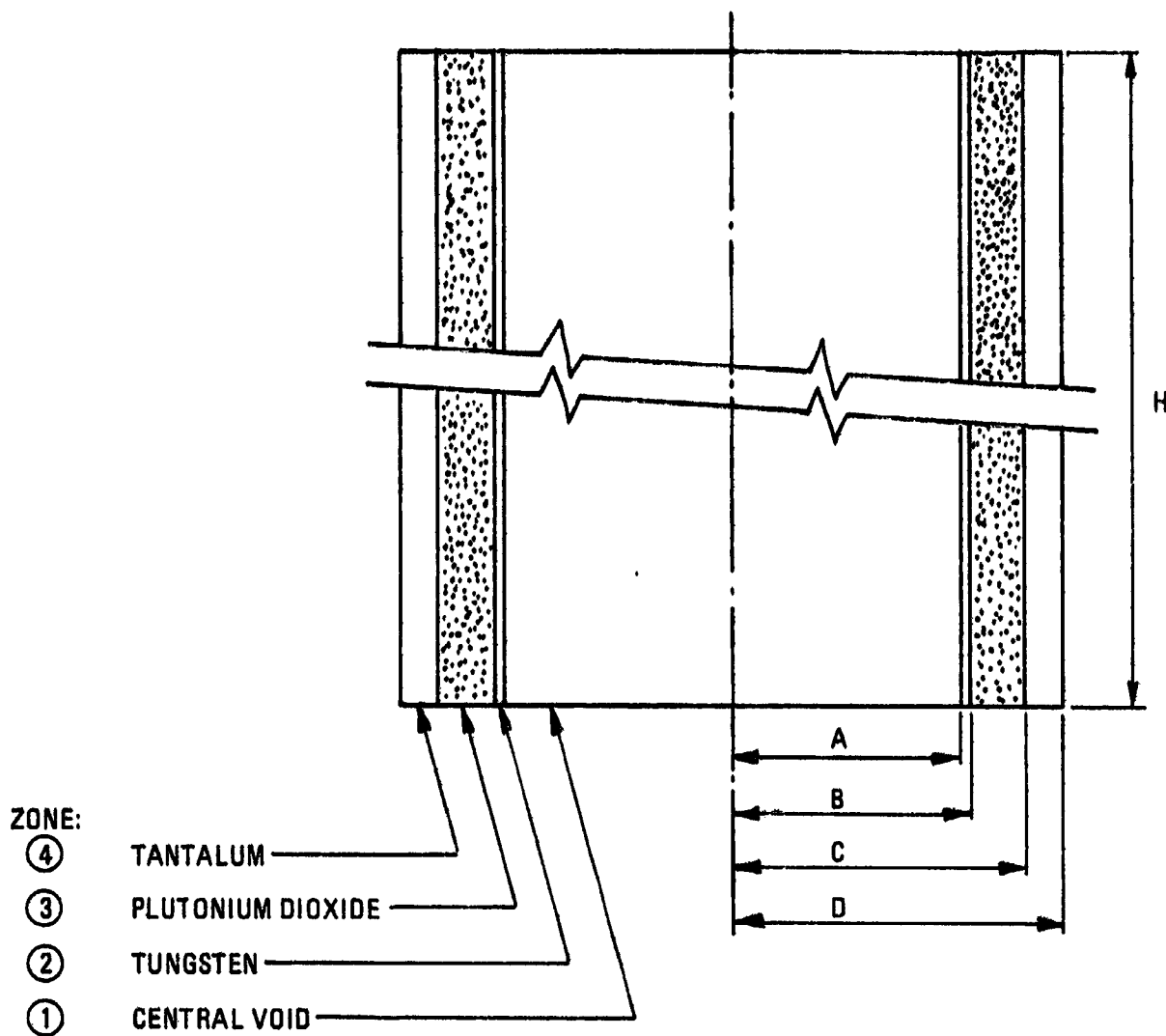


FIGURE 2-1
TYPICAL PLUTONIUM FUELLED RTG CAPSULE



DIMENSION (CM)	<u>CAPSULE POWER OUTPUT</u>		
	1575	3468	5679
A	3.234	3.234	3.234
B	3.285	3.285	3.285
C	4.023	4.761	5.499
D	4.519	5.257	5.995
H	32.188	32.188	32.188

FIGURE 2-II
GEOMETRY OF MODEL FUEL CAPSULE

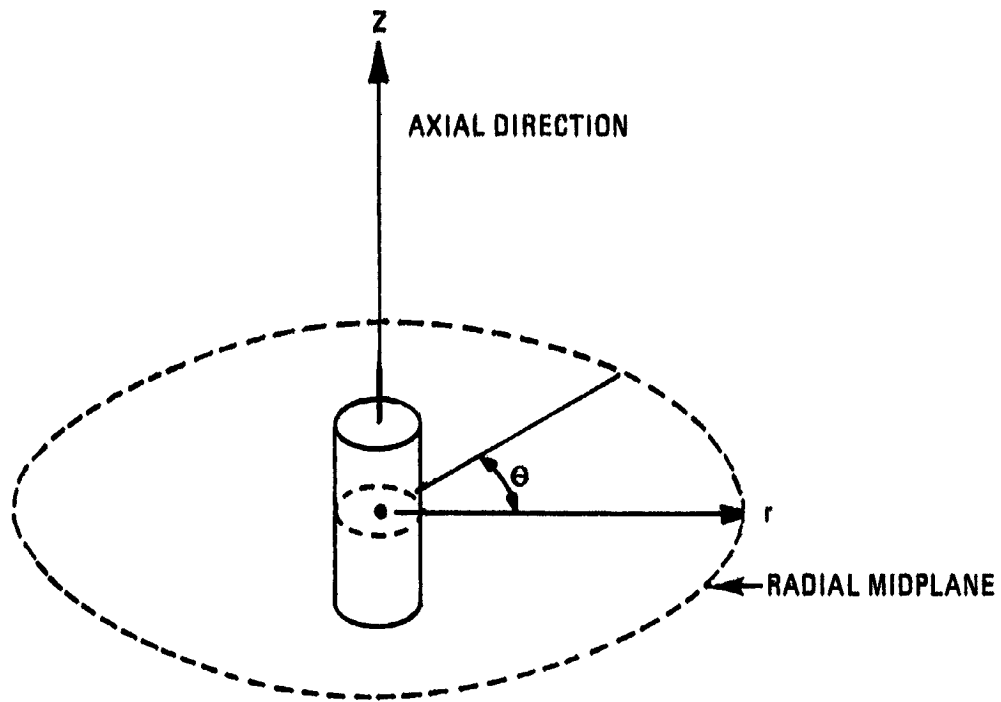


FIGURE 2-III
RTG COORDINATE SYSTEM

FIGURE 2-IV
 GAMMA PHOTON FLUX AS A FUNCTION OF DETECTOR RADIAL
 DISTANCE FROM 1575 w(th) CAPSULE AXIS WITH FUEL AGE AS THE PARAMETER

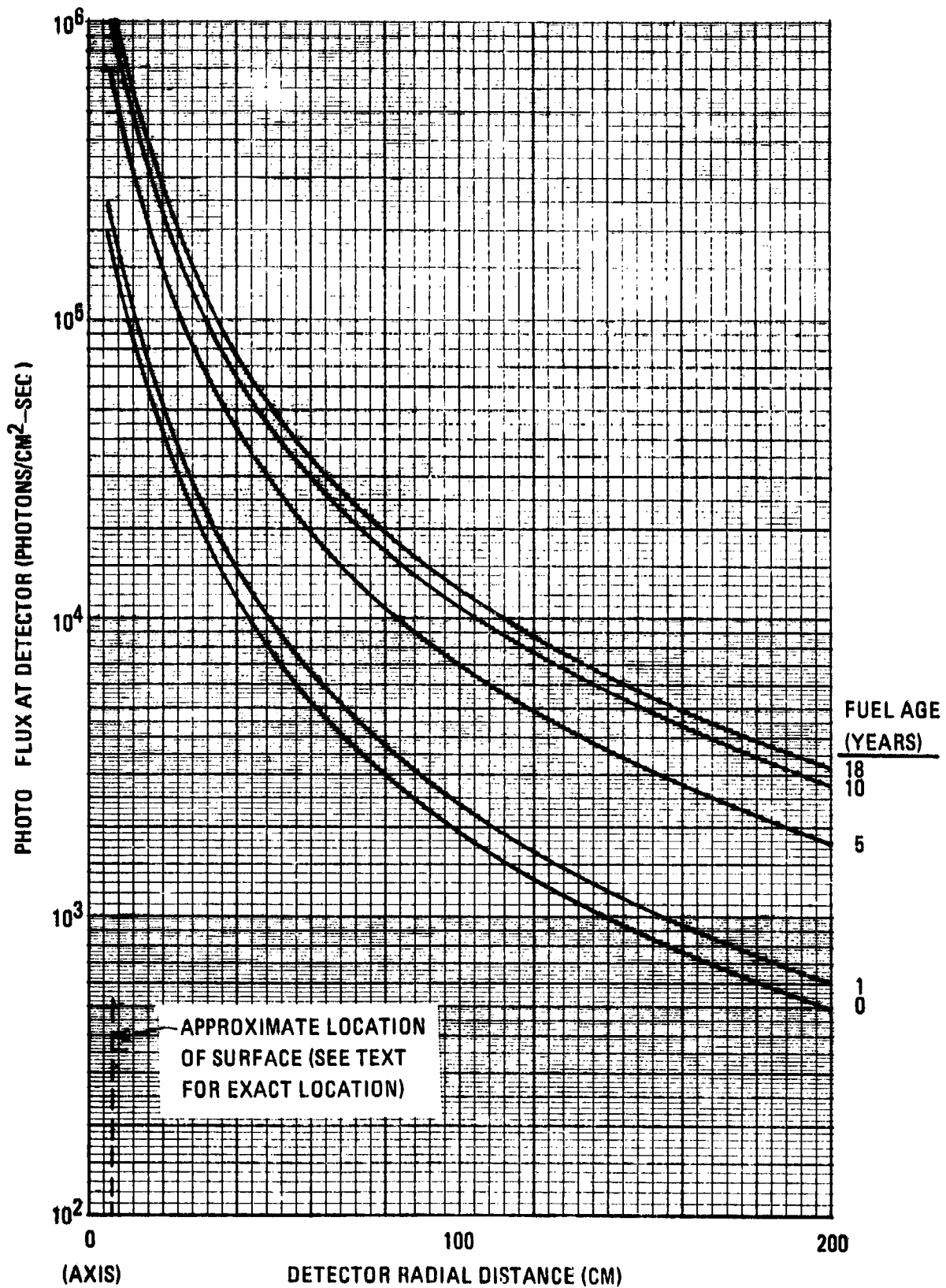


FIGURE 2-V
 GAMMA PHOTON FLUX AS A FUNCTION OF DETECTOR RADIAL
 DISTANCE FROM 3468 w(1b) CAPSULE AXIS WITH POWER AS THE PARAMETER

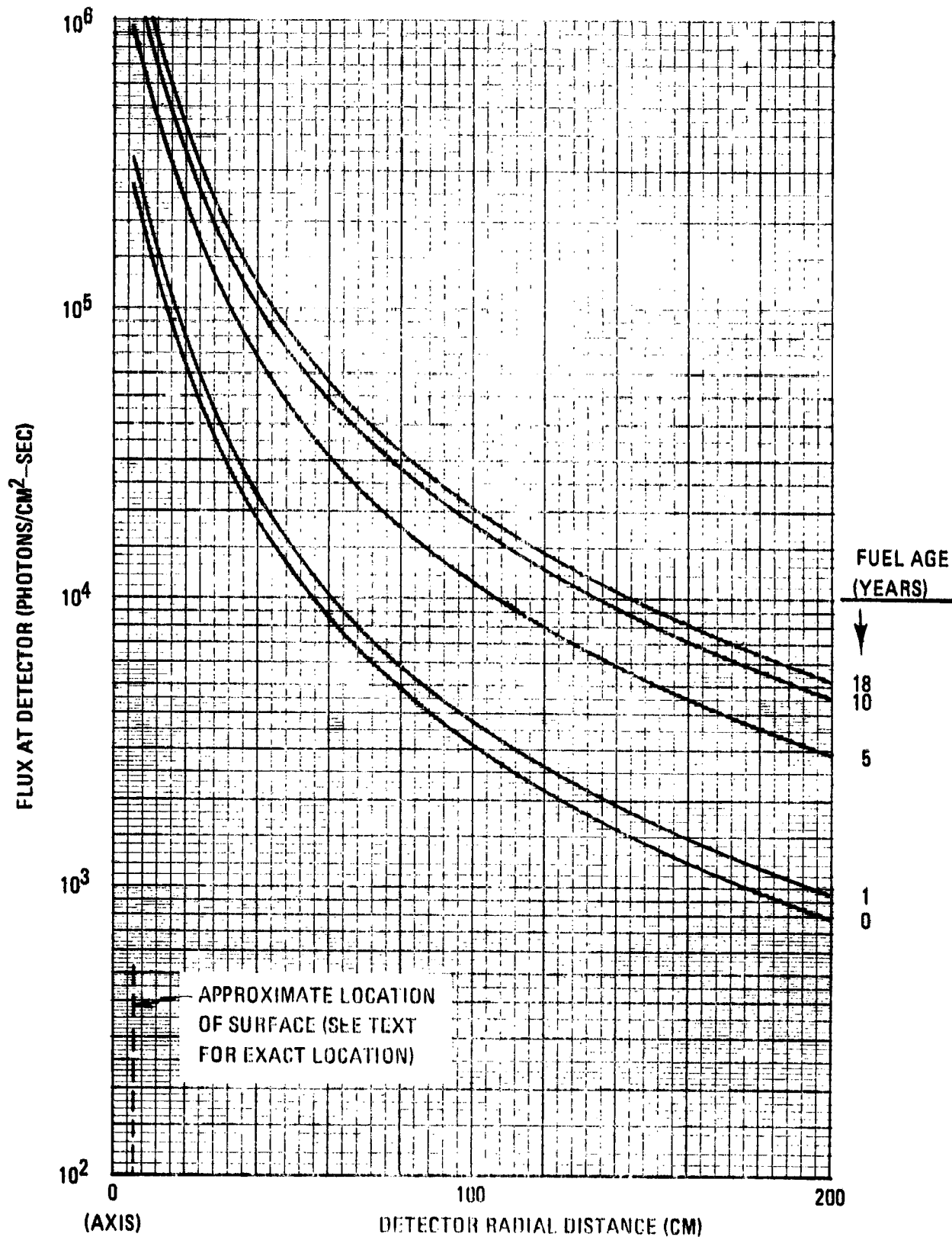


FIGURE 2- VI
 GAMMA PHOTON FLUX AS A FUNCTION OF DETECTOR RADIAL
 DISTANCE FROM 5679 w(th) CAPSULE AXIS WITH FUEL AGE AS THE PARAMETER

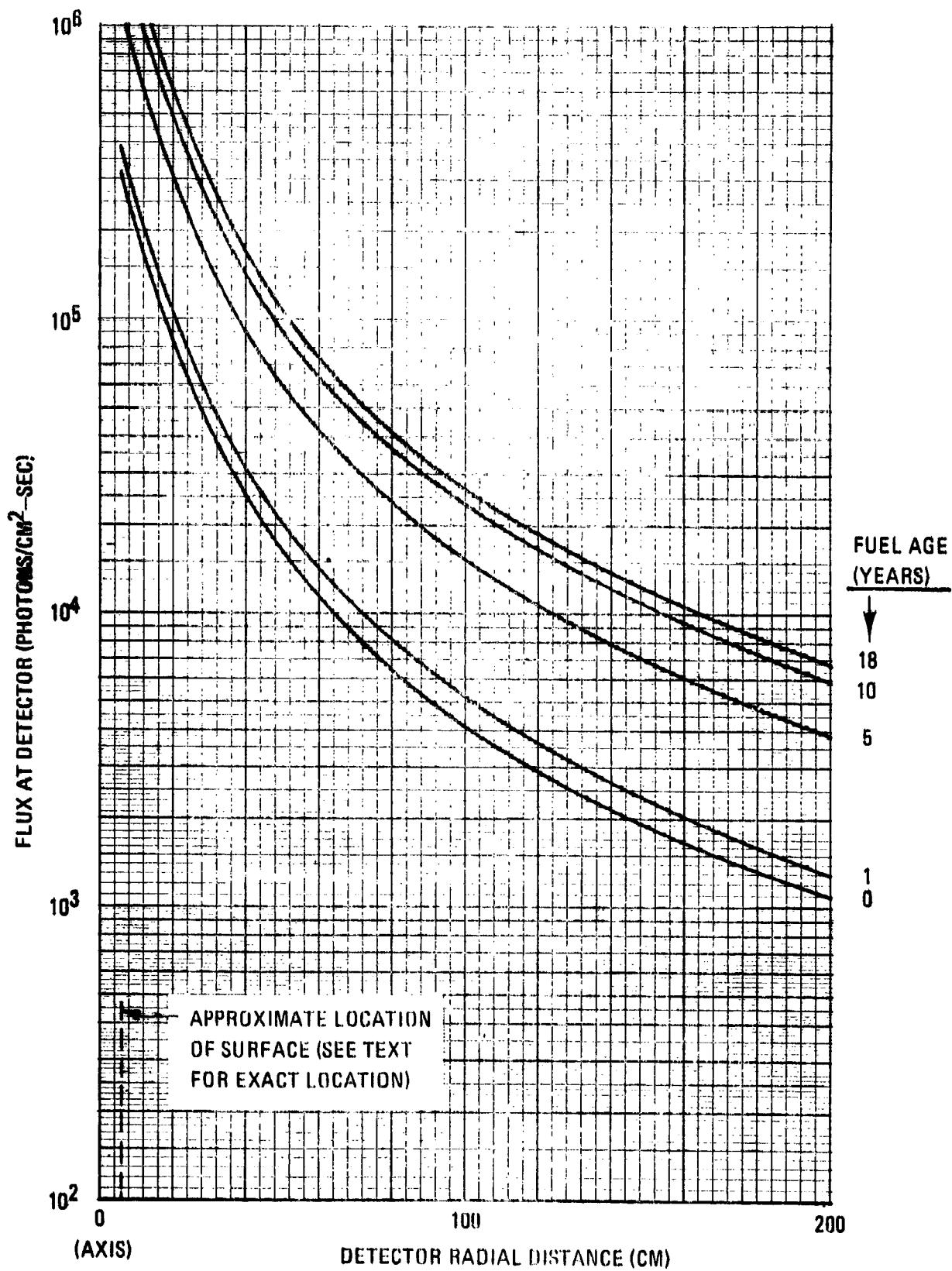


FIGURE 2-VII
 GAMMA PHOTON FLUX AS A FUNCTION OF DETECTOR AXIAL
 DISTANCE FROM 1575 w(t₀) CAPSULE MIDPLANE
 WITH FUEL AGE AS THE PARAMETER

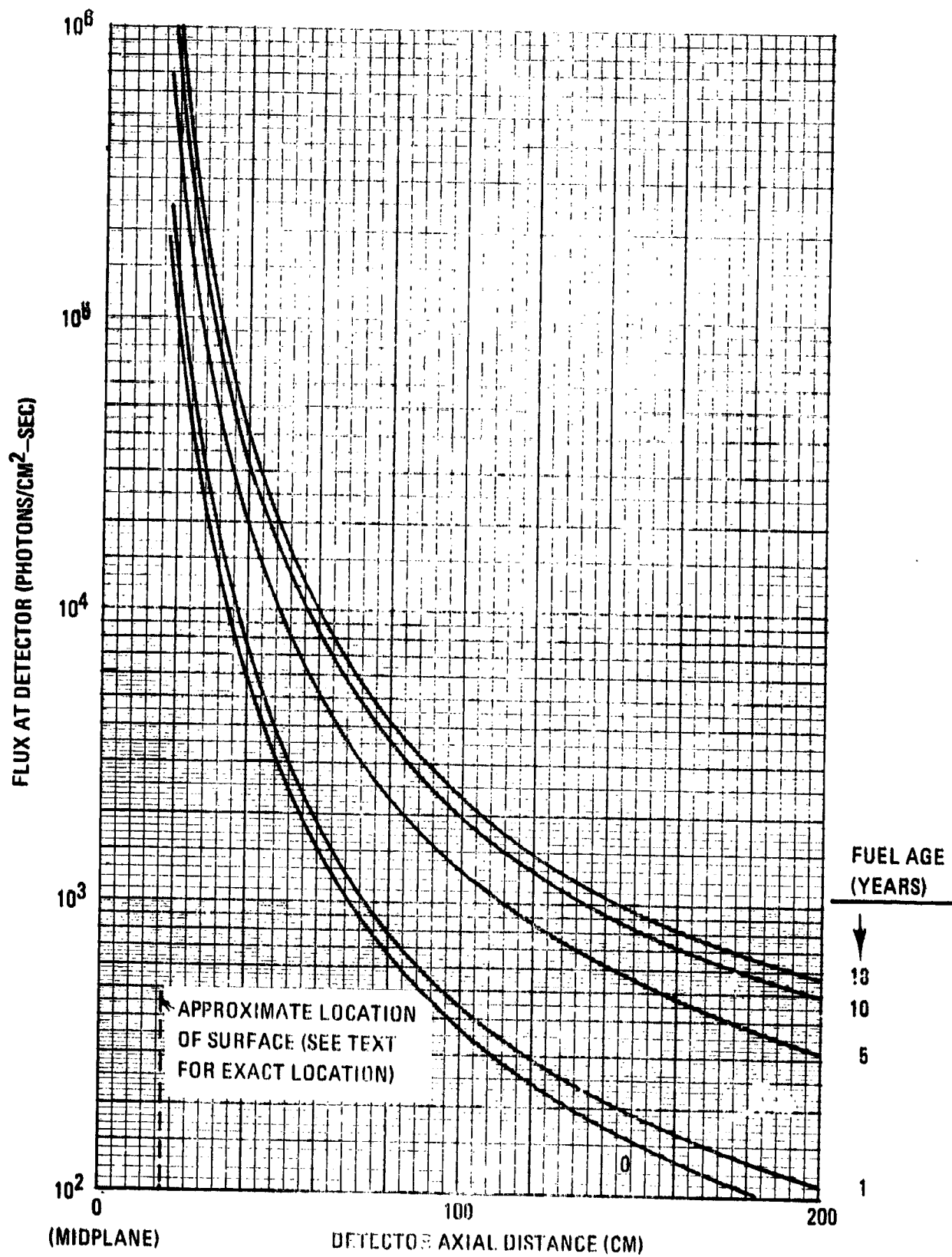


FIGURE 2-VIII
 GAMMA PHOTON FLUX AS A FUNCTION OF DETECTOR AXIAL
 DISTANCE FROM 3488 w(1b) CAPSULE MIDPLANE
 WITH FUEL AGE AS THE PARAMETER

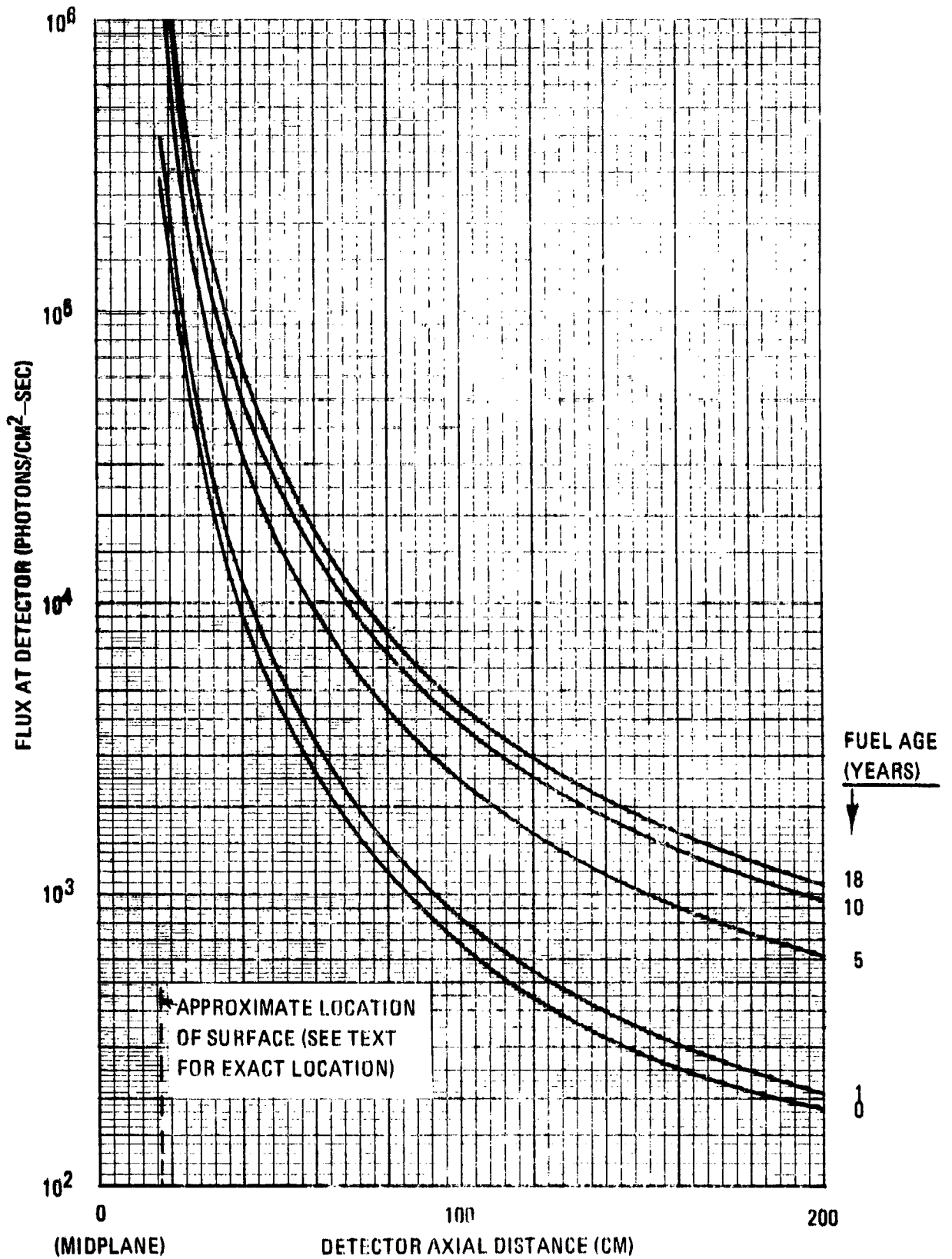


FIGURE 2-IX
 GAMMA PHOTON FLUX AS A FUNCTION OF DETECTOR AXIAL
 DISTANCE FROM 5679 w(th) CAPSULE MIDPLANE
 WITH FUEL AGE AS THE PARAMETER

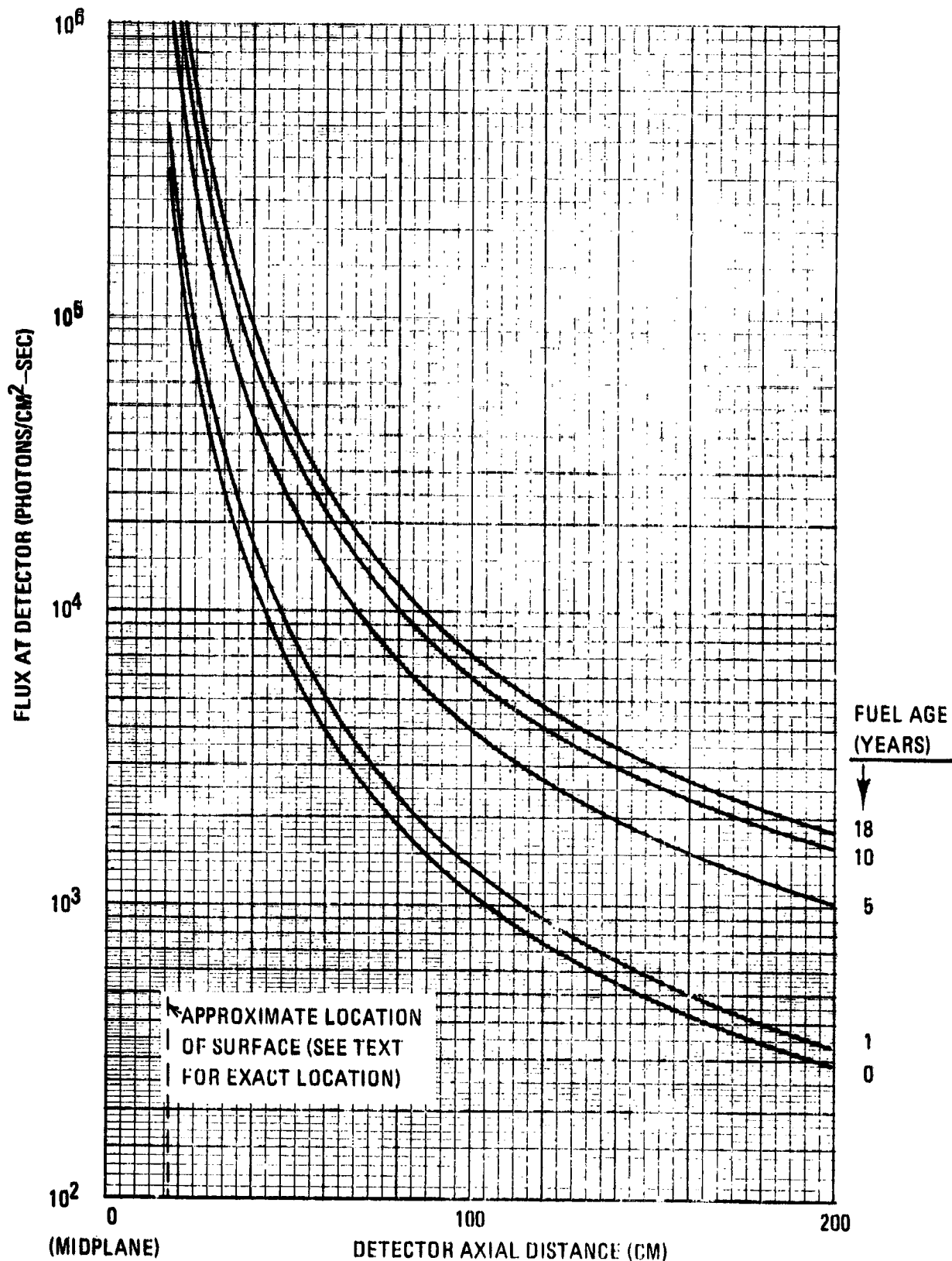


FIGURE 2-X
 GAMMA PHOTON RADIAL AND AXIAL ONE-METER PHOTON
 FLUX AS A FUNCTION OF CAPSULE POWER WITH
 FUEL AGE AS THE PARAMETER

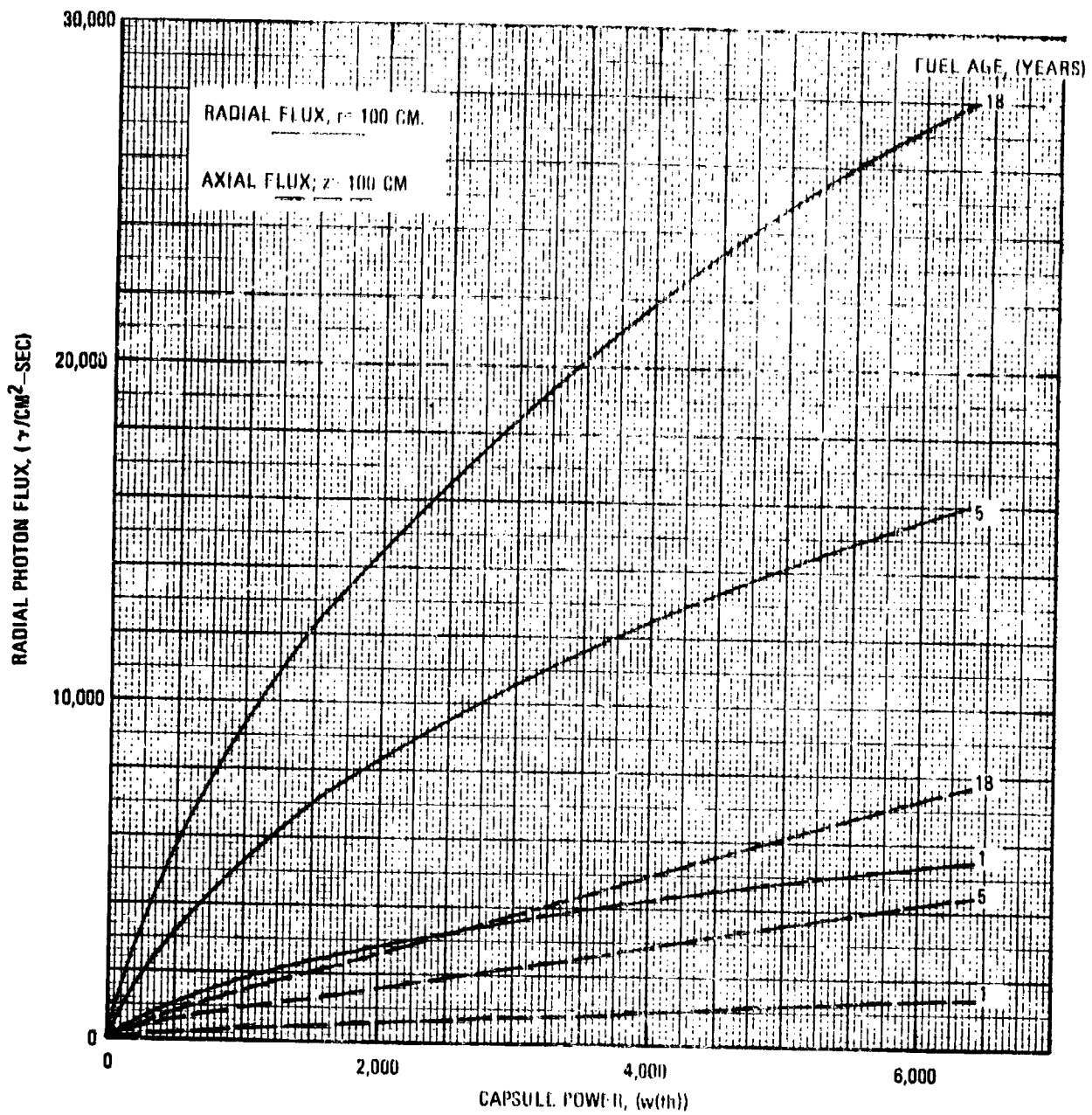


FIGURE 2-XI
ONE-METER GAMMA PHOTON RADIAL PHOTON FLUX
AS A FUNCTION OF FUEL AGE WITH CAPSULE POWER AS THE PARAMETER

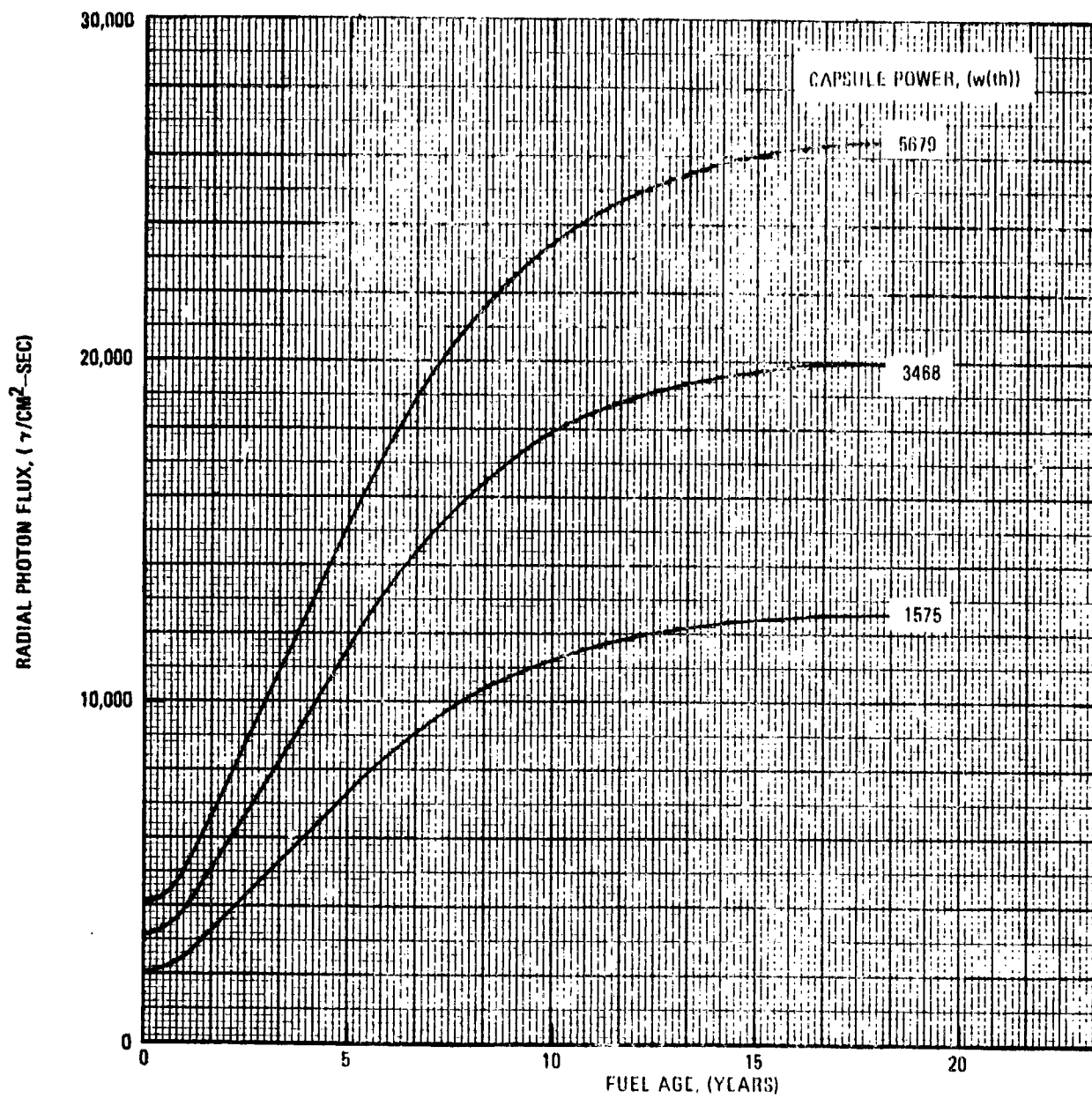


TABLE 2-1

NATURAL NUCLEAR PROPERTIES OF PLUTONIUM ISOTOPES

Isotope	Activity of Pure Isotope (dis/sec-gm)	Spontaneous Fission Half Life (years)	Fission Neutrons For Pure Isotope (n/fission)	Radio Active Half Life of Pure Isotope (years)
^{238}Pu	6.21×10^{11}	$4.9 \times 10^{10}(1,4,5)$	$2.33 \pm 0.08^{(1)}$ spontaneous	89.6 (1)
	6.63×10^{11}		$2.75 \pm 0.0118\text{E}^{(6)}$	87.4 (7)
	6.44×10^{11}		2.93 (8)	86.4 (9)
^{239}Pu	$2.27 \pm 0.04 \times 10^9$	$5.5 \times 10^{15}(1,9)$	$2.90 \pm 0.04^{(1,9,10)}$ induced	$2.44 \pm .05 \times 10^4(1,3)$
^{240}Pu	$8.36 \pm .13 \times 10^9$	$1.2 \times 10^{11}(1,11)$	$2.257 \pm 0.046^{(1,11)}$ spontaneous	$6.6 \pm .1 \times 10^3(1)$
	8.38×10^9	$1.45 \times 10^{11}(9)$		$6.58 \times 10^3(9)$
^{241}Pu	$4.24 \pm .10 \times 10^{12}$			$12.95 \pm 0.28^{(1)}$
	3.92×10^{12}			14.0 (7)
	4.16×10^{12}			13.2 (9)
^{242}Pu	$1.47 \pm .02 \times 10^8$	$8.5 \times 10^{10}(1)$	$2.18 \pm 0.09^{(1)}$ spontaneous	$3.73 \pm .05 \times 10^5(1)$
^{236}Pu	1.97×10^{13}	$3.5 \times 10^9(1,9)$	$2.30 \pm 1.9^{(1)}$	$2.85 \pm .008(1,9)$

TABLE 2-II
GAMMA PHOTONS FROM DECAY OF PLUTONIUM ISOTOPES
AND THEIR DECAY PRODUCTS

Isotope	Gamma Photon Energy (keV)	Abundance (% of Isotopic Decay)		
		Ref. (9)	Ref. (1)	Ref. (14)
^{238}Pu	17.0	13.0 (3)		
	43.6	3.8×10^{-2}	3.8×10^{-2}	
	99.6	8.0×10^{-3}	8.0×10^{-3}	7.4×10^{-3}
	152.5	10^{-3}	1.1×10^{-3}	6.3×10^{-4}
	207.8	4.0×10^{-6}	4.0×10^{-6}	1.2×10^{-5}
	742.4	9.0×10^{-6}		4.5×10^{-6}
	765.8	3.5×10^{-5}	5.0×10^{-5}	2.0×10^{-5}
	785.8	6.0×10^{-6}		2.8×10^{-6}
	807.6	6.0×10^{-5}	very small	6.0×10^{-7}
	851.3			1.2×10^{-6}
	875.0		2.0×10^{-5}	
	882.9			7.4×10^{-7}
	926.1			5.0×10^{-7}
	941.8			6.0×10^{-7}
	1091.1			3.5×10^{-7}
	1641.8			2.0×10^{-7}
1685.1		3.1×10^{-6}	1.0×10^{-7}	
^{239}Pu	17.0			$9.5 \times 10^{-2(10)}$
	38.5	7.0×10^{-3}	2.0×10^{-3}	
	41.5	2.0×10^{-2}	7.0×10^{-3}	7.0×10^{-3}
	129.6 (9) (121.0)(1)	5.0×10^{-3}	1.5×10^{-3}	
	207.0		4.4×10^{-4}	
	340.0		6.6×10^{-4}	
	375.0	1.2×10^{-3}	1.5×10^{-3}	
	414.0	1.2×10^{-3}	3.8×10^{-4}	
	650.0	8.0×10^{-5}		
	770.0	2.0×10^{-5}		
^{240}Pu	17.0			
	45.3			
	650.0	2×10^{-5}		
^{241}Pu	109.0		10^{-3}	
	145.0	1.5×10^{-4}	2.0×10^{-4}	$1.21 \times 10^{-4(12)}$
^{241}Am	66.0	36.0		
	101.0	4.0×10^{-2}		
	208.0	6×10^{-4}		
	335.0	8×10^{-4}		
	370.0	4×10^{-4}		
	663.0	5×10^{-4}		
	772.0	3×10^{-4}		
	^{237}Np	30.0	14.0	
86.0		14.0		
145.0		1.0		
^{237}U	14.0	41.0		
	33.2	16.0		
	60.0	36.0		
	298.0	23.0		

The gamma photon spectrum emitted by ^{238}Pu , ^{239}Pu , and ^{241}Pu was calculated as the abundance multiplied by the activity of the isotope at the equilibrium time considered. The activity of daughter nuclides ^{241}Am , ^{237}Np , and ^{237}U is calculated in Appendix D.

TABLE 2-III
GAMMA PHOTONS EMITTED FROM
EQUILIBRIUM FISSION

<u>Gamma. Photon Energy (MeV)</u>	<u>Number of Photons/Fission</u> ⁽¹⁵⁾	<u>Calculated Photons/Fission*</u>
0.1-0.4	1.61	1.61
0.4-0.9	4.84	4.86
0.9-1.35	0.50	0.50
1.35-1.80	0.60	0.61
1.80-2.20	0.31	0.28
2.20-2.60	0.12	0.11
2.60-3.00	0.01	0.04

* The photon yield per fission was calculated using analytic functions fitted to the above tabulated values of photon yield per fission. The functions used were:

<u>Gamma Ray Energy (MeV)</u>	<u>Function N(E) = (photons/fission)</u>
.1-.4	21.5E
.4-.65	5.77e ^E
.65-.9	22.60e ^{-1.1E}
.9-.965	-121.5E + 117.75
.965-1.35	0.38e ^{0.30E}
1.35-1.60	0.00045e ^{5.3E}
1.60-1.80	586.8e ^{-3.5E}
1.80-3.0	67.8e ^{-2.3E}

TABLE 2-IV
 GAMMA PHOTONS FROM ^{236}Pu and DAUGHTER NUCLIDES

Isotope	Gamma Photon Energy (keV)	Abundance (% of Isotope decay)		
		Ref. (1)	Ref. (9)	
^{236}Pu	46.0 ⁽¹⁾ (48.0) ⁽⁹⁾	4.7×10^{-2}	3.1×10^{-2}	
	110.0	1.2×10^{-2}	1.2×10^{-2}	
	165.0	6.6×10^{-4}	6.6×10^{-4}	
	520.0		1.7×10^{-4}	
	570.0		1.0×10^{-4}	
	645.0		2.4×10^{-4}	
	^{212}Pb	115.1		0.7
176.7			0.2	
238.6		82.0 ⁽³⁾	47.0	
300.1			3.2	
415.2			0.16	
^{212}Bi As a result of β decay (66% yield)		40.0		2.0
	288.0		0.5	
	460.0		0.8	
	727.0	7.3	7.1	
	785.0		1.1	
	893.0	6.6	0.42	
	953.0	0.2	0.10	
	1074.0 } 1079.0 }	0.66	0.60	
	1513.0	0.86	0.31	
	1800.0 } 1809.0 }	small	0.11	
	1620.0		1.8	
	^{212}Bi As a result of α decay (34% yield)	288.2		0.28
		328.0		0.110
434.0 } 453.0 } 473.0 } 493.0 }			0.42	
^{208}Tl		280.0	10.0	
		511.0	25.0	23.0
		583.0	80.0	86.0
	860.0	15.0	12.0	
	2614.0	100.0	100.0	

The gamma activity of ^{236}Pu was calculated as discussed in Appendix C.
 The radioactive decay chains and corresponding daughter nuclide activity are
 calculated in Appendix D.

*From reference (3)

TABLE 2-V
 GAMMA PHOTONS DUE TO $^{18}\text{O}(\alpha, n)^{21}\text{Ne}$ REACTION

<u>Gamma Photon Energy*</u> (MeV)	<u>Photons/gm-sec PuO₂</u>
0.35	4×10^3
1.38	8.9×10^2
1.90	1.8×10^2
2.40	1.8×10^2
2.70	1.8×10^2

*Although references (10) and (11) suggest 0.35, 1.38, 1.75 and 2.87 gamma photons, it is felt that the 1.75 MeV and 2.87 gamma rays contained the above as unresolved resonances.

The photons emitted per neutron emission, neutron emission rates and other pertinent data are presented and calculated in Appendix B.

TABLE 2-VI (a)

GAMMA PHOTON ACTIVITY AT TIME ZERO ($T = 0$)
(Photon/sec-gm PuO₂)

Energy Interval (MeV)	Decay of Isotopes and Daughters							Fission*	Total				
	238Pu (81%)	239Pu (15%)	240Pu (2.9%)	241Pu (0.8%)	241Am	237U	236Pu (1.2ppm)			212Pb	212Bi	208Tl	
6.0-7.0											5.0		
5.0-6.0											14.		
4.0-5.0											45		
3.0-4.0											147.		1.47 x 10 ²
2.0-3.0											580	360	9.4 x 10 ²
1.8-2.0											264	180	4.44 x 10 ²
1.6-1.8											400		4.0 x 10 ²
1.4-1.6											408		4.08 x 10 ²
1.2-1.4											356	890	1.25 x 10 ³
1.0-1.2	1.36 x 10 ³										415		1.78 x 10 ³
0.9-1.0	8.12 x 10 ³										433		6.56 x 10 ³
0.8-0.9	1.25 x 10 ⁴										900		1.34 x 10 ⁴
0.7-0.8	1.24 x 10 ⁵										1.004 x 10 ³		1.24 x 10 ⁵
0.6-0.7		3.0 x 10 ²		43.							50.		1.59 x 10 ³
0.5-0.6											56.2		1.30 x 10 ³
0.4-0.5		2.65 x 10 ³											3.97 x 10 ³
0.3-0.4		5.92 x 10 ³											1.13 x 10 ⁴
0.2-0.3	5.45 x 10 ⁴	1.33 x 10 ³											5.62 x 10 ⁴
.044-2	2.17 x 10 ⁸	3.63 x 10 ⁴											2.17 x 10 ⁸
.001-.044	5.91 x 10 ¹⁰	3.06 x 10 ⁵											5.91 x 10 ¹⁰
													0.0

* Includes prompt and fission product gamma photons.

TABLE 2-VI (b)

GAMMA PHOTON ACTIVITY AT TIME ZERO ($T = 0$)
(Photons/sec-gm PuO_2)

Energy Interval	Decay of Isotopes	^{236}Pu 1.2ppm	$^{18}\text{O}(\alpha, n)^{21}\text{Ne}$	Total
6.0-7.0	5			5
5.0-6.0	14			14
4.0-5.0	45			45
3.0-4.0	147			147
2.0-3.0	580		360.	940
1.8-2.0	264		180	444
1.6-1.8	400			400
1.4-1.6	408			408
1.2-1.4	356		890	1.25×10^3
1.0-1.2	1.78×10^3			1.78×10^3
0.9-1.0	8.56×10^3			8.56×10^3
0.8-0.9	1.34×10^4			1.34×10^4
0.7-0.8	1.24×10^5			1.24×10^5
0.6-0.7	1.54×10^3	50.		1.59×10^3
0.5-0.6	1.25×10^3	56.2		1.30×10^3
0.4-0.5	3.97×10^3			3.97×10^3
0.3-0.4	7.31×10^3		4.0×10^3	1.13×10^4
0.2-0.3	5.62×10^4			5.62×10^4
.044-0.2	2.17×10^8	9.1×10^3		2.17×10^8
.001-.044	5.91×10^{10}			5.91×10^{10}

TABLE 2-VII (a)

GAMMA PHOTON ACTIVITY AT TIME ONE YEAR (T=1)
(Photons/sec-gm. PuO₂)

Energy Interval (MeV)	Decay of Isotopes and Daughters								Fission*	¹⁸ O(α,n) ²¹ Ne Total		
	²³⁸ Pu (81%)	²³⁹ Pu (15%)	²⁴⁰ Pu (2.9%)	²⁴¹ Pu (0.8%)	²⁴¹ Am	²³⁷ U	²³⁶ Pu (**)	²¹² Pb			²¹² Po	²¹² Bi
6.0-7.0											5.	5
5.0-6.0											14.	14
4.0-5.0											45.	45
3.0-4.0											146.	146
2.0-3.0											9797.1	357
1.8-2.0											262.	179
1.6-1.8											397.	397
1.4-1.6											405.1	405.1
1.2-1.4											354	1237
1.0-1.2	1.35+3									536.4	412	2298
0.9-1.0	8.06+3									19.	430	8509.
0.8-0.9	1.23+4									80.	1175.7	1.45+4
0.7-0.8	1.23+5								129.	1.55+3	997	1.26+5
0.6-0.7		300.		43.					214.		1184	1780.2
0.5-0.6											1.07+4	1.20+4
0.4-0.5		2.65+3						46.1		192.3	1311	4200.4
0.3-0.4		5.92+3							514.	16.8	1378	1.18+4
0.2-0.3	5.41+4	1.33+3						1.45+4		122.5	379	2.11+5
.044-0.2	2.15+8	3.63+4						259.3			228	2.30+8
.001-.044	5.86+10	3.06+5									0.0	5.86+10

* Includes prompt and fission product gamma photons.

** 1.2 ppm

TABLE 2-VII (b)

GAMMA PHOTON ACTIVITY AT TIME ONE YEAR (T=1)
(Photons/sec-gm PuO₂)

Energy Interval	Decay of Isotopes	²³⁶ Pu 1.2ppm	¹⁸ O(α, n) ²¹ Ne	Total
6.0-7.0	5			5
5.0-6.0	14			14
4.0-5.0	45			45
3.0-4.0	146			146
2.0-3.0	576	9.8 x 10 ³	357	1.07 x 10 ⁴
1.8-2.0	262		179	441
1.6-1.8	379			397
1.4-1.6	405			405
1.2-1.4	354		883	1237
1.0-1.2	1762	536.4		2.30 x 10 ³
0.9-1.0	8.49 x 10 ³	19.		8.49 x 10 ³
0.8-0.9	1.32 x 10 ⁴	1255.7		1.446 x 10 ⁴
0.7-0.8	1.24 x 10 ⁵	1.56 x 10 ³		1.26 x 10 ⁵
0.6-0.7	1741	39.2		1780.2
0.5-0.6	1239	1.07 x 10 ⁴		1.20 x 10 ⁴
0.4-0.5	3961	239.4		4200
0.3-0.4	7812.	10.8	3.97 x 10 ³	1.18 x 10 ⁴
0.2-0.3	1.95 x 10 ⁵	1.56 x 10 ⁴		2.11 x 10 ⁵
.044-.2	2.30 x 10 ⁸	7392.3		2.30 x 10 ⁸
.001-.044	5.86 x 10 ¹⁰	380.4		5.86 x 10 ¹⁰

TABLE 2-VIII (a)

GAMMA PHOTON ACTIVITY AT TIME FIVE YEARS (T = 5)
(Photons. sec-gm PuO₂)

Energy Interval (MeV)	Decay of Isotopes and Directors										Fission*	18O(α,n) ²¹ Ne	Total
	238Pu (81%)	239Pu (15%)	240Pu (2.9%)	241Pu (0.8%)	241Am	237U	236Pu (**)	212Pb	212Bi	208Tl			
6.0-7.0											5.		5
5.0-6.0											14.		14
4.0-5.0											44.		44
3.0-4.0											142.		142
2.0-3.0										1.15+5	561.	346	1.15+5
1.8-2.0											255.	173	428
1.6-1.8											387.		387
1.4-1.6											395.		395
1.2-1.4											344.	856	1.20+3
1.0-1.2	1.31+3									6.3+3	401.		8.11+3
0.9-1.0	7.81+3									223	419.		8.45+3
0.8-0.9	1.20+4									938	870.	1.32+4	2.76+4
0.7-0.8	1.19+5			581.						1.93+4	971.		1.39+5
0.6-0.7		300.	43.	969.		14.8					1.15+3		2.48+3
0.5-0.6						16.7					1.21+3		1.26+5
0.4-0.5		2.65+3								541.	1.28+3		6.75+3
0.3-0.4		5.92+3								127	1.34+3		1.36+4
0.2-0.3	5.24+4	1.33+3								1.70+5	369.		3.52+5
.044-.2	2.09+8	3.63+4		3.45+4	6.98+7	1.79+5	2693	3045.			222.		2.75+8
.001-.044	5.69+10	3.06+5				2.83+5				4.47-3	0.0		5.69+10

* Includes prompt and fission product gamma photons.

** 1.2 ppm

TABLE 2-VIII (b)

GAMMA PHOTON ACTIVITY AT TIME FIVE YEARS (T = 5)
 (Photons/sec-gm PuO₂)

Energy Interval	Decay of Isotopes	²³⁶ Pu 1.2ppm	¹⁸ O(α, n) ²¹ Ne	Total
6.0-7.0	5			5
5.0-6.0	14			14
4.0-5.0	44			44
3.0-4.0	142			142
2.0-3.0	561	1.15 x 10 ⁵	346	1.16 x 10 ⁵
1.8-2.0	255		173	428
1.6-1.8	387			387
1.4-1.6	395			395
1.2-1.4	344		856	1.20 x 10 ³
1.0-1.2	1.71 x 10 ³	6.30 x 10 ³		8.01 x 10 ³
0.9-1.0	8.23 x 10 ³	223		8.45 x 10 ³
0.8-0.9	1.29 x 10 ⁴	1.48 x 10 ⁴		2.77 x 10 ⁴
0.7-0.8	1.21 x 10 ⁵	1.83 x 10 ⁴		1.39 x 10 ⁵
0.6-0.7	2.47 x 10 ³	14.8		2.48 x 10 ³
0.5-0.6	1.207 x 10 ³	1.25 x 10 ⁵		1.26 x 10 ⁵
0.4-0.5	3.93 x 10 ³	2.81 x 10 ³		6.74 x 10 ³
0.3-0.4	9.59 x 10 ³	127	3.85 x 10 ³	1.36 x 10 ⁴
0.2-0.3	1.69 x 10 ⁵	1.83 x 10 ⁵		3.52 x 10 ⁵
.044-.2	2.79 x 10 ⁸	5738		2.79 x 10 ⁸
.001-.044	5.69 x 10 ¹⁰	443		5.69 x 10 ¹⁰

TABLE 2-R (a)

GAMMA PHOTON ACTIVITY AT TIME TEN YEARS (T = 10)
(Photons/sec-gm PuO₂)

Energy Interval (MeV)	Decay of Isotopes and Daughters										Fission*	18O(α,n)21Ne	Total
	238Pu (81%)	239Pu (15%)	240Pu (2.9%)	241Pu (0.8%)	241Am	237U	236Pu (**)	212Pb	212Bi	208Tl			
6.0-7.0											5		5
5.0-6.0											13		13
4.0-5.0											44		44
3.0-4.0											138		138
2.0-3.0									2.04+5		543	333	2.05+5
1.8-2.0											247	167	414
1.6-1.8											375		375
1.4-1.6											382		382
1.2-1.4											334	824	1158
1.0-1.2	1.26+3							1.11+4			389		1.28+4
0.9-1.0	7.52+3							400			406		8.33+3
0.8-0.9	1.15+4							1.66+3	2.44+4		843		3.84+4
0.7-0.8	1.15+5						1039	3.24+4			941		1.50+5
0.6-0.7		3.0+2	43.			4.4	1732				1117		3.20+3
0.5-0.6						4.9			2.22+5		1170		2.23-5
0.4-0.5		2.65+3						957.	4.01+3		1237		8.86+3
0.3-0.4		5.92+3					4158	224			1301	3.7+3	1.53+4
0.2-0.3	5.05+4	1.33+3			.89+5		2079	3.0+5	2.57+3	2.04+4	358		4.66+5
.044-.2	2.01+8	3.63+4		2.70+4	1.40+5	792		5387.			216		3.26+8
.001-.044	5.47+10	3.06+5			2.21+5				7.9+3		0.0		5.47+10

* Includes prompt and fission product gamma photons.

** 1.2 ppm

TABLE 2-IX (b)

GAMMA PHOTON ACTIVITY AT TIME TEN YEARS (T = 10)
(Photons/sec-gm PuO₂)

Energy Interval	Decay of Isotopes	²³⁶ Pu 1.2ppm	¹⁸ O(α, n) ²¹ Ne	Total
6.0-7.0	5			5
5.0-6.0	13			13
4.0-5.0	44			44
3.0-4.0	138			138
2.0-3.0	543	2.04 x 10 ⁵	333	2.05 x 10 ⁵
1.8-2.0	247		167	414
1.6-1.8	375			375
1.4-1.6	382			382
1.2-1.4	334		824	1.16 x 10 ³
1.0-1.2	1.65 x 10 ³	1.113 x 10 ⁴		1.28 x 10 ⁴
0.9-1.0	7.93 x 10 ³	400		8.33 x 10 ³
0.8-0.9	1.24 x 10 ⁴	2.61 x 10 ⁴		3.85 x 10 ⁴
0.7-0.8	1.17 x 10 ⁵	3.24 x 10 ⁴		1.50 x 10 ⁵
0.6-0.7	3.20 x 10 ³	4.4		3.20 x 10 ³
0.5-0.6	1.17 x 10 ³	2.22 x 10 ⁵		2.23 x 10 ⁵
0.4-0.5	3.89 x 10 ³	4.97 x 10 ³		8.86 x 10 ³
0.3-0.4	1.14 x 10 ⁴	224	3.70 x 10 ³	1.53 x 10 ⁴
0.2-0.3	1.43 x 10 ⁵	3.23 x 10 ⁵		4.66 x 10 ⁵
.044-.2	3.26 x 10 ⁸	6.18 x 10 ³		3.26 x 10 ⁸
.001-.044	5.47 x 10 ¹⁰	7.9 x 10 ³		5.47 x 10 ¹⁰

TABLE 2-X (a)
 GAMMA PHOTON ACTIVITY AT TIME EIGHTEEN YEARS (T = 18)
 (Photons/sec-gm PuO₂)

Energy Interval (MeV)	Decay of Isotopes and Daughters										18O(α,n)21Ne	Total	
	238Pu (81%)	239Pu (15%)	240Pu (2.9%)	241Pu (0.8%)	241Am	237U	235Pu (**)	212Pb	212Bi	208Tl†			Fission*
6.0-7.0											5.	5	
5.0-6.0											13.	13	
4.0-5.0											40.	40	
3.0-4.0											131.	131	
2.0-3.0									2.34+5		519.	272	2.35+5
1.8-2.0											236.	157	393
1.6-1.8											358.		358
1.4-1.6											365.		365
1.2-1.4											316.	774	1.09+3
1.0-1.2	1.19+3								1.29+4		371.		1.44+4
0.9-1.0	7.07+3							455			387.		7.91+3
0.8-0.9	1.08+4							1910	2.81+4		805.		4.15+4
0.7-0.8	1.08+5							3.74+4			898.		1.48+5
0.6-0.7		43.									1066.		3.96+3
0.5-0.6											1116.		2.57+5
0.4-0.5									2.56+5		1180.		9.56+3
0.3-0.4											1241.	3.48+3	1.71+4
0.2-0.3	4.74+4										342.		4.84+5
.044-.2	1.89+8										206.		3.76+8
.001-.044	5.14+10										3.0		5.14+10

* Includes prompt and fission product gamma photons.

** 1.2 ppm

TABLE 2-X (b)

GAMMA PHOTON ACTIVITY AT TIME EIGHTEEN YEARS (T=18)
(Photons/sec-gm PuO₂)

Energy Interval	Decay of Isotopes	²³⁶ Pu 1.2ppm	¹⁸ O(α,n) ²¹ Ne	Total
6.0-7.0	5			5
5.0-6.0	13			13
4.0-5.0	40			40
3.0-4.0	131			131
2.0-3.0	519	2.34 x 10 ⁵	272	2.35 x 10 ⁵
1.8-2.0	236		157	393
1.6-1.8	358			358
1.4-1.6	365			365
1.2-1.4	318		774	1.09 x 10 ³
1.0-1.2	1.56 x 10 ³	1.2826 x 10 ⁴		1.44 x 10 ⁴
0.9-1.0	7.46 x 10 ³	455		7.91 x 10 ³
0.8-0.9	1.16 x 10 ⁴	3.0 x 10 ⁴		4.16 x 10 ⁴
0.7-0.8	1.10 x 10 ⁵	3.73 x 10 ⁴		1.48 x 10 ⁵
0.6-0.7	4.0 x 10 ³	1.0		4 x 10 ³
0.5-0.6	1.12 x 10 ³	2.56 x 10 ⁵		2.57 x 10 ⁵
0.4-0.5	3.83 x 10 ³	5.73 x 10 ³		9.56 x 10 ³
0.3-0.4	1.34 x 10 ⁴	258	3.48 x 10 ³	1.71 x 10 ⁴
0.2-0.3	1.12 x 10 ⁵	3.72 x 10 ⁵		4.84 x 10 ⁵
.044-.2	3.76 x 10 ⁸	7.39 x 10 ³		3.76 x 10 ⁸
.001-.044	5.14 x 10 ¹⁰	9.1 x 10 ³		5.14 x 10 ¹⁰

TABLE 2-XI
 TOTAL PHOTON ACTIVITY AT
 NOTED TIMES (Photons/sec-gm PuO₂)

Energy Interval	TIME (years)					
	0	1	5	10	18	
6.0-7.0	5	5	5	5	5	5
5.0-6.0	14	14	14	13	13	13
4.0-5.0	45	45	44	44	40	40
3.0-4.0	147	146	142	138	131	131
2.0-3.0	940	1.07 x 10 ⁴	1.16 x 10 ⁵	2.05 x 10 ⁵	2.35 x 10 ⁵	2.35 x 10 ⁵
1.8-2.0	444	441	428	414	393	393
1.6-1.8	400	397	387	375	358	358
1.4-1.6	408	405	395	382	365	365
1.2-1.4	1.25 x 10 ³	1.24 x 10 ³	1.20 x 10 ³	1.16 x 10 ³	1.09 x 10 ³	1.09 x 10 ³
1.0-1.2	1.78 x 10 ³	2.30 x 10 ³	8.01 x 10 ³	1.28 x 10 ⁴	1.44 x 10 ⁴	1.44 x 10 ⁴
0.9-1.0	8.56 x 10 ³	8.49 x 10 ³	8.45 x 10 ³	8.33 x 10 ³	7.91 x 10 ³	7.91 x 10 ³
0.8-0.9	1.34 x 10 ⁴	1.446 x 10 ⁴	2.77 x 10 ⁴	3.85 x 10 ⁴	4.16 x 10 ⁴	4.16 x 10 ⁴
0.7-0.8	1.24 x 10 ⁵	1.26 x 10 ⁵	1.39 x 10 ⁵	1.50 x 10 ⁵	1.48 x 10 ⁵	1.48 x 10 ⁵
0.6-0.7	1.59 x 10 ³	1.78 x 10 ³	2.48 x 10 ³	3.20 x 10 ³	4 x 10 ³	4 x 10 ³
0.5-0.6	1.30 x 10 ³	1.20 x 10 ⁴	1.26 x 10 ⁵	2.23 x 10 ⁵	2.57 x 10 ⁵	2.57 x 10 ⁵
0.4-0.5	3.97 x 10 ³	4.20 x 10 ³	6.74 x 10 ³	8.86 x 10 ³	9.56 x 10 ³	9.56 x 10 ³
0.3-0.4	1.13 x 10 ⁴	1.18 x 10 ⁴	1.36 x 10 ⁴	1.53 x 10 ⁴	1.71 x 10 ⁴	1.71 x 10 ⁴
0.2-0.3	5.62 x 10 ⁴	2.11 x 10 ⁵	3.52 x 10 ⁵	4.66 x 10 ⁵	4.84 x 10 ⁵	4.84 x 10 ⁵
.044-.2	2.17 x 10 ⁸	2.30 x 10 ⁸	2.79 x 10 ⁸	3.26 x 10 ⁸	3.76 x 10 ⁸	3.76 x 10 ⁸
.001-.044	5.91 x 10 ¹⁰	5.86 x 10 ¹⁰	5.69 x 10 ¹⁰	5.47 x 10 ¹⁰	5.14 x 10 ¹⁰	5.14 x 10 ¹⁰

TABLE 2-XII
MATERIAL PROPERTIES OF
MODEL FUEL CAPSULE

<u>Zone</u>	<u>Material</u>	<u>Density gm./cm³</u>	<u>Atomic Density* atoms/cm³</u>	<u>Modified Atomic Density**</u>
1	Void	0.0	0.0	
2	Tungsten (W)	19.3	.063190	4.67628
3	Plutonium Fuel (PuO ₂)	7.306***	0.01632	1.79520
	Plutonium (Pu)		0.01632	1.53408
	Oxygen (O)		0.03264	0.26112
4	Tantalum (Ta)	16.6	0.05526	4.03380

* This density corresponds to the P₀ Legendre expansion term in the Klein-Nishina cross sections.

** This density corresponds to the P₁-P₅ Legendre expansion terms in the Klein-Nishina cross sections. The P₁-P₅ Legendre terms of hydrogen were utilized and corrected by the Z (atomic number) of the isotope used in the analysis.

*** The Plutonium Dioxide fuel density, 10.7 gm/cm³, was multiplied by the volume fraction 0.683.

TABLE 2-XIII

GAMMA PHOTON SURFACE FLUX (Photons/cm²-sec)
 AT CAPSULE MIDPLANE FOR FRESH FUELS;
 SOURCE — DECAY OF ISOTOPES AND DAUGHTERS
 (INCLUDES FISSION)

Energy Interval (MeV)	Capsule Power (w(th))		5679 (k _{eff} = 0.41)
	1575 (k _{eff} = 0.17)	3468 (k _{eff} = 0.30)	
6.0-7.0	1.09274E + 01	3.11766E + 01	5.41158E + 01
5.0-6.0	3.19061E + 01	9.15588E + 01	1.58637E + 02
4.0-5.0	1.06562E + 02	3.05956E + 02	5.31846E + 02
3.0-4.0	3.59364E + 02	1.03326E + 03	1.79496E + 03
2.0-3.0	1.38919E + 03	3.96415E + 03	6.85509E + 03
1.8-2.0	6.23476E + 02	1.77177E + 03	3.05964E + 03
1.6-1.8	9.09526E + 02	2.57036E + 03	4.41956E + 03
1.4-1.6	9.56260E + 02	2.70777E + 03	4.65961E + 03
1.2-1.4	8.99081E + 02	2.55789E + 03	4.41351E + 03
1.0-1.2	2.92849E + 03	5.34024E + 03	7.61123E + 03
0.9-1.0	1.03959E + 04	1.44950E + 04	1.69881E + 04
0.8-0.9	1.49095E + 04	2.06496E + 04	2.39657E + 04
0.7-0.8	1.02619E + 05	1.28623E + 05	1.38142E + 05
0.6-0.7	2.04398E + 04	2.80276E + 04	3.19004E + 04
0.5-0.6	1.65722E + 04	2.30238E + 04	2.50728E + 04
0.4-0.5	1.24608E + 04	1.67140E + 04	1.88376E + 04
0.3-0.4	7.37900E + 03	9.72466E + 03	1.09003E + 04
0.2-0.3	2.57823E + 03	3.33692E + 03	3.71790E + 03
0.044-0.2	7.84181E + 01	9.68699E + 01	1.07720E + 02
10 ⁻³ -0.044	8.24486E - 03	1.28631E - 02	1.35308E - 02
Total	1.95648E + 05	2.65066E + 05	3.04190E + 05

TABLE 2-XV

GAMMA PHOTON SURFACE FLUX (Photons/cm²-sec)
 AT 1575 w(th) CAPSULE MIDPLANE AT NOTED FUEL AGE:
 SOURCE — ²³⁶Pu AND DAUGHTERS

Energy Interval (MeV)	Fuel Age (years)					
	0	1	5	10	18	
6.0-7.0	0.0	0.0	0.0	0.0	0.0	0.0
5.0-6.0	0.0	0.0	0.0	0.0	0.0	0.0
4.0-5.0	0.0	0.0	0.0	0.0	0.0	0.0
3.0-4.0	0.0	0.0	0.0	0.0	0.0	0.0
2.0-3.0	0.0	2.24345E + 04	2.63198E + 05	4.66864E + 05	5.35797E + 05	
1.8-2.0	0.0	1.23577E + 03	1.44979E + 04	2.57164E + 04	2.95135E + 04	
1.6-1.8	0.0	1.24820E + 03	1.46437E + 04	2.59752E + 04	2.98104E + 04	
1.4-1.6	0.0	1.26904E + 03	1.48882E + 04	2.64089E + 04	3.03082E + 04	
1.2-1.4	0.0	1.30055E + 03	1.52578E + 04	2.70645E + 04	3.10606E + 04	
1.0-1.2	0.0	2.09323E + 03	2.45596E + 04	4.35066E + 04	5.00270E + 04	
0.9-1.0	0.0	7.86781E + 02	9.23051E + 03	1.63718E + 04	1.87957E + 04	
0.8-0.9	0.0	2.00102E + 03	2.35164E + 04	4.16319E + 04	4.78951E + 04	
0.7-0.8	1.27113E - 03	2.19842E + 03	2.58259E + 04	4.57185E + 04	5.27127E + 04	
0.6-0.7	2.81568E + 01	1.11686E + 03	1.28622E + 04	2.27761E + 04	2.61946E + 04	
0.5-0.6	2.53716E + 01	4.77593E + 03	5.58239E + 04	9.89354E + 04	1.14114E + 05	
0.4-0.5	7.83508E + 00	1.61373E + 03	1.88721E + 04	3.34397E + 04	3.852334E + 04	
0.3-0.4	4.09562E + 00	9.36795E + 02	1.09120E + 04	1.93378E + 04	2.22584E + 04	
0.2-0.3	1.29844E + 00	3.21746E + 02	3.76080E + 03	6.66218E + 03	7.67152E + 03	
0.044-0.2	4.30893E - 02	8.82168E + 00	8.63979E + 01	1.89959E + 02	2.19250E + 02	
10 ⁻³ -0.044	3.67550E - 06	5.39828E - 04	5.24399E - 03	5.18950E - 03	5.73176E - 03	
Total	6.68006E + 01	4.33414E + 04	5.07936E + 05	9.00599E + 05	1.03491E + 06	

PRECEDING PAGE BLANK NOT FILMED

TABLE 2-XVI

GAMMA PHOTON SURFACE FLUX (Photons/cm²-sec)
 AT 3468 w(th) CAPSULE MIDPLANE AT NOTED FUEL AGE:
 SOURCE - ²³⁶Pu AND DAUGHTERS

Energy Interval (MeV)	Fuel Age (years)					
	0	1	5	10	18	
6.0-7.0	0.0	0.0	0.0	0.0	0.0	0.0
5.0-6.0	0.0	0.0	0.0	0.0	0.0	0.0
4.0-5.0	0.0	0.0	0.0	0.0	0.0	0.0
3.0-4.0	0.0	0.0	0.0	0.0	0.0	0.0
2.0-3.0	0.0	3.18032E + 04	3.73110E + 05	6.61826E + 05	7.59546E + 05	
1.8-2.0	0.0	1.95593E + 03	2.29467E + 04	4.07030E + 04	4.67129E + 04	
1.6-1.8	0.0	1.98543E + 03	2.32928E + 04	4.13170E + 04	4.74175E + 04	
1.4-1.6	0.0	2.02939E + 03	2.38085E + 04	4.22317E + 04	4.84673E + 04	
1.2-1.4	0.0	2.08968E + 03	2.45156E + 04	4.34864E + 04	4.99072E + 04	
1.0-1.2	0.0	3.14682E + 03	3.69208E + 04	6.54145E + 04	7.52007E + 04	
0.9-1.0	0.0	1.24267E + 03	1.45790E + 04	2.58578E + 04	2.96856E + 04	
0.8-0.9	0.0	2.76248E + 03	3.24601E + 04	5.74746E + 04	6.61082E + 04	
0.7-0.8	0.0	2.97406E + 03	3.49340E + 04	6.18518E + 04	7.12859E + 04	
0.6-0.7	3.31110E + 01	1.62855E + 03	1.88242E + 04	3.33408E + 04	3.83366E + 04	
0.5-0.6	2.90787E + 01	5.70391E + 03	6.66815E + 04	1.18180E + 05	1.36282E + 05	
0.4-0.5	9.14273E + 00	2.07093E + 03	2.42265E + 04	4.29301E + 04	4.94402E + 04	
0.3-0.4	4.73201E + 00	1.20675E + 03	1.40727E + 04	2.49406E + 04	2.87108E + 04	
0.2-0.3	1.49087E + 00	4.09212E + 02	4.76542E + 03	8.47843E + 03	9.75978E + 03	
0.044-0.2	4.81974E - 02	1.13384E + 01	1.16151E + 02	2.41751E + 02	2.78765E + 02	
10 ⁻³ -0.044	5.84410E - 06	5.83672E - 04	7.64491E - 03	7.12230E - 03	8.05833E - 03	
Total	7.76035E + 01	6.10203E + 04	7.15274E + 05	1.26827E + 06	1.45714E + 06	

TABLE 2-XVII

GAMMA PHOTON SURFACE FLUX (Photons/cm²-sec)
 AT 5679 w(th) CAPSULE MIDPLANE AT NOTED FUEL AGE;
 SOURCE — ²³⁶Pu AND DAUGHTERS

Fuel Age (years)

Energy Interval (MeV)	Fuel Age (years)					
	0	1	5	10	18	
6.0-7.0	0.0	0.0	0.0	0.0	0.0	0.0
5.0-6.0	0.0	0.0	0.0	0.0	0.0	0.0
4.0-5.0	0.0	0.0	0.0	0.0	0.0	0.0
3.0-4.0	0.0	0.0	0.0	0.0	0.0	0.0
2.0-3.0	0.0	3.55697E + 04	4.29030E + 05	7.61017E + 05	8.73382E + 05	
1.8-2.0	0.0	2.40009E + 03	2.81575E + 04	4.99460E + 04	5.73205E + 04	
1.6-1.8	0.0	2.44198E + 03	2.86498E + 04	5.08178E + 04	5.83211E + 04	
1.4-1.6	0.0	2.50142E + 03	2.93439E + 04	5.20505E + 04	5.97359E + 04	
1.2-1.4	0.0	2.57899E + 03	3.02563E + 04	5.36689E + 04	6.15932E + 04	
1.0-1.2	0.0	3.74472E + 03	4.39356E + 04	7.78499E + 04	8.94849E + 04	
0.9-1.0	0.0	1.51489E + 03	1.77726E + 04	3.15220E + 04	3.61877E + 04	
0.8-0.9	0.0	3.13671E + 03	3.68542E + 04	5.52609E + 04	7.50557E + 04	
0.7-0.8	0.0	3.34224E + 03	3.92563E + 04	6.95109E + 04	8.00953E + 04	
0.6-0.7	3.45107E + 01	1.89773E + 03	2.19725E + 04	3.89216E + 04	4.47480E + 04	
0.5-0.6	3.00675E + 01	6.05706E + 03	7.08171E + 04	1.25511E + 05	1.44717E + 05	
0.4-0.5	9.50602E + 00	2.27950E + 03	2.66709E + 04	4.72637E + 04	5.44210E + 04	
0.3-0.4	4.90504E + 00	1.33273E + 03	1.55409E + 04	2.75580E + 04	3.17184E + 04	
0.2-0.3	1.54553E + 00	4.51040E + 02	5.27576E + 03	9.34777E + 03	1.07587E + 04	
0.044-0.2	4.94647E + 02	1.25653E + 01	1.61196E + 02	2.65905E + 02	3.06467E + 02	
10 ⁻³ -0.044	6.01187E - 06	4.62359E - 04	3.17672E - 03	8.64492E - 03	9.85794E - 03	
Total	8.05843E + 01	7.02611E + 04	8.23702E + 05	1.46051E + 06	1.67785E + 06	

TABLE 2-XVIII

GAMMA PHOTON FLUX (Photons/cm²-sec) AS
 A FUNCTION OF DETECTOR POSITION FOR FRESH FUEL;
 SOURCE — DECAY OF ISOTOPES AND DAUGHTERS
 (INCLUDES FISSION)
 Capsule Power (w(th))

Detector Position (r, θ , z) (centimeters)	1575	3468	5679
4.519 cm, 0, 0	1.95648E + 05		
5.257, 0, 0	2.140 x 10 ⁵	2.65066E + 05	3.04190E + 05
5.995, 0, 0	1.950 x 10 ⁵	2.823 x 10 ⁵	3.228 x 10 ⁵
6.733, 0, 0		2.549 x 10 ⁵	2.982 x 10 ⁵
7.471, 0, 0			2.434 x 10 ⁴
40.0, 0, 0	1.184 x 10 ⁴	1.856 x 10 ⁴	4.046 x 10 ³
100.0, 0, 0	2.00 x 10 ³	3.088 x 10 ³	3.240 x 10 ⁵
0, 0, 17.7	1.870 x 10 ⁵	2.693 x 10 ⁵	1.106 x 10 ⁵
0, 0, 22.7	6.040 x 10 ⁴	8.562 x 10 ⁴	1.552 x 10 ⁴
0, 0, 37.7	7.670 x 10 ³	1.113 x 10 ⁴	1.275 x 10 ⁴
0, 0, 40.0	6.132 x 10 ³	9.092 x 10 ³	
0, 0, 100.0	3.424 x 10 ²	6.55 x 10 ²	1.065 x 10 ³

TABLE 2-XIX

GAMMA PHOTON FLUX (Photons/cm²-sec) AS
 A FUNCTION OF DETECTOR POSITION FOR FRESH FUEL;
 SOURCE — ¹⁸O(α, n)²¹Ne REACTION

Detector Position (r, θ, z) (centimeters)	Capsule Power (w(th))		
	1575	3468	5679
4.519, 0, 0	4.30457E + 03		6.93810E + 03
5.257, 0, 0	4.705 x 10 ³	6.05676E + 03	7.361 x 10 ³
5.995, 0, 0	4.288 x 10 ³	6.450 x 10 ³	6.800 x 10 ³
6.733, 0, 0		5.927 x 10 ³	5.550 x 10 ²
7.471, 0, 0			9.228 x 10 ¹
40.0	2.604 x 10 ²	4.24 x 10 ²	7.389 x 10 ³
100.0, 0, 0	4.39 x 10 ¹	7.056 x 10 ¹	2.521 x 10 ³
0, 0, 17.7	4.113 x 10 ³	6.154 x 10 ³	3.539 x 10 ²
0, 0, 22.7	1.328 x 10 ³	1.956 x 10 ³	2.907 x 10 ²
0, 0, 37.7	1.688 x 10 ²	2.544 x 10 ²	
0, 0, 40.0	1.349 x 10 ²	2.078 x 10 ²	
0, 0, 100.0	7.533	1.500 x 10 ¹	2.428 x 10 ¹

TABLE 2-XX

GAMMA PHOTON FLUX (Photon/cm²-sec) FOR 1575 w(th) CAPSULE AS
 A FUNCTION OF DETECTOR POSITION AT NOTED FUEL AGE;
 SOURCE — ²³⁶Pu AND DAUGHTERS

Detector Position (r, θ, z) (centimeters)	Fuel Age (years)							
	0	1	5	10	18			
4.519, 0, 0	6.68006E + 01	4.33414E + 04	5.07932E + 05	9.00599E + 05	1.03491E + 06			
5.257, 0, 0	7.301 x 10 ¹	4.737 x 10 ⁴	5.552 x 10 ⁵	9.844 x 10 ⁵	1.131 x 10 ⁶			
5.995, 0, 0	6.653 x 10 ¹	4.317 x 10 ⁴	5.059 x 10 ⁵	8.970 x 10 ⁵	1.0308 x 10 ⁶			
40.0, 0, 0	4.040	2.622 x 10 ³	3.073 x 10 ⁴	5.449 x 10 ⁴	6.261 x 10 ⁴			
100., 0, 0	0.681	4.421 x 10 ²	5.181 x 10 ³	9.186 x 10 ³	1.056 x 10 ⁴			
0, 0, 17.7	6.384 x 10 ¹	4.142 x 10 ⁴	4.8538 x 10 ⁵	8.606 x 10 ⁵	9.890 x 10 ⁵			
0, 0, 22.7	2.061 x 10 ¹	1.338 x 10 ⁴	1.568 x 10 ⁵	2.779 x 10 ⁵	3.194 x 10 ⁵			
0, 0, 37.7	2.619	1.700 x 10 ³	1.991 x 10 ⁴	3.531 x 10 ⁴	4.057 x 10 ⁴			
0, 0, 40.0	2.094	1.358 x 10 ³	1.592 x 10 ⁴	2.823 x 10 ⁴	3.244 x 10 ⁴			
0, 0, 100.0	0.1170	75.850	8.89 x 10 ²	1.576 x 10 ³	1.811 x 10 ³			

TABLE 2-XXI

GAMMA PHOTON FLUX (Photon/cm²-sec) FOR 3468 w(th) CAPSULE AS
 A FUNCTION OF DETECTOR POSITION AT NOTED FUEL AGE;
 SOURCE -- 236Pu AND DAUGHTERS

Detector Position (r, θ, z) (centimeters)	Fuel Age (Years)					
	0	1	5	10	18	
5.257, 0, 0	7.76035E + 01	6.10203 + 04	7.15271E + 05	1.26827E + 06	1.45714E + 06	
5.995, 0, 0	8.265 x 10 ¹	6.500 x 10 ⁴	7.618 x 10 ⁵	1.351 x 10 ⁶	1.552 x 10 ⁶	
6.733, 0, 0	7.595 x 10 ¹	5.972 x 10 ⁴	7.000 x 10 ⁵	1.241 x 10 ⁶	1.426 x 10 ⁶	
40.0, 0, 0	5.432	4.272 x 10 ³	5.007 x 10 ⁴	8.878 x 10 ⁴	1.020 x 10 ⁵	
100.0, 0, 0	0.904	7.109 x 10 ²	8.333 x 10 ³	1.478 x 10 ⁴	1.698 x 10 ⁴	
0, 0, 17.7	7.885 x 10 ¹	6.200 x 10 ⁴	7.267 x 10 ⁵	1.289 x 10 ⁶	1.481 x 10 ⁶	
0, 0, 22.7	2.507 x 10 ¹	1.971 x 10 ⁴	2.310 x 10 ⁵	4.097 x 10 ⁵	4.707 x 10 ⁵	
0, 0, 37.7	3.260	2.563 x 10 ³	3.004 x 10 ⁴	5.327 x 10 ⁴	6.120 x 10 ⁴	
0, 0, 40.0	2.662	2.093 x 10 ³	2.454 x 10 ⁴	4.350 x 10 ⁴	5.000 x 10 ⁴	
0, 0, 100.0	0.192	1.508 x 10 ²	1.767 x 10 ³	3.133 x 10 ³	3.600 x 10 ³	

TABLE 2-XXII

GAMMA PHOTON FLUX (Photons/cm²-sec) FOR 5679 w(th) CAPSULE AS
 A FUNCTION OF DETECTOR POSITION AT NOYED FUEL AGE;
 SOURCE — ²³⁶Pu AND DAUGHTERS

Detector Position (r, θ, z) (centimeters)	Fuel Age (years)					
	0	1	5	10	18	
5.995, 0, 0	8.05843E + 01	7.02611E + 04	8.23668E + 05	1.46051E + 06	1.67785E + 06	
6.733, 0, 0	8.550 x 10 ¹	7.455 x 10 ⁴	8.739 x 10 ⁵	1.550 x 10 ⁶	1.780 x 10 ⁶	
7.471, 0, 0	7.900 x 10 ¹	6.886 x 10 ⁴	8.073 x 10 ⁵	1.432 x 10 ⁶	1.645 x 10 ⁶	
40.0, 0, 0	6.4471	5.621 x 10 ³	6.590 x 10 ⁴	1.169 x 10 ⁵	1.343 x 10 ⁵	
100.0, 0, 0	1.072	9.345 x 10 ²	1.096 x 10 ⁴	1.943 x 10 ⁴	2.232 x 10 ⁴	
0, 0, 17.7	8.582 x 10 ¹	7.483 x 10 ⁴	8.772 x 10 ⁵	1.556 x 10 ⁶	1.787 x 10 ⁶	
0, 0, 22.7	2.929 x 10 ¹	2.554 x 10 ⁴	2.993 x 10 ⁵	5.308 x 10 ⁵	6.097 x 10 ⁵	
0, 0, 37.7	4.110	3.583 x 10 ³	4.201 x 10 ⁴	7,449 x 10 ⁴	8.557 x 10 ⁴	
0, 0, 40.0	3.377	2.944 x 10 ³	3.451 x 10 ⁴	6.120 x 10 ⁴	7.030 x 10 ⁴	
0, 0, 100.0	0.282	2.459 x 10 ²	2.883 x 10 ³	5.112 x 10 ³	5.872 x 10 ³	

3. NEUTRON RADIATION CHARACTERISTICS

3.1 Introduction

This report section presents the result of calculations of the neutron flux emitted by plutonium dioxide fuelled RTG capsules. Neutron flux distributions were determined as a function of energy for the three RTG model capsules already described in Section 2, namely: 1575, 3468 and 5679 w(th). The flux calculations were based on neutron yield spectra which were derived to account for plutonium spontaneous fission and both oxygen and contaminant light element (α , n) reactions.

Since the RTG emitted neutron flux is a function of the total neutron yield per gram of given plutonium dioxide, the yield spectra must be obtained as discussed in Section 3.2. Measurements and calculations of the spectrum of alpha particles and of neutrons in production plutonium dioxide fuel are presented in the literature^(1-3, 22-27). Unfortunately, there is considerable variation with respect to the emitted spectral components and their intensities.

The total neutron yield for plutonium dioxide with oxygen of natural abundance and no impurities or self multiplication may be as low as 1.7×10^4 neutrons/sec-gram of ^{238}Pu ⁽²⁸⁾. Plutonium dioxide sources larger than 100 w(th), typically have a total specific neutron yield between 2.0×10^4 and 3.0×10^4 neutrons/sec-gram Pu^{238} ^(1,28). The total specific yield may be taken as 75% due to the $^{18}\text{O}(\alpha, n)^{21}\text{Ne}$ reaction, 12% due to the spontaneous fission of ^{238}Pu and 10% due to the contaminant light element (α , n) reactions with the remaining 3% due to lesser known phenomena such as $^{17}\text{O}(\alpha, n)^{21}\text{Ne}$, (γ , n), etc. Typical yield values are:

- I. Plutonium fission ----- spontaneous fission neutron yields of 2586 (\pm 398) neutrons/sec-gm ^{238}Pu have been reported^(29,30).
- II. Oxygen (α , n) reactions ----- $^{17}\text{O}/^{18}\text{O}$ (α , n) ^{21}Ne neutron yields ranging from 12,400 to 14,500 neutrons/sec-gm ^{238}Pu , have been reported in references (1) and (28), respectively.
- III. Impurity (α , n) reactions ----- an impurity (α , n) neutron yield of 4000 neutrons/sec-gm ^{238}Pu is typical for commercial fuel, though values as high as 10,000 neutrons/sec-gm ^{238}Pu have been reported.

There are current efforts⁽²⁹⁾ to produce PuO_2 depleted in ^{17}O and ^{18}O in order to reduce the neutron emission rate to about 20% that of the natural oxygen PuO_2 .

Section 3.2.1 describes the method used to determine the neutron fission spectrum. Section 3.2.2 and Appendices G, H, I and J detail the method used to determine the $^{18}\text{O}(\alpha, n)^{21}\text{Ne}$ neutron spectrum. The impurity element (α , n) spectrum was calculated as described in Section 3.2.3 and Appendix K.

The neutron yield spectra were used as source terms for determination of neutron transport to the fuel capsule radial and axial surfaces, and surface flux spectra thus obtained. Neutron transport was calculated by the method of discrete ordinates⁽¹²⁾. Neutron flux geometric reduction from the capsule surface to exterior spatial locations was calculated by means of the removal cross section technique and point kernel geometry⁽¹³⁾. These calculations and obtained results are discussed in Section 3.3.

3.2 Neutron Source Spectra

3.2.1 Fission Neutrons

The neutron fission spectrum was determined from the reported neutron total spontaneous fission yield rate of 2.6×10^3 neutrons/sec-gm ^{238}Pu ⁽³⁰⁾. The 2.6×10^3 value does not include the spontaneous fission of ^{240}Pu because of its low abundance in the fuel and the fact that its fission rate, 29 neutrons/sec-gm ^{240}Pu , is less than the uncertainties indicated in the literature for the spontaneous fission rate of ^{238}Pu . The fission spectrum was determined from the uranium fission spectrum relationship ⁽¹⁵⁾ normalized to the plutonium total spontaneous fission yield, as

$$N(E_s) = 2.00154 \times 10^3 E_s^{1/2} \cdot \exp(-E_s/1.29), \quad (3.1)$$

where E_s is the fission neutron energy. An alternative relationship has been reported which gives the number of spontaneous fission neutrons produced per MeV per gm of ^{238}Pu as ⁽²⁴⁾

$$N(E_s) = 2.04 \times 10^3 \cdot E_s^{1/2} \cdot \exp(-E_s/1.34) \quad (3.2)$$

This relationship is based on a total spontaneous fission yield rate of 2.8×10^3 neutron/sec-gm ^{238}Pu ⁽²⁸⁾. The total number of spontaneous fission neutrons produced by ^{238}Pu in any energy interval may be obtained after integration of equation (3.1), over the energy interval, as

$$N = \int_{E_L}^{E_H} N(E_s) dE_s = 2.00154 \times 10^3 \int_{E_L}^{E_H} E_s^{1/2} \exp(-E_s/1.29) dE_s, \quad (3.3)$$

where, E_L and E_H are the lower and upper limits of the neutron energy interval in energy units of MeV.

The total spontaneous fission neutron yield rate was calculated for twenty-three (23) energy intervals, in the range 0.025 eV to 10 MeV. The results of the calculation are given in Table 3-I for the RTG plutonium dioxide fuel. In Table 3-I column 2 is the spontaneous fission yield per gm of ^{238}Pu . The spontaneous fission yield in each energy interval was divided by the total neutron fission yield to determine the spontaneous fission spectrum given in column 5 of Table-3-I.

In the neutron flux results presented later in this section, the value of k_{eff} corresponds to the ratio of the calculated total neutron fission rate in the subcritical system volume to the assumed neutron fission source normalized to unity in accord with the group distribution given in Table 3-I. The fission rate for each neutron group g , and for each volume element, was integrated as:

$$\sum_1 N_{1,g} \nu \sigma_{1,g} V_1 \quad (3.4)$$

where $N_{1,g}$ is the scalar flux (neutrons/cm²-sec); V_1 is the 1th elemental volume (cm³); and $\nu \sigma_{1,g}$ is the number of neutrons released per fission multiplied by the fission cross-section corresponding to group g . A more extensive multigroup treatment of the multiplication constant, k_{eff} , etc. is given in the references ^(17,31).

3.2.2 Oxygen (α , n) Neutrons

The oxide in the plutonium dioxide fuel source contains natural oxygen which consists of the oxygen isotopes ^{16}O , ^{17}O and ^{18}O in the relative abundances 99.759, 0.037 and 0.204% ⁽²³⁾. Alpha particles interacting

with low atomic number isotopes may give rise to the formation of very short-lived compound nuclei which promptly decay accompanied by the emission of a neutron. The cross section for this (α , n) reaction is negligible for the relatively stable ^{16}O isotope. However $^{17}\text{O}(\alpha, n)^{20}\text{Ne}$ and $^{18}\text{O}(\alpha, n)^{21}\text{Ne}$ reactions represent the principal sources of neutrons in plutonium dioxide.

The total neutron yield produced by the $^{18}\text{O}(\alpha, n)^{21}\text{Ne}$ reaction in the plutonium dioxide product fuel are tabulated in the current literature (1, 3, 4, 21, 32-35). The (α , n) neutron yields in the references are expressed as the numerical difference between the measured total neutron yield and the calculated neutron fission yield. Variations in the (α , n) spectrum result from uncertainties in the calculated fission yield and lack of knowledge of light element contaminations in the plutonium dioxide fuel. Though oxygen (α , n) neutron yields have been reported^(1, 24) information has not been given in sufficient detail to allow spectral calculations to be carried out. In the remainder of this subsection and Appendices G, H, I and J the (α , n) total neutron spectrum and the methods of calculation are presented.

In the present work, the (α , n) neutron yield from the irradiated oxygen nuclei was assumed to be totally due to the ^{18}O isotope since the maximum yield for the $^{17}\text{O}(\alpha, n)^{20}\text{Ne}$ reaction is $\sim 10\%$ of the $^{18}\text{O}(\alpha, n)^{21}\text{Ne}$ reaction yield⁽¹⁶⁾, the ^{17}O abundance is 0.037% as compared to 0.204% for ^{18}O . Further consideration of the $^{17}\text{O}(\alpha, n)^{21}\text{Ne}$ neutron yield is not possible until more experimental information becomes available.

An alpha particle of initial energy E, collides with the atoms of the transport medium and is thus degraded in energy until thermal equilibrium with

the medium is achieved. Each alpha particle collision with the ^{18}O nucleus corresponds to an inelastic (α, n) reaction providing the alpha energy is greater than the threshold energy. The threshold is the lowest energy for which the (α, n) reaction can occur. The alpha particle "slowing down" process gives rise to an energy spectrum of inelastic collision neutrons. If isotropic scattering in the center of mass coordinate system is assumed, the number of neutrons with energy E_n , generated by the alpha particle collision with ^{18}O target nuclei may be obtained as

$$N(E_n) dE_n = N(\theta_{cm}) \frac{\sin\theta_{cm}}{2} d\theta_{cm}$$

where, θ_{cm} is the scatter angle in the center of mass coordinate system. The reader may refer to texts for a discussion on the penetration of charged particles.⁽³⁶⁾

The intermediate ^{22}Ne nucleus resulting from the $^{18}\text{O}(\alpha, n)$ reaction decays to various ^{21}Ne levels as follows^(21, 32, 33):

- 55% to the ground state,
- 35% to the first excited 0.35 MeV state,
- ~ 10% to the second excited 1.73 MeV state,
- ~ 1% to the third excited 2.84 MeV state.

The (α, n) reactions were calculated for each of these inelastic collision schemes. The Q values for the reactions were taken as -0.70, -1.05, -2.43 and -3.54 MeV for ground, first, second and third states, respectively. The two alpha particles emitted by ^{238}Pu ⁽¹⁻³⁾, namely:

Energy (MeV)	Alpha Particle per Disintegration
5.495	0.72
5.452	0.28

were taken as a single 5.50 MeV alpha particle for all calculations.

The dynamics of the $^{18}\text{O}(\alpha, n)^{21}\text{Ne}$ reaction are given in Appendix G. The alpha particle energy loss per unit path length, $(dE_{\alpha}/dx)_1$, resulting from collisions with oxygen and plutonium atoms in the fuel, is discussed in Appendix H. The $^{18}\text{O}(\alpha, n)^{21}\text{Ne}$ neutron yield spectrum is discussed in Appendix I. Appendix J describes the numerical integration of the $^{18}\text{O}(\alpha, n)^{21}\text{Ne}$ spectrum over the twenty-three energy groups used in the present work.

The $^{18}\text{O}(\alpha, n)^{21}\text{Ne}$ neutron spectrum was determined for the PuO_2 product fuel in twenty-three energy groups in the range 0.025 eV to 10.0 MeV. Table 3-II presents the results of the calculations. The data are normalized to a neutron yield value of 1.22×10^4 neutrons/sec-gm ^{238}Pu ; an experimentally measured value of 1.24×10^4 neutrons/sec-gm ^{238}Pu has been obtained for reactions with ^{17}O and ^{18}O (37). Table 3-III is the spectrum normalized to unit emission.

3.2.3 Impurity (α, n) Neutron Yield

Commercial grade PuO_2 contains small quantities of uniformly mixed low atomic number impurity elements which yield neutrons through the (α, n) reaction. The neutron yield, which may be significant, varies with each commercial fuel feedstock. Thus in order to calculate the total PuO_2 neutron yield it is necessary to explicitly identify the impurity elements present. Since the yield spectra have not been generally reported they were assumed, in the present work, to be similar to the $^{18}\text{O}(\alpha, n)^{21}\text{Ne}$

yield spectra as given in Table 3-III. This assumption if the impurity concentration is relatively small and better data is unavailable.

Table 3-IV presents an analysis of a typical $\text{Pu}(\text{NO}_3)_4$ feed stock used in the production of commercial PuO_2 fuel⁽³⁸⁾. The ^{238}Pu isotope emits ~ 5.5 MeV alpha particles which in turn interact with the impurities. The 5.5 MeV alpha particles have sufficient energy to exceed the (α, n) threshold and the coulomb barrier of the low atomic numbered impurities⁽³⁹⁾. Neutron yield data for the major impurity elements are determined in Appendix K; the yield units are: neutrons/sec-gm Pu per ppm of impurity.

For example if a Li impurity of 5 ppm (by weight) is present in PuO_2 , then the neutron yield will range from, $5 \times 4.3 = 21.5$ to $5 \times 5.5 = 27.5$, neutrons/sec-gm Pu. The range variation results from the range distribution of experimental data. An excellent compilation of light element (α, n) reactions is given in Chapter I of reference (40); reference (41) is also recommended.

3.3 Neutron Fluxes

The neutron source spectra yields discussed in Section 3.2 were used to determine neutron flux distributions at the RTG surface and exterior spatial positions. The flux calculations were carried out for three fuel capsules already described in Section 2, namely: 1575, 3468 and 5679 w(th).

Figure 2-II gives the dimensions of the three model capsules and the material zones as a function of power. The material composition of the capsules' zones are detailed in Table 2-XIII.

The neutron transport to the RTG surface and exterior spatial positions was calculated using the ANISN⁽¹⁷⁾ and QAD⁽¹⁸⁾ computer codes. ANISN was used to determine surface fluxes and QAD was used to obtain exterior fluxes. The neutron collision group constants were calculated using the "Evaluated Nuclear Data File"⁽⁴²⁾ and the "R. J. Howerton Evaluated Data File"⁽⁴³⁾. The microscopic collision cross sections were averaged for twenty-three neutron groups with a neutron flux spectrum thermalized to 20°C and continuously varied as a function of energy E, up to approximately 0.2 MeV. The measured ²³⁸PuO₂⁽¹⁾ emission neutron spectrum was assumed as the fission weighted flux spectrum up to 7 MeV. From 7 MeV to 10 MeV, the ²³⁸Pu fission spectrum was assumed for weighting. Additional calculations showed that even when thermalized up to 600°C the thermal neutron fluxes remain relatively unchanged.

Table 3-V gives the calculated neutron flux as a function of energy and power at the capsule radial midplane surface for ¹⁸O (α , n) ²¹Ne and fission neutrons. Table 3-VI gives similar radial surface fluxes for fission neutrons only. The calculated values of k_{effective} are noted as 0.17, 0.30 and 0.40 for the 1575, 3468 and 5679 w(th) capsules.

Tables 3-VII, 3-VIII and 3-IX give the calculated total neutron flux at axial and radial detector positions at and beyond the capsule surface, i.e., at cylindrical coordinate positions (r, θ , z) as defined in Figure 2-III. The data in these tables corresponds to the total fluxes given in Tables 3-V and 3-VI at (r, θ , z) = (capsule radial surface, 0, 0). The total fluxes given in Tables 3-VII to 3-IX are shown graphically in Figures 3-I through 3-IV as a function of detector distance r, with capsule power as the parameter. Figures 3-I and 3-II are for the radial midplane while Figures 3-III and 3-IV are for the axial midplane. Figures 3-I and 3-III

are for $^{18}\text{O}(\alpha, n)^{21}\text{Ne}$ plus fission neutrons while Figures 3-II and 3-IV are fission neutrons only. Data for $^{18}\text{O}(\alpha, n)^{21}\text{Ne}$ may be obtained by subtraction since the values of k_{eff} are less than unity, i.e., since the fuel capsules are subcritical.

The surface neutron flux produced by the impurity light element (α, n) neutrons may be determined as

$$\Phi_1 = \Phi_0 \times \frac{Y_1}{Y_0} \quad (3.5)$$

where

Φ_0 = surface neutron flux produced by the oxygen (α, n) reaction, eg. Table 3-V minus Table 3-VI;

Y_0 = neutron yield produced by the oxygen (α, n) reaction per second per gram of Pu, eg. 9882 n/sec-gm Pu based on 80% ^{238}Pu in Pu and 1.22×10^4 n/sec-gm ^{238}Pu ;

Y_1 = neutron yield produced by the impurity element (α, n) reaction per second per gram of Pu, eg. the Appendix Table K-II data gives $Y_1 = 191 \times 10 = 1910$ n/sec-gm Pu for 10 ppm of boron (using the maximum yield per ppm of impurity value).

Equation (3.5) assumes that the light element (α, n) neutron spectrum corresponds to the $^{18}\text{O}(\alpha, n)^{21}\text{Ne}$ neutron spectrum.

An example of the use of the calculated data presented in this report section is given in Appendix F. The example computes the neutron flux at $r = 100$ cm for a capsule power of 1575 w(th), "normal" oxygen and a 100 ppm boron impurity.

FIGURE 3-1
 NEUTRON FLUX AS A FUNCTION OF DETECTOR RADIAL DISTANCE
 FROM CAPSULE AXIS WITH POWER AS THE PARAMETER
 (NEUTRON SOURCE: $^{18}\text{O}(\alpha, n)^{21}\text{Ne}$ AND FISSION)

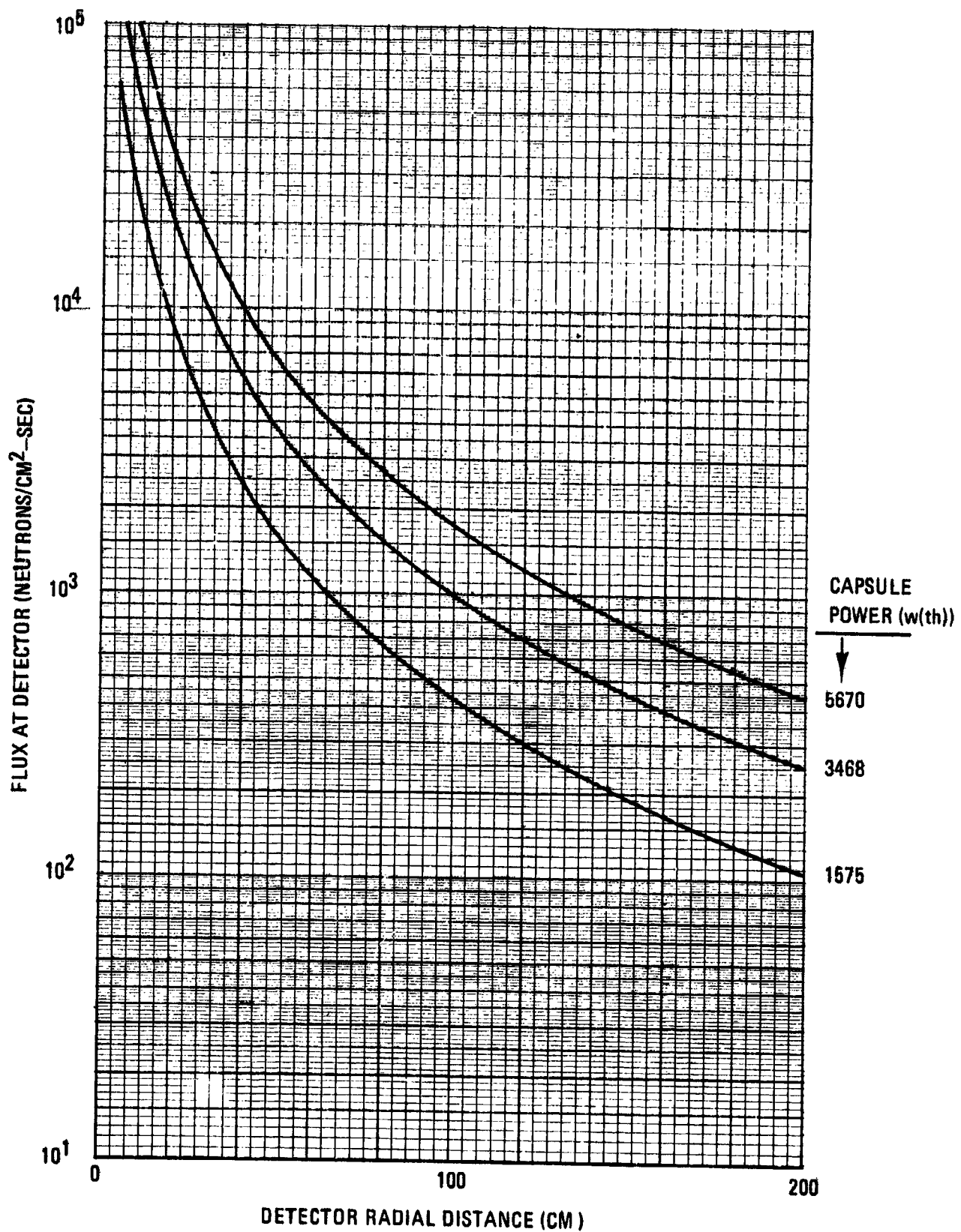


FIGURE 3-II
NEUTRON FLUX AS A FUNCTION OF DETECTOR RADIAL DISTANCE
FROM CAPSULE AXIS WITH POWER AS THE PARAMETER
(NEUTRON SOURCE: FISSION)

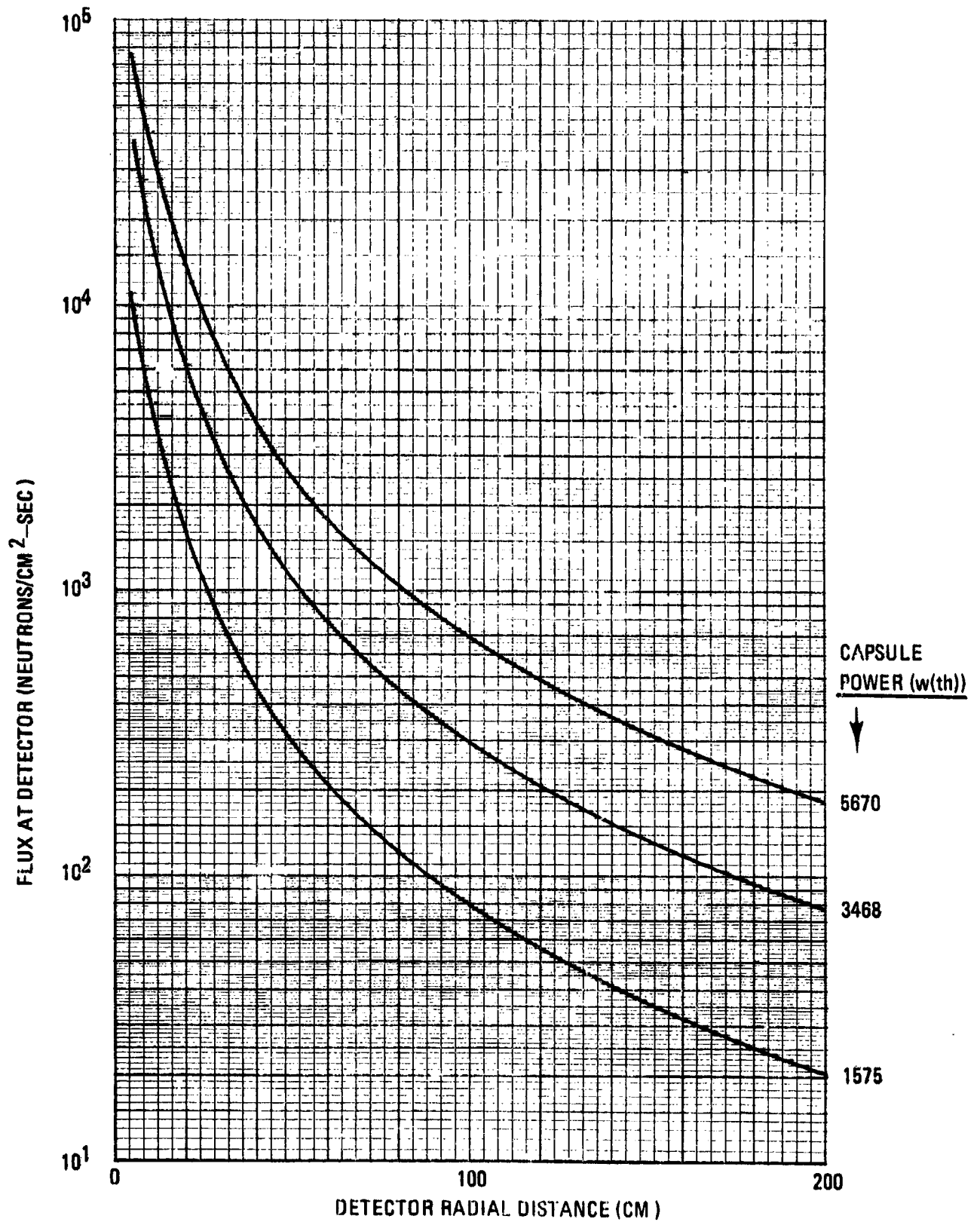


FIGURE 3-III
 NEUTRON FLUX AS A FUNCTION OF DETECTOR AXIAL DISTANCE
 FROM CAPSULE AXIS WITH POWER AS THE PARAMETER
 (NEUTRON SOURCE: $^{18}\text{O}(\alpha, n)^{21}\text{Ne}$ AND FISSION)

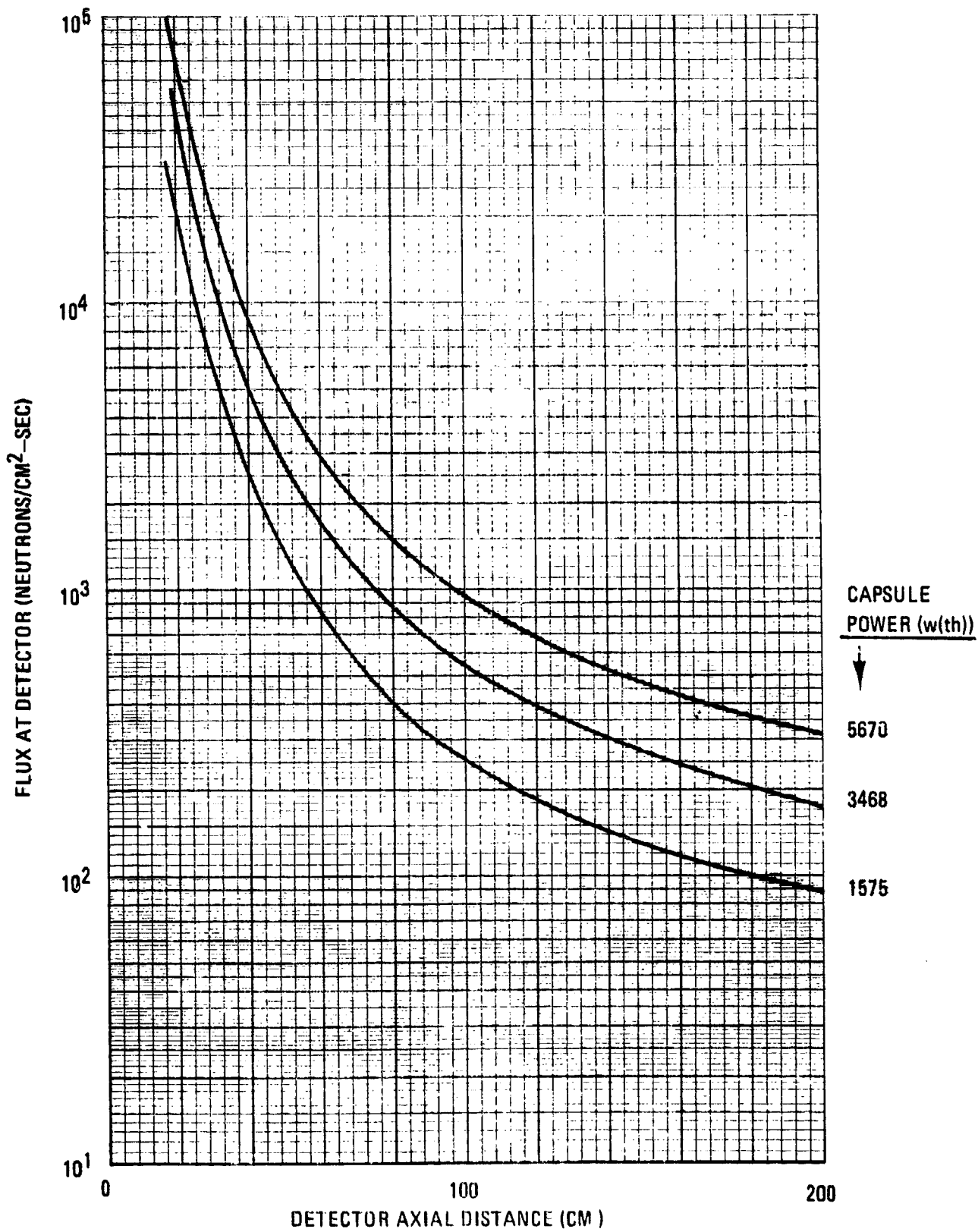


FIGURE 3-IV
 NEUTRON FLUX AS A FUNCTION OF DETECTOR AXIAL DISTANCE
 FROM CAPSULE AXIS WITH POWER AS THE PARAMETER
 (NEUTRON SOURCE: FISSION)

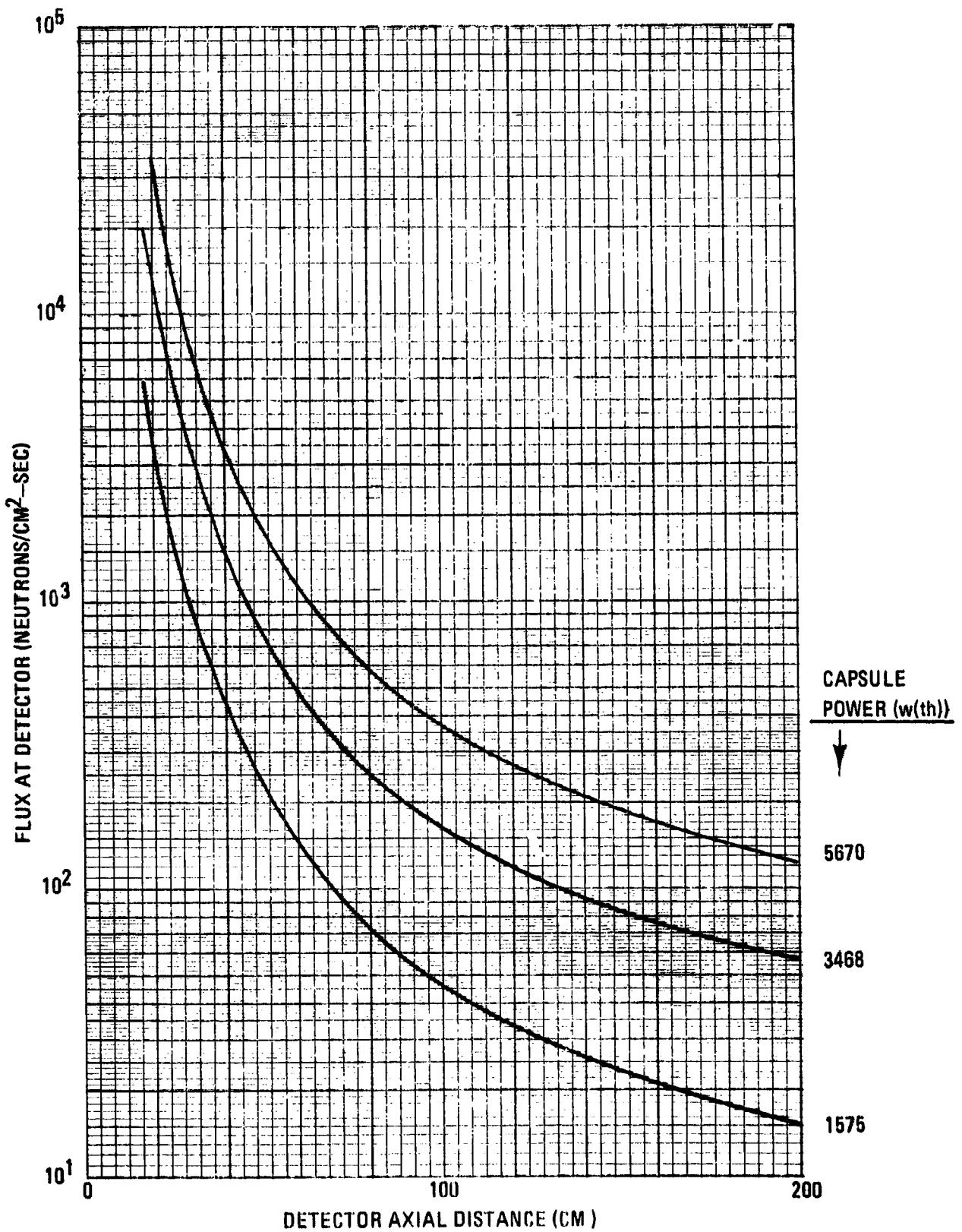


TABLE 3-1

PLUTONIUM ISOTOPE SPONTANEOUS FISSION NEUTRON SPECTRUM

Neutron Energy Interval (MeV)	Neutrons sec-gm ²³⁸ Pu	Neutrons sec-gm PuO ₂	Neutrons/sec-cm ³ (PuO ₂ Fuel)	Fission Spectrum
0.025 - 0.10 x 10 ⁻⁶	3.72 x 10 ⁻⁸	2.64 x 10 ⁻⁸	19.3 x 10 ⁻⁸	0.0
0.010 - 0.30 x 10 ⁻⁵	6.90 x 10 ⁻⁶	4.93 x 10 ⁻⁶	36.03 x 10 ⁻⁶	0.0
0.030 - 0.30 x 10 ⁻⁴	2.13 x 10 ⁻⁴	1.52 x 10 ⁻⁴	11.11 x 10 ⁻⁴	0.0
0.030 - 0.555 x 10 ⁻³	1.73 x 10 ⁻²	1.24 x 10 ⁻²	9.06 x 10 ⁻²	0.0
0.555 x 10 ⁻³ - 0.0170	2.92	2.09	15.27	.00113
0.0170 - 0.0449	9.52	6.80	49.70	.00368
0.0449 - 0.122	41.39	29.55	216.0	.01598
0.122 - 0.201	55.97	40.0	292.32	.02162
0.201 - 0.331	108.94	77.78	568.43	.04204
0.331 - 0.546	202.24	144.39	1055.2	.07805
0.546 - 0.702	152.14	108.62	793.8	.05871
0.702 - 0.90	190.74	136.18	995.22	.07361
0.900 - 1.16	237.86	169.82	1241.07	.09180
1.16 - 1.49	272.56	194.59	1422.08	.10518
1.49 - 1.91	294.11	210.0	1534.7	.11351
1.91 - 2.45	295.72	211.12	1542.9	.11412
2.45 - 3.14	266.52	190.28	1390.59	.10286
3.14 - 4.04	214.13	152.88	1117.27	.08264
4.04 - 4.46	64.58	46.11	337.0	.02493
4.46 - 5.18	76.26	54.44	397.86	.02943
5.18 - 6.66	76.51	54.62	399.17	.02952
6.66 - 8.55	30.93	15.77	115.25	.00853
8.55 - 10.0	7.00	5.00	36.54	.00270
Total	2.6 x 10 ³	1.86 x 10 ³	13.52 x 10 ³	1.0000

TABLE 3-II

TOTAL NEUTRON EMISSION FROM THE $^{18}\text{O}(\alpha, n)^{21}\text{Ne}$
REACTION IN PuO_2 FUEL*

Neutron energy interval (MeV)	Neutrons sec-gm ^{238}Pu	Neutrons sec-gm PuO_2	Neutrons** sec-cm 3	Neutrons*** sec-cm 3 (incapsulated)
2.5×10^{-8} - 10^{-7}	0.0	0.0	0.0	0.0
10^{-7} - 3.0×10^{-6}	2.673×10^{-6}	1.908×10^{-6}	2.042×10^{-5}	1.394×10^{-5}
3.0×10^{-6} - 3.0×10^{-5}	8.076×10^{-4}	5.766×10^{-4}	6.170×10^{-3}	4.214×10^{-3}
3.0×10^{-5} - 5.55×10^{-4}	5.397×10^{-2}	3.853×10^{-2}	4.123×10^{-1}	2.815×10^{-1}
5.55×10^{-4} - 1.70×10^{-2}	8.565	6.115×10^0	6.543×10^1	4.469×10^1
1.70×10^{-2} - 4.49×10^{-2}	2.070×10^1	1.478×10^1	1.582×10^2	1.060×10^2
4.49×10^{-2} - 1.22×10^{-1}	5.873×10^1	4.193×10^1	4.487×10^2	3.064×10^2
1.22×10^{-1} - 2.01×10^{-1}	7.253×10^1	5.178×10^1	5.540×10^2	3.154×10^2
2.01×10^{-1} - 3.31×10^{-1}	1.503×10^2	1.073×10^2	1.148×10^3	7.842×10^2
3.31×10^{-1} - 5.46×10^{-1}	2.450×10^2	1.749×10^2	1.672×10^3	1.275×10^3
5.46×10^{-1} - 7.02×10^{-1}	1.721×10^2	1.229×10^2	1.315×10^3	8.982×10^2
7.02×10^{-1} - 9.00×10^{-1}	2.459×10^2	1.756×10^2	1.879×10^3	1.283×10^3
9.00×10^{-1} -1.16	4.128×10^2	2.948×10^2	3.155×10^3	2.155×10^3
1.16 - 1.49	6.786×10^2	4.844×10^2	5.183×10^3	3.540×10^3
1.49 - 1.91	9.844×10^2	7.028×10^2	7.520×10^3	5.137×10^3
1.91 - 2.45	2.044×10^3	1.460×10^3	1.562×10^4	1.067×10^4
2.45 - 3.14	3.911×10^3	2.792×10^3	2.988×10^4	2.040×10^4
3.14 - 4.04	2.932×10^3	2.093×10^3	2.240×10^4	1.530×10^4
4.04 - 4.46	2.628×10^2	1.876×10^2	2.007×10^3	1.371×10^3
4.46 - 5.18	1.215×10^0	8.674×10^{-1}	9.261	5.333
5.18 - 6.66	0.0	0.0	0.0	0.0
6.66 - 8.55	0.0	0.0	0.0	0.0
8.55 - 10.00	0.0	0.0	0.0	0.0
Total	1.220×10^4	8.711×10^3		

* data normalized to 1.22×10^4 ** volume emission = $\frac{\text{Neutrons}}{\text{sec-gm PuO}_2} \times \text{density (PuO}_2)$; $\rho = 10.7 \text{ g/cc}$

*** a volume fraction 0.683 was used for this study

TABLE 3-III

 $^{18}\text{O}(\alpha, n)^{21}\text{Ne}$ NEUTRON SPECTRUM

Neutron Energy Interval (MeV)	Neutron Spectrum* (N(E))
2.5×10^{-8} - 10^{-7}	0.0
10^{-7} - 3.0×10^{-6}	0.0
3.0×10^{-6} - 3.0×10^{-5}	0.0
3.0×10^{-5} - 5.55×10^{-4}	0.0
5.55×10^{-4} - 1.70×10^{-2}	.00022
1.70×10^{-2} - 4.49×10^{-2}	.00045
4.49×10^{-2} - 1.22×10^{-1}	.0020
1.22×10^{-1} - 2.01×10^{-1}	.00216
2.01×10^{-1} - 3.31×10^{-1}	.00376
3.31×10^{-1} - 5.46×10^{-1}	.0078
5.46×10^{-1} - 7.02×10^{-1}	.00821
7.02×10^{-1} - 9.00×10^{-1}	.01019
9.00×10^{-1} -1.16	.02883
1.16 - 1.49	.04875
1.49 - 1.91	.07483
1.91 - 2.45	.17095
2.45 - 3.14	.34745
3.14 - 4.04	.26938
4.04 - 4.46	.02475
4.46 - 5.18	.000105
5.18 - 6.66	.0
6.66 - 8.55	.0
8.55 - 10.00	.0
Total	0.99983

* Number of neutrons emitted per unit neutron emitted by $^{18}\text{O}(\alpha, n)^{21}\text{Ne}$ reaction

TABLE 3-IV
ANALYSIS OF TYPICAL Pu(NO₃)₄ FEED STOCK¹ AND PLASMA SPHEROIDIZED MICROSPHERES²(40)

Batch	Impurity Elements, ppm (a)																	
	Al	B	Be	Ca	Cd	Co	Cr	Cu	Fe	Mg	Mn	Na	Ni	Pb	Si	Ti	Sn	Zn
Pu(NO ₃) ₄	12	<1	<0.5	200	<10	--	20	<2	75	<10	<5	--	50	20	60	--	<10	<50
X-001	700	600	--	400	--	1000	900	--	5100	--	100	--	600	--	600	--	--	900
X-002-3	800	--	--	700	--	900	800	600	5200	--	300	--	500	--	300	600	--	600
X-004	<200	<100	--	800	--	1500	600	--	2700	100	<200	T	<300	--	600	--	--	--
X-005	300	--	--	400	--	--	300	<100	2800	--	--	T	<100	--	T	--	--	100
X-006-8	400	<100	--	500	--	<100	400	<100	2000	200	<100	T	100	--	T	--	--	200
X-008-9	300	T	--	500	--	--	<100	--	900	100	--	T	<100	--	200	--	--	<300

(a) Analysis based on ppm of plutonium metal.

1 Pu(NO₃)₄ feed stock from Savannah River Plant.

2 Plasma microspheres from Mound Laboratory.

TABLE 3-V
 RADIAL NEUTRON FLUX AT CAPSULE SURFACE
 SOURCE: $^{18}\text{O}(\alpha, n)^{21}\text{Ne}$ AND FISSION NEUTRONS

Neutron energy Interval (MeV)	1575 w(th) $k_{\text{eff}} = 0.17$	3468 w(th) $k_{\text{eff}} = 0.30$	5670 w(th) $k_{\text{eff}} = 0.41$
10.0 - 8.55	3.043×10^1	9.518×10^1	1.770×10^2
8.55 - 6.66	9.692×10^1	3.045×10^2	5.682×10^2
6.66 - 5.18	3.351×10^2	1.057×10^3	1.977×10^3
5.18 - 4.46	3.384×10^2	1.059×10^3	1.974×10^3
4.46 - 4.04	1.329×10^3	2.590×10^3	3.826×10^3
4.04 - 3.14	1.264×10^4	2.190×10^4	2.950×10^4
3.14 - 2.45	1.800×10^4	3.243×10^4	4.500×10^4
2.45 - 1.91	1.040×10^4	1.978×10^4	2.862×10^4
1.91 - 1.49	6.351×10^3	1.304×10^4	1.993×10^4
1.49 - 1.16	6.931×10^3	1.397×10^4	2.113×10^4
1.16 - 0.90	6.139×10^3	1.250×10^4	1.900×10^4
0.90 - 0.702	4.549×10^3	1.065×10^4	1.783×10^4
0.702 - 0.546	2.801×10^3	6.770×10^3	1.161×10^4
0.546 - 0.331	2.766×10^3	6.841×10^3	1.184×10^4
0.331 - .201	1.633×10^3	4.202×10^3	7.552×10^3
.201 - .122	8.302×10^2	2.164×10^3	3.939×10^3
.122 - .0449	6.190×10^2	1.597×10^3	2.900×10^3
.0449 - .017	1.647×10^2	3.927×10^2	6.780×10^2
.017 - 555 ev	5.422×10^1	1.231×10^2	2.050×10^2
555ev - 30 ev	5.500×10^{-2}	8.930×10^{-2}	1.196×10^{-1}
30ev - 3 ev	1.964×10^{-4}	4.346×10^{-4}	7.127×10^{-4}
3ev - 0.1 ev	3.687×10^{-5}	8.067×10^{-5}	1.321×10^{-4}
.1ev - .025 ev	1.912×10^{-8}	4.020×10^{-8}	6.494×10^{-8}
Total	7.600×10^4	1.515×10^5	2.282×10^5

TABLE 3-VI
 RADIAL NEUTRON FLUX AT CAPSULE SURFACE
 SOURCE: FISSION NEUTRONS
 (neutrons/cm²-sec)

Neutron Energy Interval (MeV)	1575 w(th) k _{eff} = 0.17	3468 w(th) k _{eff} = 0.30	569 w(th) k _{eff} = 0.41
10.0 - 8.55	3.06047 x 10 ¹	9.56196 x 10 ¹	1.77633 x 10 ²
8.55 - 6.66	9.74854 x 10 ¹	3.05916 x 10 ²	5.70303 x 10 ²
6.66 - 5.18	3.37091 x 10 ²	1.06131 x 10 ³	1.98359 x 10 ³
5.18 - 4.46	3.3544 x 10 ²	1.0551 x 10 ³	1.97038 x 10 ³
4.46 - 4.04	2.8730 x 10 ²	9.0523 x 10 ²	1.69270 x 10 ³
4.04 - 3.14	9.3834 x 10 ²	2.92715 x 10 ³	5.4316 x 10 ³
3.14 - 2.45	1.27108 x 10 ³	4.11544 x 10 ³	7.86172 x 10 ³
2.45 - 1.91	1.38307 x 10 ³	4.42481 x 10 ³	8.38126 x 10 ³
1.91 - 1.49	1.40425 x 10 ³	4.50886 x 10 ³	8.56339 x 10 ³
1.49 - 1.16	1.4955 x 10 ³	4.75222 x 10 ³	8.9675 x 10 ³
1.16 - 0.90	1.37975 x 10 ³	4.32964 x 10 ³	8.10000 x 10 ³
0.90 - 0.702	1.35578 x 10 ³	4.6501 x 10 ³	9.28672 x 10 ³
0.702 - 0.546	1.04160 x 10 ³	3.51495 x 10 ³	6.98428 x 10 ³
0.546 - 0.331	1.1893 x 10 ³	3.97480 x 10 ³	7.82782 x 10 ³
0.331 - 0.201	6.9040 x 10 ²	2.43642 x 10 ³	5.0200 x 10 ³
0.201 - 0.122	3.63628 x 10 ²	1.28660 x 10 ³	2.67060 x 10 ³
0.122 - 0.0449	2.6478 x 10 ²	2.60690 x 10 ²	1.95476 x 10 ³
0.0449 - 0.017	5.6294 x 10 ¹	1.97336 x 10 ²	4.06705 x 10 ²
0.017 - 555 ev	1.4899 x 10 ¹	5.21367 x 10 ¹	1.06807 x 10 ²
555 ev - 30 ev	4.67616 x 10 ⁻³	1.60688 x 10 ⁻²	3.27270 x 10 ⁻²
30 ev - 3 ev	5.10484 x 10 ⁻⁵	1.77371 x 10 ⁻⁴	3.6205 x 10 ⁻⁴
3 ev - 0.1 ev	9.8492 x 10 ⁻⁶	3.35950 x 10 ⁻⁵	6.8110 x 10 ⁻⁵
0.1 ev - 0.025 ev	4.97321 x 10 ⁻⁹	1.65741 x 10 ⁻⁸	3.3230 x 10 ⁻⁸
Total	1.3937 x 10 ⁴	4.5532 x 10 ⁴	8.7956 x 10 ⁴

TABLE 3-VII

NEUTRON FLUX AS A FUNCTION OF DETECTOR POSITION
 CAPSULE POWER 1575 w(th) NEUTRON FLUX (neutron/cm²-sec)

Detector Position (r, θ , z) (centimeters)	¹⁸ O(α , n) ²¹ Ne and Fission Neutrons	Fission Neutrons
4.519, 0.0, 0.0	7.600 x 10 ⁴	1.394 x 10 ⁴
5.519	6.263 x 10 ⁴	1.149 x 10 ⁴
14.519	1.554 x 10 ⁴	2.851 x 10 ³
20.0	9.143 x 10 ³	1.677 x 10 ³
40.0	2.571 x 10 ³	4.716 x 10 ²
100.0	4.277 x 10 ²	7.846 x 10 ¹
500.0	1.718 x 10 ¹	3.151
0.0, 0.0, 17.6926	3.854 x 10 ⁴	7.067 x 10 ³
18.6926	3.092 x 10 ⁴	5.671 x 10 ³
20.0	2.354 x 10 ⁴	4.317 x 10 ³
27.6926	7.454 x 10 ³	1.367 x 10 ³
40.0	2.595 x 10 ³	4.759 x 10 ²
100.0	2.486 x 10 ²	4.558 x 10 ¹
500.0	6.806	1.248

TABLE 3-VII
NEUTRON FLUX AS A FUNCTION OF DETECTOR POSITION

CAPSULE POWER 3468 w(th)
(neutrons/cm²-sec)

Detector Position (r, θ , z) (centimeters)	¹⁸ O(α , n) ²¹ Ne and Fission Neutrons	Fission Neutrons
5.2570, 0.0, 0.0	1.515 x 10 ⁵	4.553 x 10 ⁴
6.2570	1.248 x 10 ⁵	3.749 x 10 ⁴
15.2570	3.357 x 10 ⁴	1.090 x 10 ⁴
20.0	2.141 x 10 ⁴	6.434 x 10 ³
40.0	6.020 x 10 ³	1.810 x 10 ³
100.0	9.975 x 10 ²	3.000 x 10 ²
500.0	4.022 x 10 ¹	1.209 x 10 ¹
0.0, 0.0, 17.6926	8.384 x 10 ⁴	2.523 x 10 ⁴
18.6926	6.801 x 10 ⁴	2.047 x 10 ⁴
20.0	5.215 x 10 ⁴	1.569 x 10 ⁴
27.6926	1.652 x 10 ⁴	4.970 x 10 ³
40.0	5.577 x 10 ³	1.678 x 10 ³
100.0	5.400 x 10 ²	1.625 x 10 ²
500.0	1.717 x 10 ¹	5.167

TABLE 3-IX
NEUTRON FLUX AS A FUNCTION OF DETECTOR POSITION

Detector Position (r, θ , z) (centimeters)	CAPSULE POWER 5679 w(th) (neutrons/cm ² -sec)	¹⁸ O(α , n) ²¹ Ne and Fission Neutrons	Fission Neutrons
5.257, 0.0, 0.0	2.282 x 10 ⁵	8.796 x 10 ⁴	
6.257	1.902 x 10 ⁵	7.332 x 10 ⁴	
15.257	5.488 x 10 ⁴	2.116 x 10 ⁴	
20.0	3.765 x 10 ⁴	1.451 x 10 ⁴	
40.0	1.058 x 10 ⁴	4.078 x 10 ³	
100.0	1.754 x 10 ³	6.759 x 10 ²	
500.0	7.047 x 10 ¹	2.716 x 10 ¹	
0.0, 0.0, 17.6926	1.373 x 10 ⁵	5.292 x 10 ⁴	
18.6926	1.126 x 10 ⁵	4.338 x 10 ⁴	
20.0	8.756 x 10 ⁴	3.375 x 10 ⁴	
27.6926	2.810 x 10 ⁴	2.083 x 10 ⁴	
40.0	9.438 x 10 ³	3.638 x 10 ³	
100.0	9.544 x 10 ²	3.678 x 10 ²	
500.0	3.200 x 10 ¹	1.233 x 10 ¹	

4. DISCUSSION OF RESULTS

Basic gamma photon and neutron source characteristics have been determined and flux data obtained for plutonium dioxide RTG fuel capsules. The fuel capsules were hypothesized based on the SNAP-27. The methods for characterizing the sources have been given in adequate detail. The calculation of the photon and neutron fluxes were carried out using computer codes in the public domain. The source data may be used as input to transport calculations in other than SNAP-27 configurations, as for example in SNAP-19 where the fuel is not annular but consists of solid discs, i.e., "hockey-pucks." Alternately the flux data in this report may be corrected to approximate data for other fuel configurations.

The results may be considered as useful starting points for analyzing RTG radiation interference with science experiments or instrumentation on space probes. Similarly it may be used to determine biological hazards in the presence of RTG's. The results may be modified as indicated for analyses of biomedical problems where PuO_2 power sources are proposed, as for example in "heart programs."

Although the data in Sections 2 and 3 do not include exposure dose information this may be readily obtained by employing standard conversion factor information^(44,45). Table 4-1 presents RTG capsule radial gamma photon total dose rate at one meter as a function of fuel age with power as a parameter. The table also indicates the percentage contribution from the source components: ^{236}Pu , ^{18}O , and Pu isotopes and daughters. It is noted that the isotopes and daughters are the major source (~ 97%) component in fresh fuel, whereas ^{236}Pu is the major source in aged fuel (~ 91%). Figure 4-1 gives the one meter radial and axial dose rate as a function of fuel age for

the 1575 w(th) model capsule; this size approximates SNAP-27. Reference (46) gives radial and axial experimental values of 8 and 1.6 mr/hour for a two year old 1500 w(th) SNAP-27. Allowing for the 5% difference in source power, this value is in very good agreement with the present calculations as seen in Figure 4-I.

The capsule surface neutron flux data given in Table 3-V and the reference (45) conversion factors were used to obtain the surface dose rate for a 1575 w(th) capsule. The data in Table 3-VII was used to convert surface dose rates to one-meter radial and axial dose rates of 52.4 and 30.5 mrem/hr. Since these dose rates are based on source yield data which accounts only for $^{18}\text{O}(\alpha, n)^{21}\text{Ne}$ reactions and fission, a 'correction' for (α, n) impurity reactions is required. If impurities concentrations are not identified but total yield data is, an estimation of the (α, n) impurity flux may be carried out. Reference (24) gives total neutron yield for SNAP-27-1 as $2.2 \pm 0.1 \times 10^4$ neutrons/sec-gm ^{238}Pu , and the dose rates above (52.4 and 30.5 mrem/hr) are based on 1.48×10^4 neutron/sec-gm ^{238}Pu , which suggests an impurity yield of 0.72×10^4 neutron/sec-gm ^{238}Pu , i.e., an additional $\sim 49\%$ yield. For this yield radial and axial total neutron dose rates of 78 and 45 mrem/hour are predicted. The actual total neutron yield value depends on the PuO_2 quality control during the production process. If the total neutron yield is taken as 19,000 neutrons/sec-gm ^{238}Pu , the SRP value as in reference (37), then radial and axial total neutron dose rates of 64 and 38 mrem/hour are predicted. These dose rates may be compared with references (47, 48) radial and axial measurements of 93 and 42 mrem/hour, respectively. The reference data represents a mean for three different capsules.

Since the experimental dose data of the references includes laboratory neutron and photon scattering it is suggested that this may be the major

reason for the difference between experiment and prediction. The backscatter dose is a function of experiment geometry, structural material composition and thickness as well as neutron and photon spectral distribution. For gamma photons the increase in excess of the direct dose, resulting from concrete floor and wall scatter, would be only $\sim 5\%$ ⁽⁵⁹⁾. It is possibly for this reason that the above gamma photon predictions are in good agreement with experiment. The increase in excess of the direct dose for neutrons is considerably greater for concrete floor and wall scatter, with a value of $\sim 30\%$ estimated as probable; this percentage is based on estimates using references (50) and (51) albedo data. In order to obtain an accurate determination of backscatter the details of the specific experiment are required. A '30% backscatter' for neutrons would increase the radial and axial total direct-dose rates of 64 and 38 mrem/hours to yield 'laboratory dose' rates of 83 and 49 mrem/hour respectively. These dose rates are within the experimental data accuracy of 93 and 42 mrem/hour $\pm 20\%$ ⁽⁴⁷⁾.

FIGURE 4-1
1675 w(th) CAPSULE GAMMA PHOTON DOSE RATE
AT 1.0 METER AS A FUNCTION OF FUEL AGE

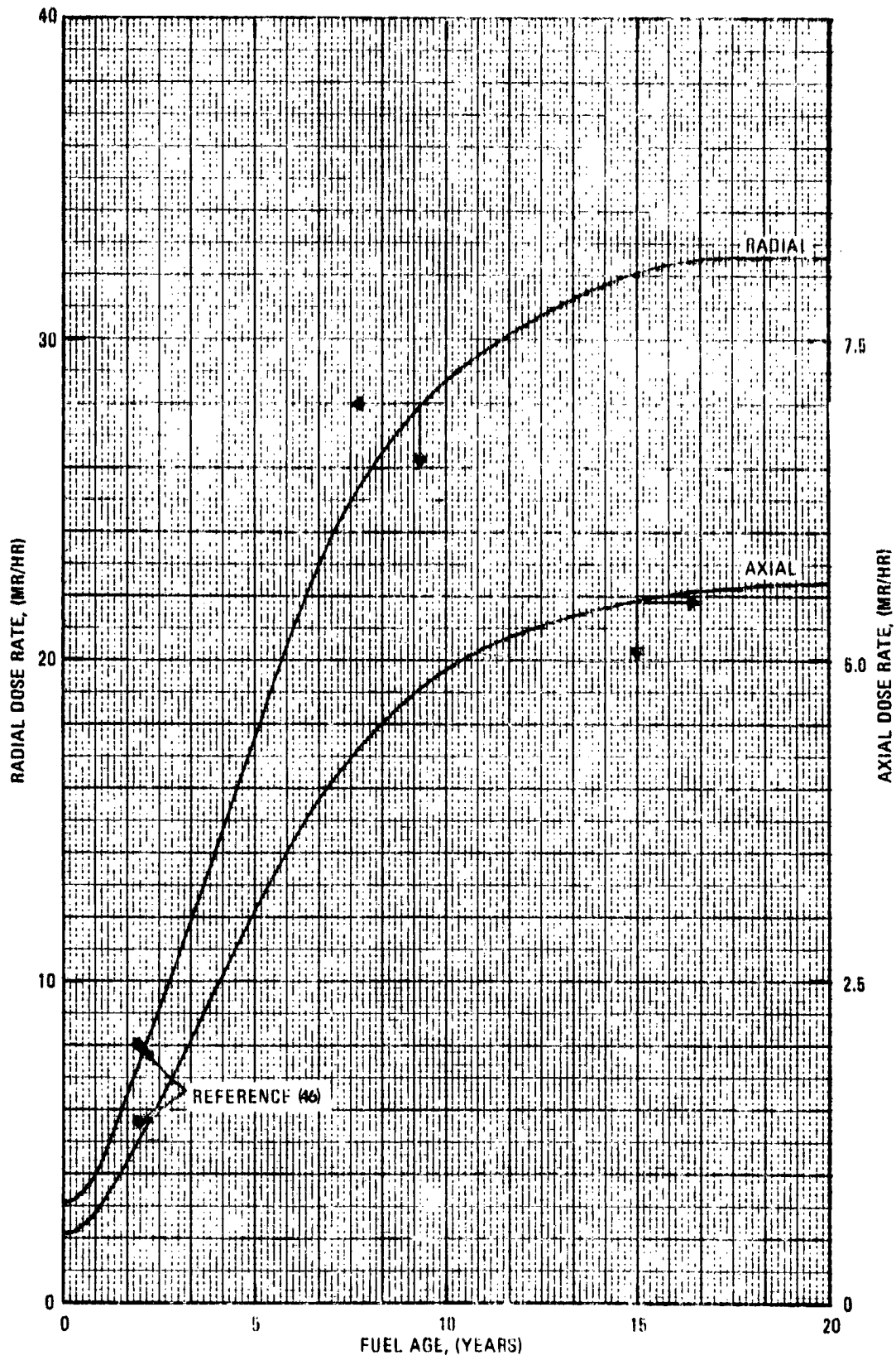


TABLE 4-1

RADIAL GAMMA PHOTON TOTAL DOSE RATE AT
1.0 METER AS A FUNCTION OF PuO₂ AGE

PHOTON SOURCE	POWER (w(th))	TIME (Years)				TOTAL DOSE RATE (mrem/hour)
		0	1	5	10	
Total	1575	3.07	4.30	17.54	28.73	32.53
Total	3468	4.94	6.95	26.57	46.84	53.05
Total	5679	6.68	9.34	37.89	61.96	70.15

RELATIVE CONTRIBUTION OF SOURCE COMPONENTS TO TOTAL DOSE RATE (PERCENT)

²³⁶ Pu	~0	28.7	22.5	89.3	90.5
¹⁸ O	3.5	2.5	0.6	0.4	0.3
Isotopes & Daughters	96.5	69.8	16.9	10.3	9.1
Total	100	100	100	100	100

APPENDIX A
 GAMMA ACTIVITY DUE TO DIRECT DECAY OF
²⁴¹Pu AND DAUGHTER NUCLIDES

The direct decay of ²⁴¹Pu yields a 145 keV gamma photon whose intensity is obtained as:

$$\text{photons/sec-gm PuO}_2 = 3.92 \times 10^{12} \frac{\text{dis}}{\text{sec-gm } ^{241}\text{Pu}} \times (.008) \times (.881) \times (\text{abundance})$$

where

$$0.008 \text{ is the fraction } \frac{\text{gm } ^{241}\text{Pu}}{\text{gm Pu}}$$

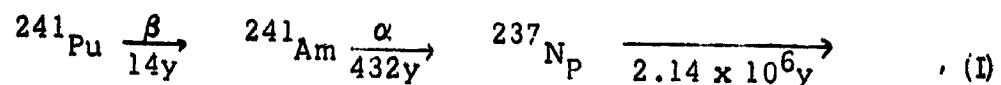
and

$$0.881 \text{ is the fraction } \frac{\text{gm Pu}}{\text{gm PuO}_2}$$

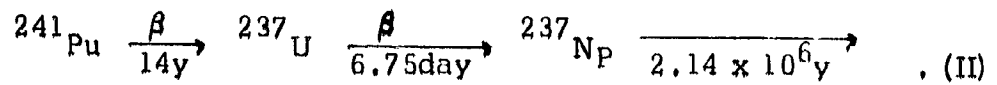
Thus, the 145 keV photon activity is obtained as

$$\begin{aligned} &= 3.92 \times 10^{12} \frac{\text{dis}}{\text{sec-gm } ^{241}\text{Pu}} \times .008 \times .881 \times 1.6 \times 10^{-6} \\ &= 4.42 \times 10^4 \frac{\text{photons (145 keV)}}{\text{sec-gm PuO}_2} \end{aligned}$$

There are two decay modes available to ²⁴¹Pu. The gamma photon yields of the ²⁴¹Pu daughter isotopes in these chains is presented in the remainder of this appendix. The decay chains available to ²⁴¹Pu are:



and

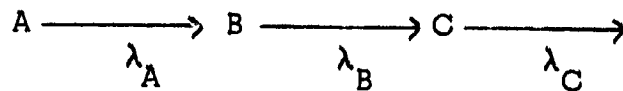


Decay Chain I

Decay chain I gives rise to a gamma spectrum which is calculated from the following abundances⁽⁹⁾:

<u>Gamma Energy (keV)</u>	<u>Abundance (% of isotope decay)</u>
60	36.
101	4×10^{-2}
208	6×10^{-4}
335	8×10^{-4}
370	4×10^{-4}
663	5×10^{-4}
772	3×10^{-4}

The gamma activity may be calculated from the Bateman equation. Where the decay chain is represented as:



the activity of ${}^{241}\text{Am}$, represented by $B\lambda_B$, is obtained as

$$N_B \lambda_B = \frac{\lambda_B \lambda_A}{\lambda_B - \lambda_A} \left\{ e^{-\lambda_A t} - e^{-\lambda_B t} \right\} \times N_{AO}$$

where

$N_B \lambda_B$ = dis/sec, of daughter nuclide B,

N_{AO} = initial number of atoms A; equal to Avagadros number

(N_O) divided by the gm-atomic mass of the parent A, given as M_A

The decay constants λ_A , λ_B corresponding to the parent and daughter nuclides were calculated as, $\lambda_A = .0495 \text{ year}^{-1} = 1.567 \times 10^{-9} \text{ sec}^{-1}$

$$\lambda_B = .001604 \text{ year}^{-1}$$

The activity of ^{241}Am is thus obtained as

$$\frac{\text{dis}}{\text{sec-gm PuO}_2} = \left(\frac{\text{gm } ^{241}\text{Pu}}{\text{gm PuO}_2} \right) \times \left(\frac{N_O}{M_A} \right) \left(\frac{\lambda_A \lambda_B}{\lambda_B - \lambda_A} \right) (e^{-\lambda_A t} - e^{-\lambda_B t}) \times (\text{abundance})$$

Decay Chain II

Decay chain II yields four photon lines which may be calculated from the relationship;

$$\frac{\text{photons}}{\text{sec-gm PuO}_2} = \left(\frac{\lambda_A N_O}{M_A} e^{-\lambda_A t} \right) \left(\frac{\text{gm } ^{241}\text{Pu}}{\text{gm PuO}_2} \right) \times (\text{abundance}) \times (\text{yield})$$

where the yield is assumed as 2.3×10^{-5}

The photon energy and abundances assumed, were ⁽⁹⁾;

<u>Gamma Energy (keV)</u>	<u>Abundance (% of isotope decay)</u>
14.	41.
33.2	16.
60.0	36.
208.0	23.

The expression, $e^{-\lambda At}$, gives the decay factor as:

Time (years)	0	1	5	10	18
Decay Factor	1.0	0.952	0.781	0.610	0.410

APPENDIX B
TABULATION OF PROMPT FISSION AND
EQUILIBRIUM FISSION PRODUCT GAMMA PHOTONS

This appendix presents tabulations of prompt fission and equilibrium fission product gamma photon emission. The tabulations are given in support of Section 2 of this report.

TABLE B-I
 PROMPT FISSION AND EQUILIBRIUM FISSION
 PRODUCT GAMMA PHOTONS*

Gamma Ray Energy Interval (MeV)	Prompt Fission Gamma Spectrum	Equil. Fission Product Gamma Spectrum	Total Fission Gamma Spectrum
7.0-6.0	0.007	0.0	0.007
6.0-5.0	0.020	0.0	0.020
5.0-4.0	0.060	0.003	0.063
4.0-3.0	0.179	0.027	0.207
3.0-2.0	0.538	0.267	0.815
2.0-1.8	0.198	0.173	0.371
1.8-1.6	0.247	0.312	0.559
1.6-1.4	0.308	0.267	0.575
1.4-1.2	0.384	0.117	0.501
1.2-1.0	0.478	0.106	0.584
1.0-0.9	0.302	0.307	0.609
0.9-0.8	0.380	0.888	1.268
0.8-0.7	0.479	0.9910	1.470
0.7-0.6	0.602	1.077	1.679
0.6-0.5	0.758	1.000	1.758
0.5-0.4	0.954	0.905	1.859
0.4-0.3	1.201	0.753	1.954
0.3-0.2	0.0	0.538	0.538
0.2-0.044	0.0	0.323	0.323
0.044-0.001	0.0	0.0	0.0

* Tabulation units are: "Number of photons emitted/fission."

TABLE B-II
 PROMPT FISSION AND EQUILIBRIUM FISSION
 PRODUCT GAMMA PHOTONS

Gamma Ray Energy Interval (MeV)	Total Fission Gamma Spectrum (γ /fission)	Photons ⁽¹⁴⁾ sec-gm PuO ₂		
		keff=0.17*	0.30*	0.41*
7.0-6.0	0.007	5.0	10.0	15.1
6.0-5.0	0.020	14.0	28.2	43.0
5.0-4.0	0.063	45.0	88.8	1.355 x 10 ²
4.0-3.0	0.207	147.0	291.9	4.451 x 10 ²
3.0-2.0	0.815	5.787 x 10 ²	11.492 x 10 ²	1.752 x 10 ³
2.0-1.8	0.371	2.634 x 10 ²	5.231 x 10 ²	7.977 x 10 ²
1.8-1.6	0.559	3.969 x 10 ²	7.882 x 10 ²	1.202 x 10 ³
1.6-1.4	0.575	4.083 x 10 ²	8.108 x 10 ²	1.236 x 10 ³
1.4-1.2	0.501	3.557 x 10 ²	7.064 x 10 ²	1.077 x 10 ³
1.2-1.0	0.584	4.147 x 10 ²	8.234 x 10 ²	1.256 x 10 ³
1.0-0.9	0.609	4.324 x 10 ²	8.587 x 10 ²	1.309 x 10 ³
0.9-0.8	1.268	9.003 x 10 ²	17.879 x 10 ²	2.726 x 10 ³
0.8-0.7	1.470	10.044 x 10 ²	20.727 x 10 ²	3.161 x 10 ³
0.7-0.6	1.679	11.921 x 10 ²	23.674 x 10 ²	3.610 x 10 ³
0.6-0.5	1.758	12.482 x 10 ²	24.788 x 10 ²	3.780 x 10 ³
0.5-0.4	1.859	13.200 x 10 ²	26.212 x 10 ²	3.997 x 10 ³
0.4-0.3	1.954	13.874 x 10 ²	27.552 x 10 ²	4.202 x 10 ³
0.3-0.2	0.538	3.820 x 10 ²	7.586 x 10 ²	1.157 x 10 ³
0.2-0.044	0.323	2.294 x 10 ²	4.554 x 10 ²	.695 x 10 ³
0.044-0.001	0.0	0.0	0.0	0.0

* The fission rates determined for this study ⁽¹⁴⁾ were 710, 1410 and 2150 n/sec-gm PuO₂, for the 1575, 3468 and 5679 w(th) sources, respectively.

APPENDIX C
²³⁶Pu GAMMA PHOTON ACTIVITY

The gamma photon activity due to ²³⁶Pu contamination in the PuO₂ fuel was based on a 1.2 ppm impurity.

The activities were calculated as follows:

$$\frac{\text{dis}}{\text{sec-gm } ^{236}\text{Pu}} = 1.97 \times 10^{13} \frac{\text{dis}}{\text{sec}} \times e^{-\lambda t} \times (\text{abundance}),$$

and

$$\frac{\text{dis}}{\text{sec-gm PuO}_2} = \frac{\text{dis}}{\text{sec-gm } ^{236}\text{Pu}} \times \frac{(\text{gm } ^{236}\text{Pu})}{(\text{gm PuO}_2)}$$

The results of the calculations are tabulated as:

Gamma Energy ⁽⁹⁾ (keV)	Abundance ⁽⁹⁾ (% of isotope decay)	$\frac{\text{photons}}{\text{sec-gm } ^{236}\text{Pu}}$	$\frac{\text{photons}}{\text{sec-gm PuO}_2}$
48	3.1×10^{-2}	6.107×10^9	6.46×10^3
110	1.2×10^{-2}	2.364×10^9	2.50×10^3
165	6.6×10^{-4}	13.0×10^7	13.75×10^1
520	1.7×10^{-4}	3.35×10^7	3.54×10^1
570	1.0×10^{-4}	1.97×10^7	2.08×10^1
645	2.4×10^{-4}	4.728×10^7	5.00×10^1

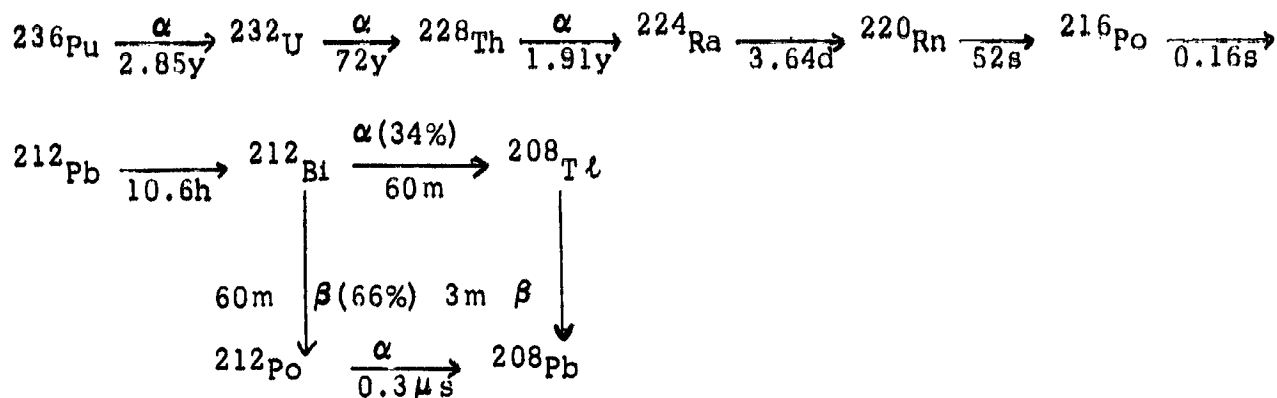
The expression, $e^{-\lambda t}$, was calculated to obtain the decay factor as:

Time (years)	0	1	5	10	18
Decay Factor	1.0	0.784	0.296	0.087	0.013

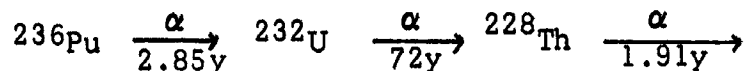
APPENDIX D

^{236}Pu DAUGHTER NUCLIDE GAMMA PHOTON ACTIVITY

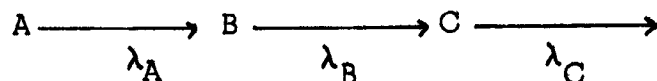
The activity of the ^{236}Pu daughter nuclides was determined from the growth of ^{228}Th , using the Bateman equation. The decay chain for this family is:



The gamma photon activity is controlled by the growth of the 1.91 year ^{228}Th . It may be calculated from the Bateman expression where



is represented as:



The final nuclide activity may be written as

$$\lambda_C N_C = \lambda_C N_{A0} \left[\frac{\lambda_A \lambda_B e^{-\lambda_A t}}{(\lambda_B - \lambda_A)(\lambda_C - \lambda_A)} + \frac{\lambda_A \lambda_B e^{-\lambda_B t}}{(\lambda_A - \lambda_B)(\lambda_C - \lambda_B)} + \frac{\lambda_A \lambda_B e^{-\lambda_C t}}{(\lambda_A - \lambda_C)(\lambda_B - \lambda_C)} \right] \times$$

x (yield) x (abundance) x (concentration)

where

N = number of atoms of daughter C ,

$$N_{Ao} = \frac{M_A N_O}{M_A} ,$$

M_A = actual mass of ^{236}Pu in PuO_2 ,

M_A = gram atomic mass = 236 gm ,

N_O = 0.6023×10^{24} , Avogadro Number ,

λ_A = $.24316 \text{ year}^{-1}$, ^{236}Pu decay constant ,

λ_B = $0.009365 \text{ year}^{-1}$, ^{236}U decay constant ,

λ_C = $0.36474 \text{ year}^{-1}$, ^{228}Th decay constant .

The activity of ^{228}Th as a function time was calculated as:

<u>TIME (years)</u>	<u>dis/sec-gm ^{236}Pu</u>
1	2.738×10^{10}
5	3.2216×10^{11}
10	5.6957×10^{11}
18	7.1566×10^{11}

When applied to PuO_2 fuel in which the concentration of ^{236}Pu may vary, the activity of the ^{228}Th per gm of PuO_2 , becomes:

^{236}Pu Concentration (ppm)	^{228}Th Nuclide Activity/gm- PuO_2			
	1	5	10	18
1.2	2.8815×10^4	3.383×10^5	5.981×10^5	6.891×10^5
0.8	1.021×10^4	2.256×10^5	3.987×10^5	4.594×10^5
0.6	1.441×10^4	1.692×10^5	2.990×10^5	3.445×10^5
0.1	0.240×10^4	2.819×10^4	4.984×10^4	5.742×10^4

APPENDIX E

$^{18}\text{O}(\alpha, n)^{21}\text{Ne}$ GAMMA PHOTON ACTIVITY

The $^{18}\text{O}(\alpha, n)^{21}\text{Ne}$ reaction yields gamma photons as well as neutrons. If the total neutron emission rate for ^{238}Pu is assumed as 1.9×10^4 n/sec-gm ^{238}Pu (14), then 1.24×10^4 , 0.26×10^4 and 0.4×10^4 n/sec-gm ^{238}Pu are the emission rate components for the $^{18}\text{O}(\alpha, n)^{21}\text{Ne}$, spontaneous fission and (α, n) impurity interactions, respectively. (37) The photon activity for ^{18}O reactions may be obtained as

$$\frac{\text{photons}}{\text{sec-gm } ^{238}\text{Pu}} = 1.24 \times 10^4 \frac{n}{\text{sec-gm } ^{238}\text{Pu}} \times \text{photons/neutron emitted,}$$

and thus

$$\frac{\text{photons}}{\text{sec-gm PuO}_2} = \frac{\text{photon}}{\text{sec-gm } ^{238}\text{Pu}} \times 0.714$$

Gamma photon activities were calculated as

<u>Gamma Photon Energy (MeV)</u>	<u>Photons emitted/ neutron emission (1)</u>	<u>Photons sec-gm ^{238}Pu</u>	<u>Photons sec-gm PuO₂</u>
0.35	0.45	$.558 \times 10^4$	$.400 \times 10^4$
1.38	0.10	$.124 \times 10^4$	$.089 \times 10^4$
1.90	0.02	$.025 \times 10^4$	$.018 \times 10^4$
2.40	0.02	$.025 \times 10^4$	$.018 \times 10^4$
2.70	0.02	$.025 \times 10^4$	$.018 \times 10^4$

These photon emission rates may be corrected for the decrease in ^{238}Pu activity, using the decay factor $e^{-.007734 \text{ year}^{-1}t}$ which yields

TIME (years)	0	1	5	10	18
Decay Factor	1.0	0.992	0.962	0.926	0.870

APPENDIX F
EXAMPLE FLUX CALCULATIONS

An example gamma photon flux and an example neutron flux calculation are presented in this appendix. Both calculations are for a point located at a radial distance of 100 cm. from a 1575 w(th) capsule. Normal (^{18}O undepleted) oxygen is assumed in each case.

1. The gamma photon flux for a 5 year old PuO_2 fuel containing a ^{236}Pu impurity of 1.6 ppm is obtained as follows:

From Table XVIII, the 'Decay of Isotopes and Daughters' flux	= 2,000 $\gamma/\text{cm}^2\text{-sec}$
From Table XIX the $^{18}\text{O}(\alpha, N)^{21}\text{Ne}$ flux	= 44 $\gamma/\text{cm}^2\text{-sec}$
From Table XX the ^{236}Pu and Daughters' Flux x (1.6/1.2)	= 5,181 $\gamma/\text{cm}^2\text{-sec}$
Total flux	= 8,952 $\gamma/\text{cm}^2\text{-sec}$

An estimate of the dose corresponding to this flux may be obtained, using Table 4-I, as

$$\begin{aligned}
 &= 17.54 \times 0.175 + 17.54 \times 0.825 (1.6/1.2) \\
 &= 22.4 \text{ mrem/hour}
 \end{aligned}$$

The above calculation assumes that only ^{236}Pu change with age is significant. The oxygen flux yield may be corrected (x 0.962) using the table given in Appendix E. This calculation may be corrected for other capsule power values by interpolation, as in Figure 2-X.

2. The neutron flux for PuO_2 fuel containing a 100 ppm boron (only) impurity is obtained as follows:

From Table 3-VII the
 $^{18}\text{O}(\alpha, n)^{21}\text{Ne}$ + Fission Neutron' flux = $427.7 \text{ n/cm}^2\text{-sec}$

From Table 3-VII the
'Fission Neutron' flux = $78.5 \text{ n/cm}^2\text{-sec}$

Thus, $^{18}\text{O}(\alpha, n)^{21}\text{Ne}$ flux = $349.2 \text{ n/cm}^2\text{-sec}$

Appendix Table K-II gives the boron yield (maximum) as 46.9 n/sec-gm Pu per ppm or 4690 n/sec-gm Pu per 100 ppm. From Equation (3.5) the boron impurity flux is determined as

$$\begin{aligned} &= 349.2 \times 4,690/9,882 \text{ n/cm}^2\text{-sec} \\ &= 156.7 \text{ n/cm}^2\text{-sec} \end{aligned}$$

The total flux is simply equal to

$$156.7 + 427 = 593.4 \text{ n/cm}^2\text{-sec}$$

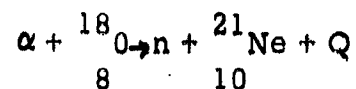
An estimate of the dose rate corresponding to this flux may be obtained by scale-factoring the 52.4 mrem/hour dose rate given in the text of Section 4 as

$$= 52.4 \times (593.4/427.7) = 72.7 \text{ mrem/hour.}$$

The above may be obtained for other power values by repeating the calculations for 3468 and 5679 w(th) and interpolating at the desired power.

APPENDIX G
THE DYNAMICS OF THE $^{18}\text{O}(\alpha, n)^{21}\text{Ne}$ REACTION

The (α, n) reaction may be considered as an inelastic collision between two initial systems and the reaction written as



The total kinetic energy of the interacting system corresponds to the kinetic energy of the alpha particle

$$E_{\alpha} = E_f - Q$$

where

Q is the energy equivalent of the difference between the masses of the initial reactants and product involved.

It can be shown that the total kinetic energy before the collision in the center of mass coordinate system is the sum of the kinetic energy of the incident alpha particle and oxygen target nucleus. The reaction masses and energies may be defined as follows:

- M_{α} = the rest mass of the alpha particle,
- M_{O} = the rest mass of the oxygen atom,
- M_{N} = the rest mass of the neutron,
- M_{Ne} = the rest mass of the neon atom,
- E_{α} = the kinetic energy of the alpha particle in the laboratory system,

- E_{α}' = the kinetic energy of the alpha particle in the center of mass coordinate system,
 E_n = the kinetic energy of the neutron in the laboratory system of coordinates,
 E_n' = the kinetic energy of the neutron in the center of mass coordinate system.

The total kinetic energy prior to collision may be written as

$$E_i' = E_{\alpha} \left(\frac{M_o}{M_o + M_{\alpha}} \right),$$

the total energy of the incident alpha particle relative to the target nucleus.

The total energy of the incident alpha particle in the center of mass system is

$$E_{\alpha}' = E_{\alpha} \left(\frac{M_o}{M_o + M_{\alpha}} \right)$$

The energy of the emitted neutron in the center of mass coordinate system is obtained as

$$E_n' = \left(\frac{M_{NE}}{M_{NE} + M_N} \right) \left[Q + \left(1 - \frac{M_{\alpha}}{M_N + M_{NE}} \right) E_{\alpha} \right]$$

which reduces to

$$E_n' = \left(\frac{M_{NE}}{M_N + M_{NE}} \right) \left\{ Q + \frac{M_o E_{\alpha}}{M_o + M_{\alpha}} \right\} = \left(\frac{M_{NE}}{M_N + M_{NE}} \right) (Q + E_{\alpha}')$$

The emitted neutron energy in the laboratory system of coordinates is E_n where

$$E_n = E_n' + \frac{M_N M_\alpha}{(M_O + M_\alpha)^2} E_\alpha + \frac{M_N M_\alpha}{(M_O + M_\alpha)} \sqrt{\frac{2E_\alpha}{M_\alpha}} \sqrt{\frac{2E_n'}{M_N}} \cos \theta_{cm}$$

This expression relates the neutron energy in the laboratory system, E_n , to the incident alpha particle energy, E_α and the angle of scatter, θ_{cm} , in the center of mass coordinate system.

The kinetic energy of the emitted neutron is determined from the Q value of the reaction, the incident alpha particle energy, E_α , and the angle of scatter in the center of mass coordinate system as

$$E_n = a(E_\alpha) + b(E_\alpha) \cos \theta_{cm}$$

where

$$a(E_\alpha) = \frac{M_{NE}}{M_N + M_{NE}} \left\{ Q + \frac{M_O}{M_O + M_\alpha} E_\alpha \right\} + \frac{M_N M_\alpha}{(M_O + M_\alpha)^2} E_\alpha$$

and

$$b(E_\alpha) = \frac{M_N M_\alpha}{(M_O + M_\alpha)} \left(\frac{2E_\alpha}{M_\alpha} \right)^{1/2} \left(\frac{2}{M_N} \left\{ \frac{M_{NE}}{M_N + M_{NE}} \left(Q + \frac{M_O}{M_O + M_\alpha} E_\alpha \right) \right\} \right)^{1/2}$$

If the probability of emission into an angle, θ_{cm} , in the center of mass coordinate system, is isotropic, then $p(\theta_{cm}) = (\sin \theta_{cm})/2$, is the probability of scatter such that

$$\int_{0^{\circ}}^{180^{\circ}} p(\theta_{cm}) d\theta_{cm} = \int_{0^{\circ}}^{180^{\circ}} \frac{\sin \theta_{cm}}{2} d\theta_{cm} = \int_{-1}^{+1} 1/2 d(\cos \theta_{cm}) = \int_{-1}^{+1} 1/2 d\mu = 1$$

where

$$d\mu = d(\cos \theta_{cm}).$$

Rewriting

$$\begin{aligned} \sin \theta_{cm} &= (1 - \cos^2 \theta_{cm})^{1/2} \\ &= \left(1 - \left(\frac{E_n - a}{b} \right)^2 \right)^{1/2} = \left(\frac{b^2 - E_n^2 + 2E_n a - a^2}{b^2} \right)^{1/2} \end{aligned}$$

the probability of scatter can be rewritten

$$\int_{a+b}^{a-b} \frac{1}{\pi b^2} \left(b^2 - a^2 - E_n^2 + 2E_n a \right)^{1/2} dE_n = 1$$

This equation gives the probability of scatter in the center of mass coordinate system in terms of $a(E_\alpha)$, $b(E_\alpha)$, and E_n which are parameters of the alpha particle and emitted neutron energy in the laboratory system of coordinates. It integrates to unity for particles scattered over all angles of emission. The equation expresses a uniform distribution of scattered neutrons in the laboratory coordinate system.

APPENDIX H

ALPHA PARTICLE ENERGY LOSS PER UNIT PATH LENGTH

Alpha particles are emitted during the decay of ^{238}Pu with an energy of 5.50 MeV. They eventually lose this energy by collision with the oxygen and plutonium atoms present in the PuO_2 fuel. The loss in energy, per unit of path length traveled by the alpha particle, may be determined from the expression:

$$\sum_1 \left. \frac{dE_\alpha}{dx} \right|_1 = \sum_1 3.8117 \times 10^3 \frac{Z_1}{E_\alpha} N_1 \ln \left\{ \frac{5.4823 \times 10^2 E_\alpha}{I_1} \right\}$$

where

I_1 = the mean excitation energy ⁽⁵²⁾ of the material species, 1.

The mean excitation energy was assumed to be 91eV and 893eV for the oxygen and plutonium isotopes ⁽³⁶⁾.

E_α = the energy of the alpha particle (MeV)

Z_1 = the atomic number of the scattering nucleus 1,

N_1 = the atomic density of the scattering nucleus (atoms/cm³).

A more detailed discussion of this subject is given in the excellent article by Fano ⁽³⁶⁾.

APPENDIX I
 $^{18}\text{O}(\alpha, n) ^{21}\text{Ne}$ NEUTRON YIELD

The 5.5 MeV alpha particles emitted by the radioactive decay of plutonium 238 interact with ^{18}O by a inelastic collision to produce neutrons. The alpha particle in this (α, n) reaction will have a maximum energy of 5.50 MeV and a possible minimum threshold energy

$$E_{th} = -(1 + \frac{m_{\alpha}}{m_u}) Q$$

Q is the energy equivalent of the difference in masses of reactants and products of the reaction. This term is discussed in more detail in Appendix G.

The incident alpha particle with energy $E_{th} \leq E_{\alpha} \leq 5.5$ MeV collides with ^{18}O and forms the compound nucleus ^{22}Ne . The ^{22}Ne emits a neutron and decays to the excited and ground state levels of ^{21}Ne . The yield and Q values from this reaction were given in Section 3.3 as: 55% to the ground state ($Q = -0.70$ MeV), 35% to the first excited state ($Q = -1.05$ MeV), 10% to the second excited states ($Q = -2.43$ MeV), and 1% to the third excited state ($Q = -3.54$ MeV).

The number of neutrons produced in each energy group j and the corresponding Q value of the reaction was calculated according to the relationship:

$$N_j(Q) = \frac{\int_{E_{\alpha}} \sigma(E_{\alpha}) E_{\alpha} \int_{\mu(E_j+1)}^{\mu(E_j)} 1/2 du dE_{\alpha}}{3.8117 \times 10^3 \left[16 \log_e \left\{ \frac{.4823 \times 10^2 E_{\alpha}}{91} \right\} + 94 \log_e \left\{ \frac{5.4823 \times 10^2 E_{\alpha}}{893} \right\} \right]}$$

where

$\sigma(E_\alpha)$ = the cross section for the formation of the ^{22}Ne (39),

E_α = the energy of the alpha particle in MeV.

$\mu(E_{j+1}), \mu(E_j)$ are the lower and upper values of $\cos\theta_{cm}$ from which the energy group j can be produced.

The number of neutrons produced in each energy group j , by the decay of the compound nucleus through ^{22}Ne all possible decay channels, was calculated as

$$N_j = 0.55 N_j(-0.70) + 0.35 N_j(-1.05) + 0.10 N_j(-2.43) + 0.01 N_j(-3.54)$$

where

$N_j(-0.70), N_j(-1.05), N_j(-2.43),$ and $N_j(-3.54)$ are the number of neutrons produced from the particular Q value reaction.

The sum, $\sum_j N_j$ is determined as the total number of neutrons produced in the $^{18}\text{O}(\alpha, n)^{21}\text{Ne}$ reaction. The fraction $N_j/\sum_j N_j$ as calculated for an arbitrary 10,000 groups j , is plotted in Figure I-I.

The equation relating the neutron energy, E_n , the incident alpha particle energy, E_α in the laboratory system of coordinates, to the angle of scatter, θ_{cm} in the center of mass coordinate system is

$$E_n = a(E_\alpha) + b(E_\alpha) \cos \alpha_{cm}$$

This equation has been derived and discussed in Appendix G.

To illustrate the relationship between E_n , E_α and θ_{cm} (angle of scatter), Figure I-II was tabulated for the following conditions:

$Q = -0.70$ MeV; the Q value for the inelastic collision which will yield the ground state of ^{21}Ne .

M_{NE} (mass of $^{21}_{10}\text{Ne}$ isotope) = 21.00000 a.m.u.,

M_{N} (mass of incident neutron) = 1.008665 a.m.u.,

M_{O} (mass of target nucleus ^{18}O) = 17.999160 a.m.u.,

M_α (mass of alpha particle) = 4.001506 a.m.u. where a.m.u. is the standard atomic mass unit.

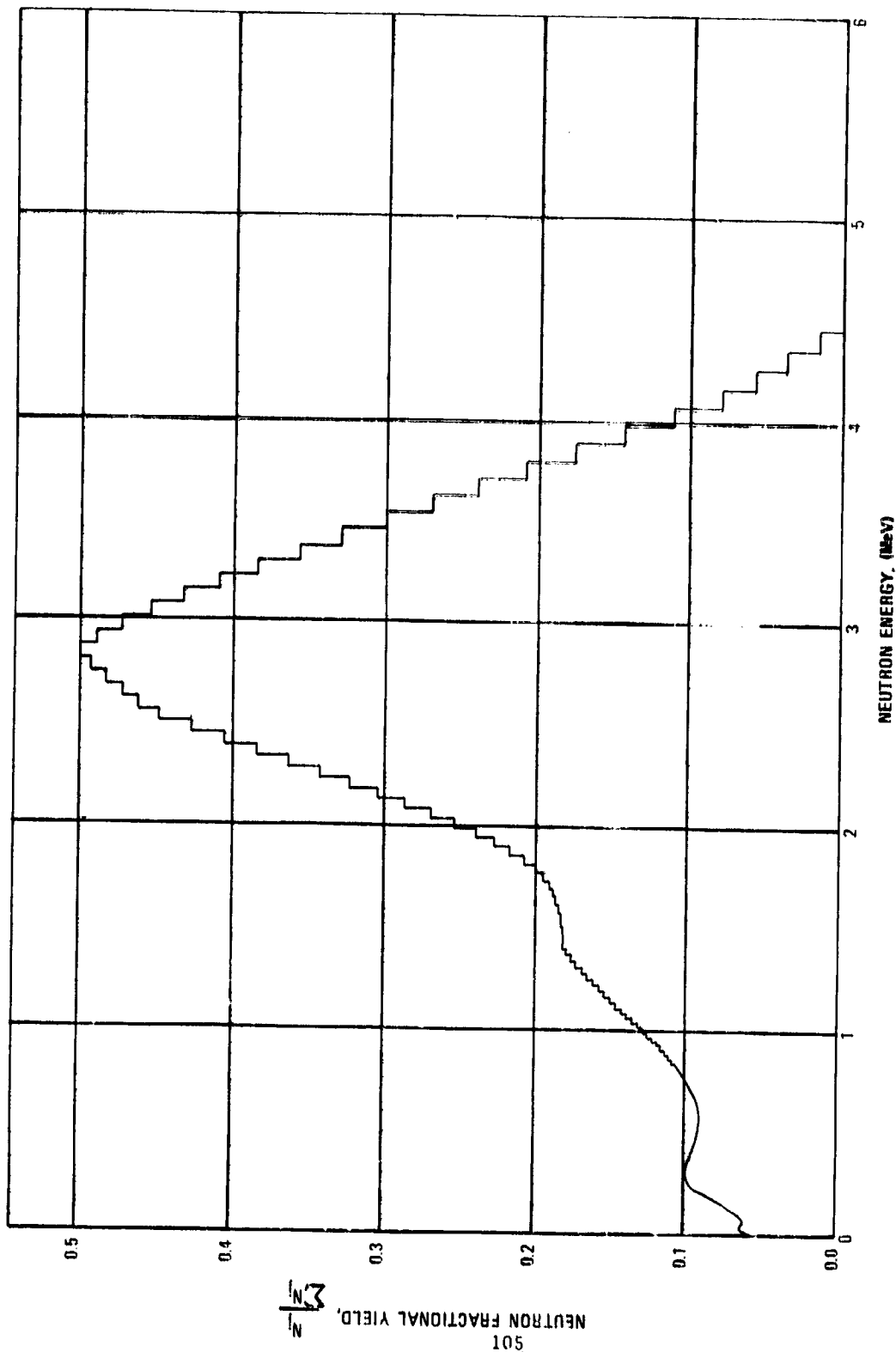


FIGURE I-1
NEUTRON FRACTIONAL YIELD AS A FUNCTION OF ENERGY

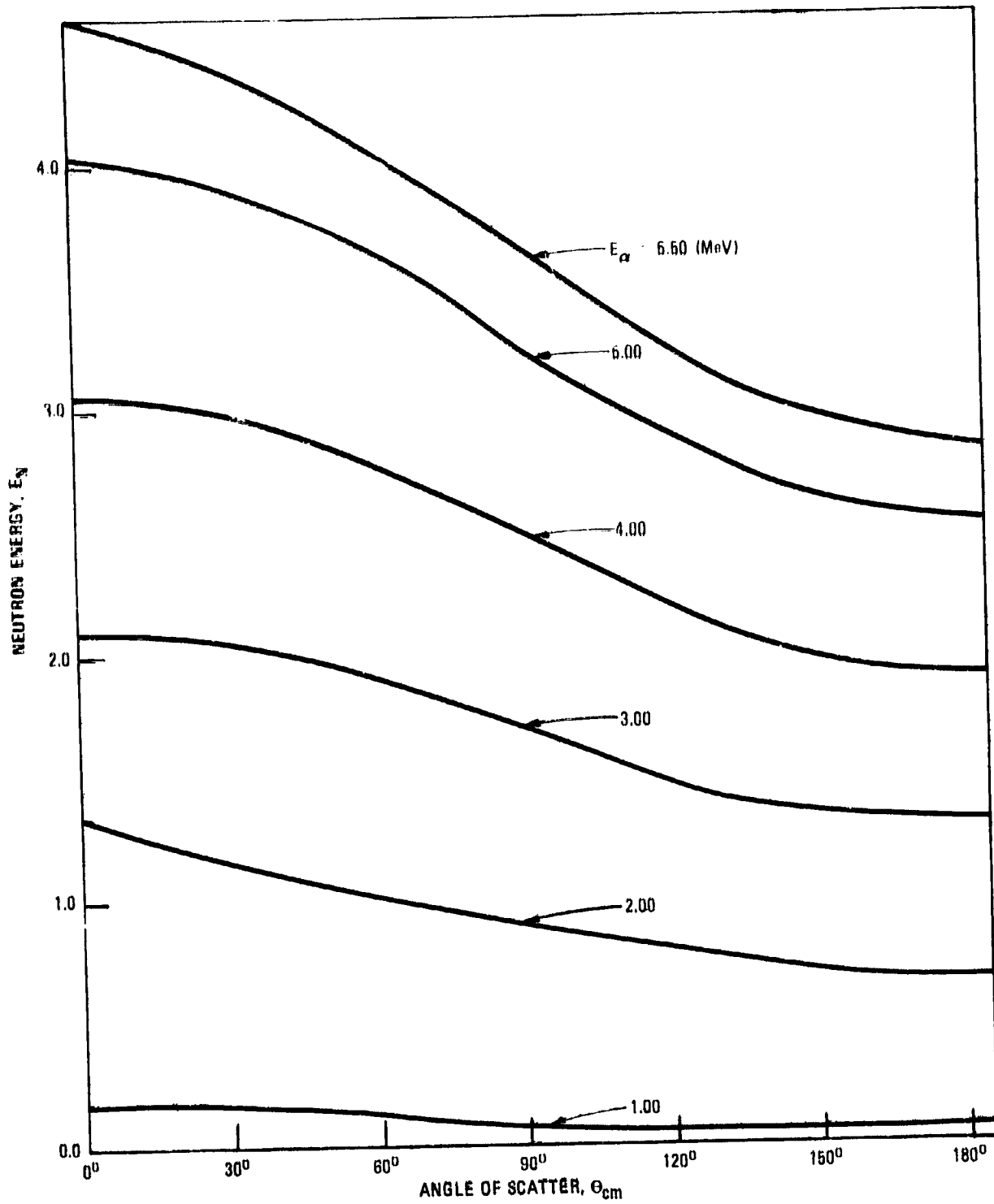


FIGURE I-II
 NEUTRON ENERGY AS A FUNCTION OF ANGLE OF SCATTER
 IN THE C-M SYSTEM WITH ALPHA PARTICLE ENERGY AS THE PARAMETER

APPENDIX J

INTEGRATION OF $^{18}\text{O}(\alpha, n)^{21}\text{Ne}$ SPECTRAL YIELD

$$\sum_{j=E_L}^{E_H} N(E_j) = 1.22 \times 10^4 \frac{\text{neutrons}}{\text{sec-gm}^{238}\text{Pu}} \sum_{j=E_L}^{E_H} N_j / \sum_j N_j \quad (3.5)$$

where

$$N_j = 0.55 N_j (Q = -0.70 \text{ MeV}) + 0.35 N_j (Q = -1.05 \text{ MeV}) + 0.10 N_j (Q = -2.43 \text{ MeV}) + 0.01 N_j (Q = -3.54 \text{ MeV}) \quad (3.6)$$

and

$\sum_j N_j$ = the total number of neutrons produced by the $^{18}\text{O}(\alpha, n)^{21}\text{Ne}$ reaction.

$N(E_j)$ = the number of neutrons in the laboratory system, between E_L and E_H , the lower and upper energy limit of the interval.

The number of neutrons in each group i , for each Q value, was numerically integrated according to the relationship:

$$N_j(Q) = \int_{E_\alpha} \frac{\sigma(E_\alpha)}{\sum_i \left(\frac{dE_\alpha}{dx} \right)_i} \left\{ \int_{\mu(E_{j+1})}^{\mu(E_j)} 1/2 d\mu \right\} dE_\alpha \quad (3.7)$$

where

$\mu(E)$ = cosine of the scattering angle in the center of mass coordinate system,

- N_j = the number of neutrons in each group j in the laboratory system of coordinates ($j = 10,000$ was used in the calculations),
 $\sigma(E_\alpha)$ = the compound (α, n) nuclear cross-section for the ^{18}O reaction⁽³⁹⁾, corrected to the laboratory system of coordinates,
 E_α = the range of the alpha particle energy appropriate to group j and each value of Q .

Since isotropic scattering is assumed in the center of mass coordinate system, the integral in equation (3.7)

$$\int_{\mu(E_{j+1})}^{\mu(E_j)} \frac{1}{2} d\mu = \int_{\mu(E_{j+1})}^{\mu(E_j)} \frac{1}{2} d(\cos\theta_{cm}) = \int_{\mu(E_{j+1})}^{\mu(E_j)} \frac{1}{2} \sin\theta_{cm} d\theta_{cm}, \quad (3.8)$$

corresponds to the neutron distribution, in the C. M. coordinate system, contributing to group j in the laboratory coordinate system.

If the compound nuclear cross sections $\sigma(E_\alpha)$ are plotted as a function of incident alpha particle energy, Shapiro⁽³⁹⁾ suggests that although the distribution will have the correct shape, the numerical values of the compound nuclear cross sections may be low. To correct for this fact the fraction

$$\frac{\sum_{j=E_1}^{E_H} N_j}{\sum_j N_j} \quad (3.9)$$

was calculated and multiplied by 1.22×10^4 neutrons/sec-gm ^{238}Pu , the experimentally measured yield of the $^{18}\text{O}(\alpha, n)^{21}\text{Ne}$ inelastic neutron reaction rate in PuO_2 (the normalizing value of the total yield from the $^{18}\text{O}(\alpha, n)^{21}\text{Ne}$ reaction).

The nuclear cross sections for the formation of the compound nucleus $^{21}_{10}\text{Ne}$ were determined from the tabulated quantities of Table J-I, with $g = 4$ and $v_0/B = 1.0$ as given by Shapiro⁽³⁹⁾. The cross sections calculated by this method are normally given in terms of the alpha particle energies in the center of mass coordinate system. Table J-I gives the alpha particle energies, converted from the C. M. to the laboratory system and the corresponding calculated nuclear cross sections.

Although the data of Baird and Willard⁽³³⁾ is an excellent source of nuclear cross sections for the $^{18}\text{O}(\alpha, n)$ reaction, the lowest alpha particle energy is 2.25 MeV and thus the data is difficult to interpret for averaged cross sections near the resonance peaks; data for alpha particle energies down to at least 1.0 MeV is desirable.

If the relationship between neutron energy group, j , alpha particle energy, E_α and the angle of scatter, $\cos\theta_{\text{cm}} = \mu$, in Appendix G, is written as

$$\mu(E_j) = \alpha E_j + \beta,$$

then the following combination of integration limits apply for each neutron energy group j and value of Q , where, $\mu(E_j) = (+1)$, (-1) and $(> -1$ and $< +1)$ are defined as cases A, B and C, respectively:

$$\frac{\mu(E_j) - \mu(E_{j+1})}{2}$$

$$\text{A-A} = (1 - 1)/2; \text{ no neutrons in group } j$$

$$\text{A-B} = (1 - (-1))/2 = 1; \text{ all neutrons are in group } j$$

- A-C = $(1 - (\alpha E_{j+1} + \beta)) / 2$; some of the neutrons are in group j
- B-A cannot occur since, $\mu(E_j) > \mu(E_{j+1})$
- B-B = $(-1 - (-1.01)) / 2$; no neutrons in group j
- B-C same as B-A
- C-A same as B-A
- C-E = $(\alpha E_j + \beta + 1) / 2$; some neutrons are in group j
- C-C = $\alpha(E_j - E_{j+1}) / 2$; some neutrons are in group j

TABLE J-I

NUCLEAR CROSS SECTIONS FOR FORMATION
OF $^{18}\text{O}(\alpha, n)^{21}\text{Ne}$ COMPOUND NUCLEUS⁽³⁹⁾

<u>E_α (MeV)</u>	<u>$\sigma(E_\alpha)$ (10^{-24} barns)</u>
1.222	2.52×10^{-3}
1.834	10.69×10^{-3}
2.445	17.32×10^{-3}
3.056	48.36×10^{-3}
3.667	23.75×10^{-3}
4.278	166.04×10^{-3}
4.890	189.30×10^{-3}
5.501	198.13×10^{-3}

APPENDIX K
CONTAMINANT LIGHT ELEMENT (α, n) NEUTRON YIELD

Low atomic number elements present as contaminants ⁽¹⁾, which are uniformly mixed with the plutonium isotopes in the commercial PuO₂ fuel, produce additional neutrons by the (α, n) reaction with the impurity given element ^(3, 53, 54).

The neutron yield N_y , for the $X(\alpha, n)Y$ reaction with the given impurity element X, where X is uniformly mixed with the PuO₂, may be obtained as

$$N_y = K \lambda N_{pu} T_x \frac{S_x N_x}{S_{pu} N_{pu} + S_x N_x}$$

where

the yield is the number of neutrons produced per gm of Pu per million parts by weight of the contaminant element, X,

K = the ²³⁸Pu fraction of plutonium,

λ = the ²³⁸Pu disintegration constant,

N_x = the number of atoms of element X,

N_{pu} = the number of atoms of the plutonium present,

T_x = the thick target yield for the element X (yield produced by the alpha particle incident on the thick target composed of the element X).

S_x = the atomic stopping power for the alpha particle incident on material species, x.

Neutron yields were calculated using the thick target yields and atomic stopping powers data given in Table K-I.

The (α , n) neutron yield N_y was calculated using the approximate relationship

$$N_y = K\lambda T_x \left(\frac{N_0}{A_x} \right) \left(\frac{S_x}{S_{pu}} \right) = 1.4897 \times 10^8 K \left(\frac{T_x}{A_x} \right) \left(\frac{S_x}{S_{pu}} \right) .$$

where

$N_0 = 6.024 \times 10^{23}$, Avogadro number,

$A_x =$ the atomic mass of the element x .

If minimum and maximum values of the ratio of the atomic stopping powers are multiplied by the minimum and maximum thick target yield, respectively, Table K-II yields result.

TABLE K-I
DATA FOR LIGHT ELEMENT (α, n) YIELD

Element	Ratio of Atomic Stopping Powers (S_x/S_{pu})		Thick Target Yields (in units of 10^{-6} neutrons/alpha)	
	$S_x/S_{pu}^{(2)*}$	$S_x/S_{pu}^{(52)}$	$T_x^{(54)}$	$T_x^{(53)}$
Li	.1038	.13	2.4	2.4(28)**
Be	.1320	.17	72.	84.4 \pm 0.9
B	.1579	.20	21.	19.6 \pm 0.2
C	.1821	.23	.09	0.113 \pm .015
N	.2047	-	.01	-
O	.2260	.29	.061	.068 \pm .011
F	.2462	.31	10.4	11.6 \pm .2
Na	.2837	.34	1.3	1.5(28)**
Mg	.3013	.36	1.2	1.33 \pm .04
Al	.3180	.37	.64	.76 \pm .03
Si	.3342	.42	.15	.168 \pm .020

* $S_x/S_{pu} = \left(\frac{Z_x}{\sqrt{Z_x + 7}} \right) / \left(\frac{Z_{pu}}{\sqrt{Z_{pu} + 7}} \right)$, where Z = atomic number.

** these uncertainties were given as +25%, -40%.

TABLE K-II
 LIGHT ELEMENT (α, n) YIELD
 (neutrons/sec-gm Pu, per ppm impurity)

Element	Maximum Yield*	Minimum Yield*	Yield ⁽²⁾
Li	5.5	4.3	4.6
Be	191.0	126.5	133.
B	46.9	35.1	41.
C	.3	.2	.2
N	-	-	-
O	.2	.1	.1
F	22.7	13.2	18.0
Na	2.7	1.5	2.2
Mg	2.4	1.8	2.1
Al	1.3	.9	1.0
Si	.3	.2	.2

* The maximum and minimum yields are not observed yields, but calculated using all possible thick target yields and stopping powers given in the literature. The values will include uncertainties in the observed thick target yields when used by the reader.

REFERENCES

1. STODDARD, D. H. and ALBENESIUS, E. L., "Radiation Properties of ^{238}Pu Produced for Isotopic Power Generators," DF-794, Savannah River Laboratory (1965).
2. "Plutonium-238 and Plutonium-210 Data Sheets," MLM-1441, Monsanto Research Corporation (November 1967).
3. MATLACK, G. M. and METZ, C. F., "Radiation Characteristics of Plutonium-238," LA-3696, Los Alamos Scientific Laboratory (1967).
4. TSENER, E. M., KHABAKHPASHEV, A. G. and PIRKIN, J. A., "Gamma Rays from Po-O^{18} Neutron Source," Soviet Physics JETP, 37 (10) No. 4 (1960) 806.
5. DRUIN, V. A., PERELYGIN, V. P. and KHLEBNIKOV, G. R., "Spontaneous Fission Periods of Np^{237} , Pu^{238} and Pu^{242} ," Soviet Physics JETP, 13, 5 (November 1961) (English Translation) 913.
6. DUNFORD, C., private communication (January 1970).
7. ANDERSON, E., private communication (March 1969).
8. PRINCE, A., "Thermal Neutron Cross Sections and Resonance Integrals for Transuranium Isotopes," Proceedings of Conference on Neutron Cross Sections and Technology, NBS Special Publication 299, Vol. II, Washington, D. C. (4-7 March, 1968).
9. LEDERER, C. M., HOLLANDER, J. M. and PERLMAN, I., "Table of Isotopes," Sixth Edition, John Wiley and Sons, Inc. (1967).
10. TERRELL, JAMES, "Distribution of Fission Neutron Numbers," Physical Review 108, 3, 783-789 (1957).
11. ASPLUND-NILSSON, I., CONDE, H., and STARFELT, N., "Average Number of Prompt Neutrons Emitted in the Spontaneous Fission of U^{238} and Pu^{240} ," Nuc. Sci. and Eng., 15 (1963) 213.
12. STEVENS, P. N., "Use of the Discrete Ordinates S_n Method in Radiation Shielding Calculations," Nuc. Eng. and Design, 13, 3 (1970) 395.

13. TRUBEY, D. K., "Kernel Methods for Radiation Shielding," *Nuc. Eng. and Design*, 13, 3 (1970) 423.
14. BUBERNACK, J., MATLACK, G. M., METZ, C. F., "Neutrons and Gamma Radiations from Pu-238," *Trans. Am. Nuc. Soc.*, Vol. II, No. 2, P. 457 (1968).
15. _____ "Reactor Physics Constants," ANL-5800, Argonne National Laboratory (1958).
16. SERDYUKOVA, I. A., KHABAKHPASHEV, A. G. and ISENTER, E. M., "Investigation of the (α , n) Reaction on Oxygen," *Izvest Akad Nauk SSSR Ser Fiz.* 21 (1957) 1017.
17. ENGLE, W. W., Jr., "ANISN, A One Dimensional Discrete Ordinates Transport Code with Anisotropic Scattering," K-1693 (March 1967); RSIC/ORNL Code Package CCC-82.
18. MALENFANT, P. E., "QAD, A Series of Point Kernel General Purpose Shielding Programs," LA-3573, Los Alamos Scientific Laboratory (April 1967); RSIC/ORNL Code Package CCC-48.
19. LATHROP, V. D., "GAMLEG - A Fortran Code to Produce Multigroup Cross Sections for Photon Transport Calculations," LA-3267, Los Alamos Scientific Laboratory (April 1965).
20. PRONKO, J. G., OLSEN, W. C., and SAMPLE, J. T., "Levels in ^{21}Ne Using ^{18}O (α , n) ^{21}Ne Reaction," *Nuclear Physics*, 83 (1966) 321.
21. PRONKO, J. G., ROLFS, C. and MAIER, H. J., "The 2.791 MeV and 2.87 MeV States in ^{21}Ne ," *Nuclear Physics*, A94 (1967) 561.
22. HEROLD, T. R., "Neutron Spectrum of $^{238}\text{PuO}_2$, DP-MS-67-51, Savannah River Laboratory, E. I. du Pont de Nemours Co., Aiken, South Carolina, 29801.
23. HEROLD, T. R., "Neutron Spectrum of $^{238}\text{PuO}_2$," *Nuc. App. and Tech.* 14 (1968).
24. ANDERSON, M. E. and NEFF, R. A., "Neutron Emission Rates and Energy Spectra of Two ^{238}Pu Power Sources," *Nuc. App. and Tech.*, 7 (1969) 62.

25. ARNOLD, E. D., "IAEA Engineering Compendium on Radiation Shielding: Chapter 2.1.2, Neutron Sources," Oak Ridge National Laboratory.
26. MEYER, C. T., ANDERSON, H. F. and KAHLE, J. B., "Calculated Dose Rates for Plutonium-238 Dioxide," MLM-1460, Monsanto Research Corp. (1968).
27. HICKS, D. A., ISE, J., Jr., and PYLE, R. V., "Probabilities of Prompt Neutron Emission from Spontaneous Fission," Phys. Rev. 101, 3 (1956) 1016.
28. ANDERSON, M. EDWARD, Private Communication (March 1970).
29. MULLINS, L. J. and LEARY, J. A., "Plutonium-238 for Biomedical Applications," Nuc. App. and Tech., 6 (1969) 287.
30. HYDE, E. K., PERLMAN, I. and SEABORG, G. T., "The Nuclear Properties of Heavy Elements," Volume II, Prentice-Hall, Inc. (1964).
31. LATHROP, K. D., "DTF-IV, A Fortran IV Program for Solving the Multigroup Transport Equation with Anisotropic Scattering," LA-3373, Los Alamos Scientific Laboratory Report (1965).
32. SAUTER, G. D. and BOWMAN, C. D., "The (α , n) Cross Sections on ^{17}O , ^{18}O ," UCRL-14260, University of California Radiation Laboratory.
33. BAIRD, J. K. and WILLARD, H. B., "Level Structure on Ne^{22} and Si^{30} from the Reaction $\text{O}^{18}(\alpha, n)\text{Ne}^{21}$ and $\text{Mg}^{26}(\alpha, n)\text{Si}^{29}$," Phys. Rev., 128, 1 (October 1962) 299.
34. HESS, W. N., "Neutrons from (α , n) Sources," UCRL-3839, University of California, Lawrence Radiation Laboratory (July 1957); Annals of Physics, 2 (1959) 115.
35. BONNER, T. W., KRAUS, Jr., A. A., MARION, J. B., and SCHIFFER, J. P., "Neutrons and Gamma Rays from the Alpha Particle Bombardment of Bc^9 , B^{10} , B^{11} , C^{13} and O^{18} ," Phys. Rev., Ed 102, 5 (June, 1956) 1348.

36. FANO U., "Penetration of Protons, Alpha Particles, and Mesons," National Academy of Sciences, National Research Council Publication 1133 (1964) (Report No. 39, Nuc. Sci. Series).
37. ALBENESIUS, E. L., private communication to V. Keshishian (March, 1969)
38. BROWN, PAUL E., private communication to General Electric Company Missile and Space Division (July 1969).
39. SHAPIRO, M. M., "Cross Sections for the Formation of the Compound Nucleus by Charged Particles," Phys. Rev., 90, 2 (1953) 171.
40. MARION, J. B. and FOWLER, J. L., (Editors), "Fast Neutrons," "Fast Neutron Physics," Vol. 1, Interscience Publishing Co., New York (1960).
41. HOWERTON, R. J., BRAFF, D. L., CAHILL, W. J. and CHAZAN, N., "Thresholds for He⁴ Induced Reactions," UCRL-14005, University of California, Lawrence Radiation Laboratory (1964).
42. _____ "Evaluated Nuclear Data File," Cross Section Education Center, Brookhaven National Laboratory, New York.
43. HOWERTON, R. J., "Evaluated Nuclear Data File," Lawrence Radiation Laboratory, Livermore, California.
44. ROCKWELL III, THEODORE, Editor, "Reactor Shielding Design Manual," D. Van Nostrand Company, Inc., New York, (1956).
45. "Protection Against Neutron Radiation Up to 30 Million Electron Volts," National Bureau of Standards Handbook 63 (April 1967).
46. LOFFREDA, J., "Radiation Fields about a Pu²³⁸O₂ Heat Source," IPSO-PIR-3401, General Electric Company Missile and Space Division, Philadelphia, Pa. (Dec. 1970).
47. BROWN, P. E., "Radiation from SNAP-27 Sources," IPSO-PIR-2394, General Electric Company Missile and Space Division, Philadelphia, Pa. (Dec. 1968).
48. MUSEN, L. G., and PROSSER, D. L., "Neutron and Gamma Dose Rates from SNAP-27 Heat Sources No. 2 and 6," Monsanto Research Corp. Report, Mound Laboratory, Miamisburg, Ohio (March 1970).

49. CHILTON, A. B., "Backscattering for Gamma Rays from a Point Source Near a Concrete Plane Surface," University of Illinois, Engineering Experiment Station, Bulletin 471, Vol. 62, No. 36 (Nov. 1964).
50. SONG, Y. T., "A Semiempirical Formula for Differential Dose Albedo for Neutrons on Concrete," TN-589, U. S. Naval Civil Engineering Laboratory, Port Hueneme, California (March 1964).
51. WELLS, M. B., "Reflection of Thermal Neutrons and Neutron Capture Gamma Rays from Concrete," RRA-M44, Radiation Research Associates, Texas (1964).
52. BADER, M., PIXLEY, R. E., MOZER, F. S. and WHALING, W., "Stopping Cross Section of Solids for Protons, 50-600 keV," Phys. Rev., 103, 1 (1956) 32.
53. GORSHOV, G. V., ZYABKIN, V. A. and TSVETKOV, O. S., "Neutron Yield from the Reaction (α , n) in Be, B, C, O, F, Mg, Al, Si," Atomnaya Energiya, 13, 1 (July 1962) 65.
54. ROBERTS, J. H., "Neutron Yields of Several Light Elements Bombarded with Polonium Alpha Particles," United States Atomic Energy Commission Report MDCC-731 (Jan. 1947).